



# **NAVAL POSTGRADUATE SCHOOL**

**MONTEREY, CALIFORNIA**

## **THESIS**

**ANALYSIS OF A NON-DEVELOPING TROPICAL  
CIRCULATION SYSTEM DURING TROPICAL CYCLONE  
STRUCTURE (TCS08) FIELD EXPERIMENT**

by

Steven C. Malvig

December 2009

Thesis Advisor:  
Second Reader:

Patrick Harr  
Russell Elsberry

**Approved for public release; distribution is unlimited**

<b>REPORT DOCUMENTATION PAGE</b>			<i>Form Approved OMB No. 0704-0188</i>	
Public reporting burden for this collection of information is estimated to average 1 hour per response, including the time for reviewing instruction, searching existing data sources, gathering and maintaining the data needed, and completing and reviewing the collection of information. Send comments regarding this burden estimate or any other aspect of this collection of information, including suggestions for reducing this burden, to Washington headquarters Services, Directorate for Information Operations and Reports, 1215 Jefferson Davis Highway, Suite 1204, Arlington, VA 22202-4302, and to the Office of Management and Budget, Paperwork Reduction Project (0704-0188) Washington DC 20503.				
<b>1. AGENCY USE ONLY (Leave blank)</b>		<b>2. REPORT DATE</b> December 2009	<b>3. REPORT TYPE AND DATES COVERED</b> Master's Thesis	
<b>4. TITLE AND SUBTITLE</b> Analysis of a Non-Developing Tropical Circulation System During the Tropical Cyclone Structure (TCS08) Field Experiment			<b>5. FUNDING NUMBERS</b>	
<b>6. AUTHOR</b> Steven C. Malvig				
<b>7. PERFORMING ORGANIZATION NAME(S) AND ADDRESS(ES)</b> Naval Postgraduate School Monterey, CA 93943-5000			<b>8. PERFORMING ORGANIZATION REPORT NUMBER</b>	
<b>9. SPONSORING /MONITORING AGENCY NAME(S) AND ADDRESS(ES)</b> N/A			<b>10. SPONSORING/MONITORING AGENCY REPORT NUMBER</b>	
<b>11. SUPPLEMENTARY NOTES</b> The views expressed in this thesis are those of the author and do not reflect the official policy or position of the Department of Defense or the U.S. Government.				
<b>12a. DISTRIBUTION / AVAILABILITY STATEMENT</b> Approved for public release; distribution is unlimited			<b>12b. DISTRIBUTION CODE</b>	
<b>13. ABSTRACT</b>  The objective of this research is to analyze the non-developing Tropical Circulation System (TCS025) utilizing data collected during the Tropical Cyclone Structure 2008 (TCS-08) and The Observing System Research and Predictability Experiment (THORPEX) Pacific Asian Regional Campaigns (T-PARC). Aircraft dropwindsondes, special ELDORA radar observations, and analyzed ECMWF model fields are used to define the three-dimensional structure at key times during the lifecycle of TCS025.  Two TCS025-related Mesoscale Convective Systems (MCSs) were examined with observations from Air Force WC-130J and Navy Research Lab P-3 flights. On 28 August 2008, dropwindsonde and ELDORA wind fields identified a cyclonic circulation associated with an MCS (MCS-G). However, the upper-level and lower-level circulations were disconnected around the 850 hPa level. The upper-level circulation propagated southward with the MCS-G convection while the lower-level circulation progressed poleward. On 29 August 2008, dropwindsonde and ELDORA wind fields identified a broad cyclonic circulation associated with another MCS (MCS-H). However, the center of circulation was northwest of MCS-H convection. It appears mid- and upper-level circulations associated with the MCS convection propagated southward with the convection while the low-level cyclonic circulation, under influence of the low-level background flow, progressed poleward. Without continued vertical coupling, TCS025 did not become a tropical depression.				
<b>14. SUBJECT TERMS</b> Electra Doppler Radar (ELDORA), Tropical Cyclone Structure (TCS08), TCS08, Tropical Cyclone Formation, Tropical Circulation System (TCS), TCS025			<b>15. NUMBER OF PAGES</b> 93	
			<b>16. PRICE CODE</b>	
<b>17. SECURITY CLASSIFICATION OF REPORT</b> Unclassified	<b>18. SECURITY CLASSIFICATION OF THIS PAGE</b> Unclassified	<b>19. SECURITY CLASSIFICATION OF ABSTRACT</b> Unclassified	<b>20. LIMITATION OF ABSTRACT</b> UU	

THIS PAGE INTENTIONALLY LEFT BLANK

**Approved for public release; distribution is unlimited**

**ANALYSIS OF A NON-DEVELOPING TROPICAL CIRCULATION SYSTEM  
DURING THE TROPICAL CYCLONE STRUCTURE (TCS08) FIELD  
EXPERIMENT**

Steven C. Malvig  
Lieutenant, United States Navy  
B.S., Saint Cloud State University, 2003

Submitted in partial fulfillment of the  
requirements for the degree of

**MASTER OF SCIENCE IN METEOROLOGY AND OCEANOGRAPHY**

from the

**NAVAL POSTGRADUATE SCHOOL  
December 2009**

Author: Steven C. Malvig

Approved by: Patrick Harr  
Thesis Advisor

Russell Elsberry  
Second Reader

Philip Durkee  
Chairman, Department of Meteorology

## **ABSTRACT**

The objective of this research is to analyze the non-developing Tropical Circulation System (TCS025) utilizing data collected during the Tropical Cyclone Structure 2008 (TCS-08) and The Observing System Research and Predictability Experiment (THORPEX) Pacific Asian Regional Campaigns (T-PARC). Aircraft dropwindsondes, special ELDORA radar observations, and analyzed ECMWF model fields are used to define the three-dimensional structure at key times during the lifecycle of TCS025.

Two TCS025-related Mesoscale Convective Systems (MCSs) were examined with observations from Air Force WC-130J and Navy Research Lab P-3 flights. On 28 August 2008, dropwindsonde and ELDORA wind fields identified a cyclonic circulation associated with an MCS (MCS-G). However, the upper-level and lower-level circulations were disconnected around the 850 hPa level. The upper-level circulation propagated southward with the MCS-G convection while the lower-level circulation progressed poleward. On 29 August, 2008, dropwindsonde and ELDORA wind fields identified a broad cyclonic circulation associated with another MCS (MCS-H). However, the center of circulation was northwest of MCS-H convection. It appears mid- and upper-level circulations associated with the MCS convection propagated southward with the convection while the low-level cyclonic circulation, under influence of the low-level background flow, progressed poleward. Without continued vertical coupling, TCS025 did not become a tropical depression.

## TABLE OF CONTENTS

<b>I.</b>	<b>INTRODUCTION.....</b>	<b>1</b>
A.	<b>MOTIVATION .....</b>	<b>1</b>
B.	<b>TROPICAL MESOSCALE CONVECTIVE SYSTEMS .....</b>	<b>2</b>
C.	<b>TROPICAL CIRCULATION SYSTEMS DURING TCS08.....</b>	<b>4</b>
D.	<b>ELDORA BACKGROUND .....</b>	<b>5</b>
<b>II.</b>	<b>METHODOLOGY .....</b>	<b>7</b>
A.	<b>ECMWF GLOBAL MODEL.....</b>	<b>7</b>
B.	<b>DROPWINDSONDES.....</b>	<b>8</b>
D.	<b>ELDORA DATA .....</b>	<b>10</b>
C.	<b>SATELLITE DATA.....</b>	<b>14</b>
<b>III.</b>	<b>ANALYSIS .....</b>	<b>17</b>
A.	<b>SYNOPTIC OVERVIEW OF TCS025.....</b>	<b>17</b>
1.	<b>24 August 2008 .....</b>	<b>17</b>
2.	<b>25 August 2008 .....</b>	<b>19</b>
3.	<b>26 August 2008 .....</b>	<b>21</b>
4.	<b>27 August 2008 .....</b>	<b>23</b>
5.	<b>28 August 2008 .....</b>	<b>25</b>
6.	<b>29 August 2008 .....</b>	<b>27</b>
7.	<b>Synoptic Summary.....</b>	<b>30</b>
B.	<b>MESOSCALE CONVECTION ANALYSIS.....</b>	<b>30</b>
1.	<b>MTSAT-1R Imagery 0930 UTC 25 August – 0730 UTC 26 August .....</b>	<b>31</b>
2.	<b>MTSAT-1R Imagery 0930 UTC 26 August – 0730 UTC 27 August .....</b>	<b>32</b>
3.	<b>MTSAT-1R Imagery 0930 UTC 27 August – 0730 UTC 28 August .....</b>	<b>34</b>
4.	<b>MTSAT-1R Imagery 0930 UTC 28 August – 0730 UTC 29 August .....</b>	<b>35</b>
C.	<b>AIRCRAFT DROPWINDSONDE ANALYSIS.....</b>	<b>37</b>
1.	<b>USAF WC-130J Dropwindsondes 26–27 August .....</b>	<b>37</b>
2.	<b>USAF WC-130J and NRL P-3 Dropwindsondes 27–28 August ....</b>	<b>42</b>
3.	<b>USAF WC-130J and NRL P-3 Dropwindsondes 28–29 August ....</b>	<b>46</b>
D.	<b>ELDORA ANALYSIS .....</b>	<b>49</b>
1.	<b>NRL P-3 ELDORA Flight 28 August 2008.....</b>	<b>50</b>
1.	<b>NRL P-3 ELDORA Flight 29 August 2008.....</b>	<b>60</b>
E.	<b>SYNOPTIC OVERVIEW 30 AUGUST THROUGH 1 SEPTEMBER 2008.....</b>	<b>64</b>
1.	<b>30 August 2008 .....</b>	<b>64</b>
2.	<b>31 August 2008 .....</b>	<b>66</b>
2.	<b>1 September 2008 .....</b>	<b>68</b>
<b>IV.</b>	<b>CONCLUSIONS .....</b>	<b>71</b>

A.	SUMMARY .....	71
B.	RECOMMENDATIONS.....	73
LIST OF REFERENCES .....		75
INITIAL DISTRIBUTION LIST .....		77

## LIST OF FIGURES

Figure 1.	MTSAT-1R enhanced infrared imagery showing several mesoscale convective systems within TCS025 at 2030 UTC 24 August 2008.....	5
Figure 2.	ELDORA scan technique showing the dual radar beam, tilted fore and aft of a plane normal to the fuselage (Hildebrand et al. 1996).....	6
Figure 3.	Timeline of USAF WC-130J and NRL P-3 missions flown on TCS025 during TCS08.....	9
Figure 4.	Flight pattern and dropwindsonde locations for the second USAF WC-130J flight of TCS025 during 1953 UTC 27 August - 0515 UTC 28 August. Yellow line is the flight path of the NRL P-3 with ELDORA. ....	9
Figure 5.	(a) MTSAT IR imagery of TCS025 at 0230 UTC 28 August. (b) RF05 ELDORA reflectivity and NRL P-3 flight path for portion of TCS025 indicated by the black box in (a).....	11
Figure 6.	(a) MTSAT IR imagery of TCS025 at 0230 UTC 28 August. (b) RF05 ELDORA reflectivity and NRL P-3 flight path for portion of TCS025 indicated by the black box in (a).....	12
Figure 7.	(a) Forward-looking raw ELDORA reflectivity (dBz) (top) and velocity over ground ( $\text{m s}^{-1}$ ) (bottom) before processing with Solo. (b) Processed reflectivity (top) and velocity over ground (bottom) using automated algorithm in Solo.....	13
Figure 8.	(a) MTSAT IR imagery at 1230 UTC 24 August 2008, and the 1200 UTC 24 August (b) ECMWF analyzed 200 hPa streamlines and geopotential (m), and (c) 850 hPa analyzed streamlines and geopotential (m). Streamline color indicates speed according to color scale on right in $\text{m s}^{-1}$ . ....	18
Figure 9.	Upper-level divergence (contoured at $10^{-5} \text{ s}^{-1}$ ) at 1200 UTC 24 August between 150-300 hPa superposed on MTSAT water vapor imagery. ....	19
Figure 10.	As in Figure 8, except MTSAT imagery at 1230 UTC 25 August and ECMWF analyses at 1200 UTC 25 August.....	20
Figure 11.	As in Figure 9, except at 1200 UTC 26 August 2008.....	21
Figure 12.	As in Figure 8, except MTSAT imagery at 1230 UTC 26 August and ECMWF analyses at 1200 UTC 26 August.....	22
Figure 13.	As in Figure 8, except MTSAT imagery at 1230 UTC 27 August and ECMWF analyses at 1200 UTC 27 August.....	24
Figure 14.	The analyzed 200 hPa – 850 hPa streamlines of vertical wind shear ( $\text{m s}^{-1}$ , see color bar) at 1200 UTC 27 August 2008 from the ECMWF. ....	25
Figure 15.	As in Figure 8, except MTSAT imagery at 1230 UTC 28 August and ECMWF analyses at 1200 UTC 28 August.....	26
Figure 16.	As in Figure 8, except MTSAT imagery at 1230 UTC 29 August and ECMWF analyses at 1200 UTC 29 August.....	28
Figure 17.	Convergence between 850-925 hPa (contoured units of $10^{-5} \text{ s}^{-1}$ ) at 1200 UTC 29 August 2008 superimposed on MTSAT-IR imagery.....	29
Figure 18.	The analyzed 200 hPa – 850 hPa streamlines of vertical wind shear ( $\text{m s}^{-1}$ , see color bar) at 1200 UTC 29 August 2008 from the ECMWF. ....	29



Figure 19.	MTSAT infra-red imagery each 2 h between 0930 UTC 25 August and 0730 UTC 26 August. In each image, the center latitude is 20°N and the longitudinal domain is 145°E to 165°E in 5° increments. ....	32
Figure 20.	MTSAT infra-red imagery each 2 h between 0930 UTC 26 August and 0730 UTC 27 August. In each image, the center latitude is 20°N and the longitudinal domain is 145°E to 165°E in 5° increments. The panels outlined in black indicate the period of a NRL P-3 with ELDORA mission. ....	33
Figure 21.	MTSAT infra-red imagery each 2 h between 0930 UTC 27 August and 0730 UTC 28 August. In each image, the center latitude is 20°N and the longitudinal domain is 145°E to 165°E in 5° increments. The panels outlined in black indicate the period of a WC-130J and NRL P-3 with ELDORA mission. ....	35
Figure 22.	MTSAT infra-red imagery each 2 h between 0930 UTC 28 August and 0730 UTC 29 August. In each image, the center latitude is 20°N and the longitudinal domain is 145°E to 165°E in 5° increments. The panels outlined in black indicate the period of a WC-130J and NRL P-3 with ELDORA mission. ....	36
Figure 23.	The WC-130J flight track between 1800 UTC 26 August – 0730 UTC 27 August 2008 displayed on the MTSAT enhanced IR imagery at 0130 UTC 27 August 2008. Circles identify approximate locations of dropwindsonde launches. ....	38
Figure 24.	Dropwindsonde winds for WC-130J flight 1800 UTC 26 August - 0730 UTC 27 August at (a) 950 hPa, (b) 850 hPa, (c) 700 hPa, and (d) 500 hPa. ...	39
Figure 25.	(a) Geostationary MTSAT IR imagery and WC-130J flight track from 1800 UTC 26 August – 0730 UTC 27 August 2008. (b) East-west vertical cross-section along 150°E-155°E at 20°N (black line in the MTSAT imagery panel (a)). Horizontal winds are defined by the barbs with one long barb equal to 10 m s <sup>-1</sup> . Contours are vertical velocity in m s <sup>-1</sup> and relative humidity in percent shaded. ....	41
Figure 26.	WC-130J flight track from 1953 UTC 27 August – 0515 UTC 28 August 2008 superposed on MTSAT IR imagery from 0330 UTC 28 August. Larger red circles identify approximate locations of dropwindsonde launches. Yellow line indicates flight path of the NRL P-3. ....	43
Figure 27.	Dropwindsonde winds for WC-130J flight 2000 UTC 27 August - 0500 UTC 28 August at (a) 950 hPa, (b) 850 hPa, (c) 700 hPa, and (d) 500 hPa. The circled wind barb coincides to the skew-T plot in Figure 29. ....	44
Figure 28.	Skew-T profile of TCS025 at 19.2°N, 152.3°E at 0110 UTC 28 August 2008. ....	45
Figure 29.	Satellite-derived upper-level winds from CIMMS at 1000 UTC 28 August between 150-300 hPa superposed on MTSAT water vapor imagery. ....	46

Figure 30.	WC-130J flight track from 2100 UTC 28 August – 0700 UTC 29 August 2008 superposed on MTSAT IR imagery from 0330 UTC 29 August. Red circles identify approximate locations of dropwindsonde launches. Yellow line indicates flight path of the NRL P-3 from 2240 UTC 28 August – 0615 UTC 29 August 2008. Red line is the path of the T-PARC Driftsonde launched from Hawaii.....	47
Figure 31.	Low-level winds from QuickSCAT imagery at 1827 UTC 28 August. ....	48
Figure 32.	Dropwindsonde winds for WC-130J flight 2100-0700 UTC 28 and 29 August at (a) 950 hPa, (b) 850 hPa, (c) 700 hPa, and (d) 500 hPa. ....	49
Figure 33.	The P-3 flight path, flight-level winds, and ELDORA reflectivity (dBz; scale at the bottom) at 2.5 km altitude 0140-0510 UTC 28 August 2008. ....	51
Figure 34.	Analyzed ECMWF streamlines, WC-130J and P-3 dropwindsondes at 850 hPa between 2000 UTC 27 August – 0600 UTC 28 August, and ELDORA winds ( $\text{m s}^{-1}$ : $10 \text{ m s}^{-1}$ scale at bottom) at 1.5 km between 0150-0410 UTC 28 August 2008. ....	52
Figure 35.	Analyzed ELDORA winds at 3 km ( $\text{m s}^{-1}$ : $10 \text{ m s}^{-1}$ scale at bottom) and WC-130J dropwindsondes at 700 hPa during 0150-0410 UTC 28 August 2008.....	53
Figure 36.	As in Figure 34, except for 700 hPa and 3 km.....	54
Figure 37.	As in Figure 35, except for 500 hPa and 6 km.....	55
Figure 38.	As in Figure 34, except for 500 hPa and 6 km.....	56
Figure 39.	As in Figure 34, except for 300 hPa and 9.5 km.....	57
Figure 40.	Analyzed ECMWF streamlines, NRL P-3 and WC-130J dropwindsondes, and ELDORA reflectivity and winds during 0345-0410 UTC 28 August 2008. (a) 1.5 km, 850 hPa, (b) 3 km, 700 hPa, (c) 4.5 km, 600 hPa, and (d) 6 km, 500 hPa. ....	59
Figure 41.	The P-3 flight path, flight-level winds, and ELDORA reflectivity (dBz) at 1.5 km altitude from 0010 UTC - 0615 UTC 29 August 2008.....	61
Figure 42.	Analyzed ECMWF streamlines, WC-130J dropwindsondes at 850 hPa between 2100 UTC 28 August – 0500 UTC 29 August, and ELDORA reflectivity (dBz) and winds ( $\text{m s}^{-1}$ ) at 1.5 km during 0020-0415 UTC 29 August 2008.....	62
Figure 43.	Analyzed ELDORA winds (3 km) and WC-130j dropwindsondes (700 hPa) during 0020-0415 UTC 29 August 2008.....	63
Figure 44.	As in Figure 8, except MTSAT imagery at 1230 UTC 30 August and ECMWF analyses at 1200 UTC 30 August.....	65
Figure 45.	As in Figure 8, except MTSAT imagery at 1230 UTC 31 August and ECMWF analyses at 1200 UTC 31 August.....	67
Figure 46.	As in Figure 8, except MTSAT imagery at 1230 UTC 1 September and ECMWF analyses at 1200 UTC 1 September. ....	69

THIS PAGE INTENTIONALLY LEFT BLANK

## **LIST OF ACRONYMS AND ABBREVIATIONS**

DoD	Department of Defense
ECMWF	European Centre for Medium-range Weather Forecasts
ELDORA	Electra Doppler Radar
GPS	Global Positioning System
IR	Infrared
JTWC	Joint Typhoon Warning Center
LLCC	Low-level Circulation Center
MCS	Mesoscale Convective System
MSLP	Minimum Sea-Level Pressure
NCAR	National Center for Atmospheric Research
NRL	Naval Research Laboratory
NSF	National Science Foundation
ONR	Office of Naval Research
SST	Sea-Surface Temperature
T-PARC	THORPEX Pacific Asian Regional Campaign
TC	Tropical Cyclone
TCS	Tropical Circulation System as defined during TCS08/T-PARC
TCS08	Tropical Cyclone Structure-08
TD	Tropical Depression
THORPEX	The Observing System Research and Predictability Experiment
TS	Tropical Storm
TUTT	Tropical Upper Tropospheric Trough
TY	Typhoon
USAF	United States Air Force
VHT	Vortical Hot Tower
WNP	Western North Pacific
YOTC	Year of Tropical Convection

THIS PAGE INTENTIONALLY LEFT BLANK

## **ACKNOWLEDGMENTS**

I would like to thank my thesis advisor Professor Patrick Harr for his guidance, knowledge, and patience and Professor Russell Elsberry for his help in editing. I would also like to thank Michael Bell for his ELDORA expertise and willingness to help and Elizabeth Sanabia for her countless hours of assistance. I would also like to thank Bob Creasy for his assistance with anything and everything computer-related. Finally, I would like to thank my friends and fellow US Navy METOC officers for their support and motivation.

THIS PAGE INTENTIONALLY LEFT BLANK

# **I. INTRODUCTION**

## **A. MOTIVATION**

The western North Pacific (WNP) is an extremely active region for tropical cyclone (TC) development with an average of 31 named systems per year (JTWC 2008). Tropical cyclones can occur in every month of the year with the peak activity in August and September. Although WNP TCs occur at a high frequency, the ability to forecast TC development is a difficult endeavor even for the most experienced forecaster. In recent years, advances in remote sensing observations have greatly improved the ability to accurately forecast TC tracks and estimate intensity. However, predicting development or non-development of a tropical circulation system (TCS) into a TC remains a complex problem. One of the challenges of TC forecasting in the WNP is the lack of in situ observations. Because of the immense size of the WNP basin, data from ocean buoys are sparse and land-based radar is virtually ineffective. Additionally, direct measurements from reconnaissance aircraft, such as those in the western Atlantic and occasionally in the Northeast Pacific, are rare. Due to the potentially devastating economic and social effects of TC landfall impacts, a better understanding of TC development, including formation, structure, and transition is required.

From August through October 2008, a major international TC field experiment was conducted in the WNP. The Tropical Cyclone Structure (TCS08) program was conducted in cooperation with the THORPEX Pacific Asian Regional Campaign (T-PARC) to increase the understanding of TC formation, intensification, structure, and extratropical transition to improve forecasting. Due to the large number of military assets and operations in the WNP, the ability to accurately forecast TCs is of great importance to the Department of Defense (DoD). The leading sponsors of TCS08 were the U. S. Office of Naval Research (ONR), the U. S. Naval Research Laboratory, and the U. S. Air Force (USAF). Participants included a wide range of civilian and military personnel from all over the world including Japan, Australia, and Taiwan. A large array of data collection methods were employed, which include Doppler radar, Doppler wind lidar, and dropwindsondes launched from aircraft (Elsberry and Harr 2008).



One of the primary goals for TCS08 was to study the mesoscale contribution to TC development including the role of mesoscale convective systems (MCSs) in the development process. The focus of this thesis will be a case study of a non-developing TCS (TCS025) that was made up of multiple MCSs. In situ measurements, specifically those obtained by the Navy Research Laboratory (NRL) P-3 aircraft with the National Science Foundation (NSF)/ National Center for Scientific Research (NCAR) Electra Doppler radar (ELDORA) and the USAF WC130J aircraft, are used to better understand the dynamic and thermodynamic structure of individual MCSs that are embedded in a non-developing TCS. The MCS characteristics to be investigated include 3-D airflow characteristics, deep convection response to vertical wind shear, and the 3-D variability of convection in the vertical over time. Additionally, model analyses from the European Centre for Medium-range Weather Forecasts (ECMWF) and satellite data were utilized.

## **B. TROPICAL MESOSCALE CONVECTIVE SYSTEMS**

The synoptic-scale conditions that can lead to TC formation are relatively well understood. Monsoon troughs, monsoon depressions, easterly tropical waves, and tropical upper tropospheric troughs (TUTTs) are some of the tropical weather phenomena that can serve as an incipient disturbance for a developing TC. These synoptic-scale systems, together with ideal thermodynamic and dynamic conditions such as conditional instability, low-level vorticity, and low vertical wind shear, are known to be favorable for TC development (Gray 1968). Within an incipient disturbance, tropical cloud clusters may exist and be composed of one or multiple MCSs. How the organization of multiple MCSs within a TCS that then leads to development of a TC is an aspect of TC formation that is not well understood. Many of these systems form in the WNP every year, yet very few of them actually develop into TCs. According to Montgomery (2006), they tend to form in association with synoptic-scale disturbances such as tropical easterly waves. While it is understood that these structures are important to TC formation, the mesoscale processes that lead to development or non-development are not completely understood in part due to the limited number of observations of their 3-D structure.

There are two leading theories as to how one MCS or multiple MCSs may lead to TC formation. In the “top-down” formation, strong mid-level convergence generates positive mid-level vorticity near the base of the stratiform cloud region of the MCS (Simpson et al. 1997). Warming due to latent heat release combined with cooling from evaporation of rain below the stratiform cloud leads to a vertical potential temperature gradient at the stratiform base. Mesoscale convergence and stretching occurs just above the cloud base and leads to a positive potential vorticity anomaly with a circulation on the scale of the stratiform cloud. This mid-level positive vorticity anomaly causes lifting of unstable air in the boundary layer below. If this interaction takes place for an extended period of time, the positive vorticity anomaly will translate down to the surface where the circulation may tap the energy associated with the warm ocean to develop further. Additionally, multiple mid-level vortices associated with an ensemble of MCSs within a TCS may merge to increase the horizontal and vertical extent of the mid-level vortex

The hypothesized application in TCS08 of the top-down formation related to monsoon depressions was that MCSs that formed in the convective regions with strong low-level winds and large vertical wind shear would be transient and be axisymmetrized into the mean flow (Elsberry and Harr 2008). However, a MCS that formed in the central region of weak wind and weak vertical wind shear in the monsoon depression would be sustained longer and undergo re-generation. The persistent positive potential vorticity anomaly generated by these MCSs would then combine with the monsoon depression circulation to form a deep, warm-core, vorticity column that would evolve into a tropical depression (TD).

In the “bottom-up” formation, a favorable tropical environment could produce multiple vortical hot towers (VHTs) (Montgomery et al, 2006). These VHTs contain extremely strong updrafts that stretch the column and therefore increase the low-level convergence and produce cyclonic vorticity. Multiple VHTs in the vicinity of each other can merge and strengthen this low-level convergence. This convergence leads to a mesoscale spin-up of winds in the lower troposphere (Elsberry and Harr 2008), which enhances the air-sea fluxes of heat and momentum that are needed to sustain deep

convection and continue to lower sea-level pressure (SLP). Lowering SLP increases surface winds that enhance the air-sea fluxes. This positive feedback interaction is what is required for TC development.

### **C. TROPICAL CIRCULATION SYSTEMS DURING TCS08**

The primary strategy used by TCS08 scientists to monitor the early stages of TC development was to observe and track TCSs. Local regions of convection were identified by satellite and numbered to catalog TCSs. Each of these systems was the subject of analysis and discussion of structure and potential for TC development as possible targets for aircraft missions. From early August to early October, a total of 51 numbered TCSs were monitored in the WNP. Of these TCSs, 12 reached a minimum of tropical depression (TD) intensity. Of these 12, four never intensified beyond TD status, four reached tropical storm (TS) status, and four eventually intensified into a typhoon (TY).

Since only 12 TCs developed from the 51 TCSs that were monitored, many long-lived TCSs never developed. One of these was TCS025 that was identified on 2100 UTC 24 August at approximately 600 km northeast of Guam (Figure 1). This relatively broad system of tropical convection initially showed promise for further development as synoptic scale conditions at the time were favorable. For the next ten days until 3 September, convection continued to flare up and die down, but a consistent low-level circulation center (LLCC) did not develop, and TCS025 was never upgraded to TD status. Because of its proximity to TCS08/TPARC flight operations out of Guam and potential for development, this TCS was chosen for further investigation with the NRL P-3 and the USAF WC-130J. Of particular interest was the use of ELDORA to examine the structure of the MCSs that were embedded in TCS025. Two ELDORA missions, conducted on 28 and 29 August, were flown on this system and will be discussed later.

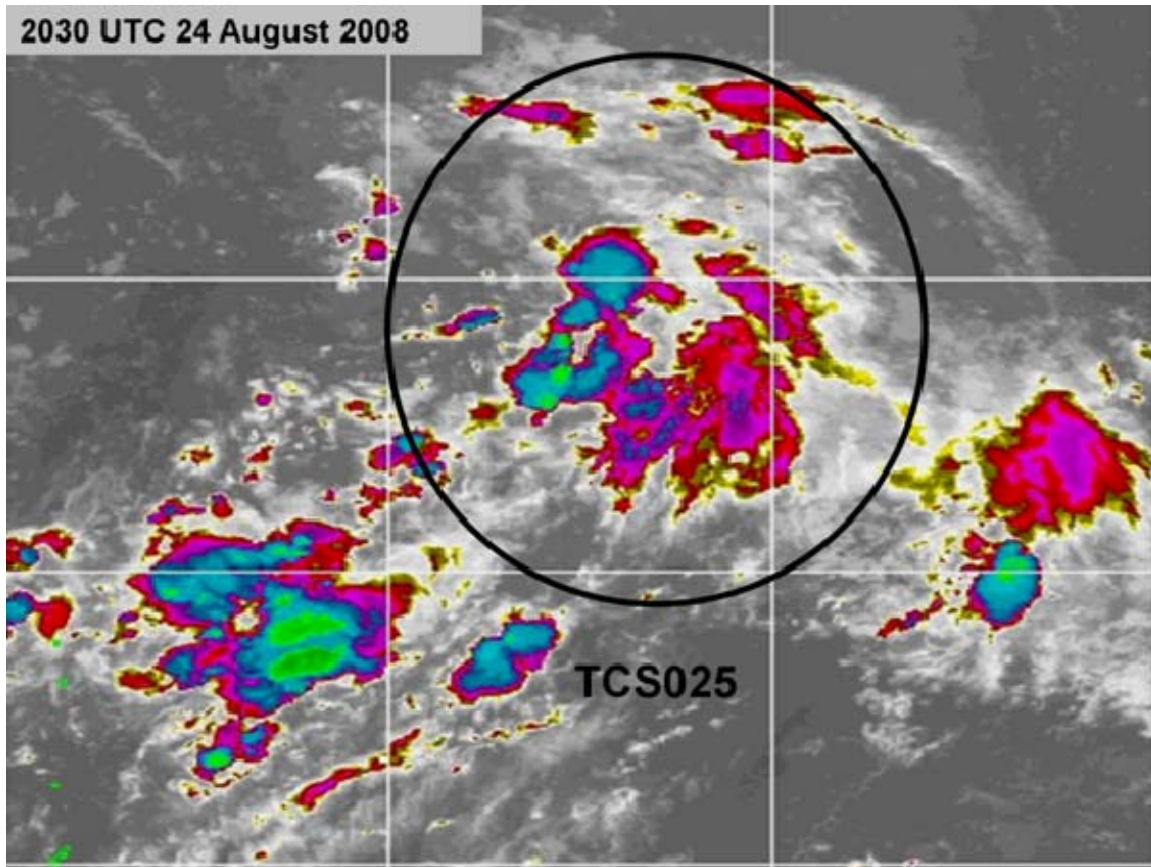


Figure 1. MTSAT-1R enhanced infrared imagery showing several mesoscale convective systems within TCS025 at 2030 UTC 24 August 2008.

#### **D. ELDORA BACKGROUND**

For the combined TCS08 and T-PARC field experiment, the ELDORA radar was mounted on a P-3 aircraft operated by the Naval Research Lab (NRL). The ELDORA was developed under a joint effort between the National Center for Atmospheric Research (NCAR) and the Centre de Recherche en Physique de L'Environnement Terrestre et Planetaire (CRPE), France. The first deployment of ELDORA was during Tropical Oceans-Global Atmosphere Coupled Ocean-Atmospheric Response Experiment (TOGA COARE) in January and February 1993 (<http://www.eol.ucar.edu/rsf/eldora/eldora.html>). This dual-Doppler radar was designed to provide high-resolution measurements of air motion and rainfall characteristics of large storms that are too remote to observe by conventional ground radar. The forward and aft antennas are mounted on the tail of the aircraft and spin longitudinally about the axis of the aircraft (Figure 2). These two

antennae point slightly ahead and slightly back, respectively, and provide two wind components. Using the conservation of momentum, a 3-D structure of the storm is produced that can then be sliced to produce 2-D plots at various elevations in the storm.

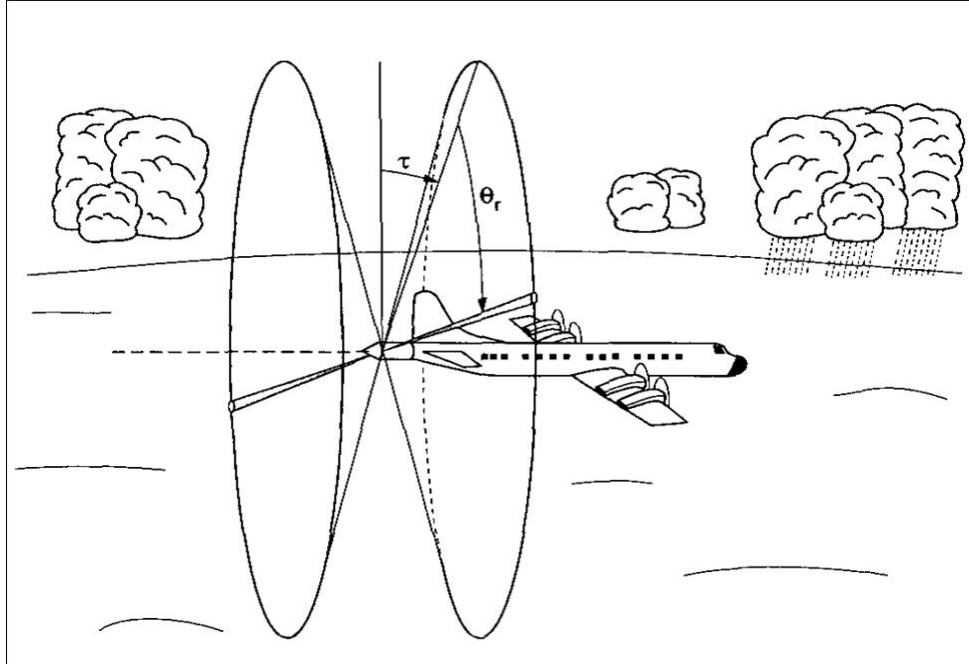


Figure 2. ELDORA scan technique showing the dual radar beam, tilted fore and aft of a plane normal to the fuselage (Hildebrand et al. 1996).

During TCS08, the NRL P-3 was flown out of Andersen Air Base on Guam. This area of the WNP routinely sees TC development and was therefore an ideal location for flight operations. One limitation of the NRL P-3 is that it is only equipped with a forward sector-scanning weather radar which makes it insufficient for safe navigation at night in regions of deep convection. Therefore, the NRL P-3 was deployed in the early morning hours following the peak in convective activity that typically occurs prior to dawn. The primary use of this aircraft was to study the mesoscale convective vortex (MCV) that is often detected in the stratiform rain region following the nocturnal convective maximum. During August to October, ELDORA was deployed on the NRL P-3 for a total of 21 missions. These missions included investigating developing and non-developing TCSs, TDs, TYs, and an extratropical system.

## **II. METHODOLOGY**

One of the great challenges for TC forecasters in the WNP is the lack of available data. Few rawinsondes are deployed, ship reports are sporadic and can be unreliable, shore-based Doppler radar winds are ineffective beyond 60 miles from shore, and buoy observations cannot cover the immense size of the WNP basin. Forecasters have had to rely on remote sensing and computer models to predict development, intensification, and track.

Forecast accuracy can be greatly enhanced if in situ observations are obtainable. This can give forecasters a three-dimensional data set of an assortment of meteorological variables that would improve TC forecasting. The principal method to acquire these data is by reconnaissance aircraft. Aircraft are used frequently in the Atlantic and the eastern North Pacific to investigate TCs, but are uncommon in the WNP.

During TCS08, two aircraft, the WC-130J and the NRL P-3, were made available to collect meteorological data through a variety of methods. This analysis of TCS025 makes use of data collected by dropwindsondes launched from both aircraft and the NCAR ELDORA deployed aboard the NRL P-3. Additionally, ECMWF model fields and satellite imagery are used to analyze periods before and after flights and for in situ observation comparisons.

### **A. ECMWF GLOBAL MODEL**

The ECMWF global model data assimilation system provided a  $\frac{1}{4}$ -degree horizontal grid resolution and 25 hPa vertical resolution analyses at 0000, 0600, 1200, and 1800 UTC. This system, which was introduced in 2006, uses a triangular truncation (T799) numerical scheme and a semi-Lagrangian, two-time-level, semi-implicit formulation. Wind, temperature, surface pressure and humidity observations are assimilated using a four-dimensional multivariate variational technique every 12 hours. These high-resolution model analyses were made available for TCS08 via the Year of Tropical Convection (YOTC) archive. For this study, wind, geopotential, and vorticity fields are used as a baseline to define the overall environment of TCS025, and for

comparison with ELDORA data. The ECMWF fields are also used to describe the synoptic conditions of the WNP from the time of TCS025 identification through dissipation. Model fields are also used to evaluate in situ measurements from WC-130J and NRL P-3 flights

## **B. DROPWINDSONDES**

From 1 August through 30 September 2008, the USAF Reserve 53rd Weather Squadron (Hurricane Hunter) provided two WC-130Js for a variety of in situ measurements during TCS08 including the NCAR Global Positioning System (GPS) dropwindsonde. The NRL P-3 was also fitted with the NCAR dropwindsonde and provided an additional tool for vertical profile measurements. This dropwindsonde, which is based on GPS satellite navigation, provides wind measurements with accuracies of  $0.5\text{-}2.0\text{ m s}^{-1}$  and a vertical resolution of  $\sim 5\text{ m}$  (Hock and Franklin 1999). The USAF WC-130J and NRL P-3 flew a total 47 missions during TCS08 and launched between 10 and 30 dropsondes for each mission.

During the investigation of TCS025, the WC-130J flew three separate missions (Figure 3) from Andersen Air Base on Guam and launched an average of 30 dropwindsondes each flight. For each of the three flights, the WC-130J aircraft flew in a variety of patterns including a lawn mower, square spiral (Figure 4), and modified spiral box. Flight level was approximately 8500 m ( $\sim 350\text{ hPa}$ ) and dropwindsondes were launched in a pre-determined pattern to gain multiple vertical profiles in both east-west and north-south orientations.

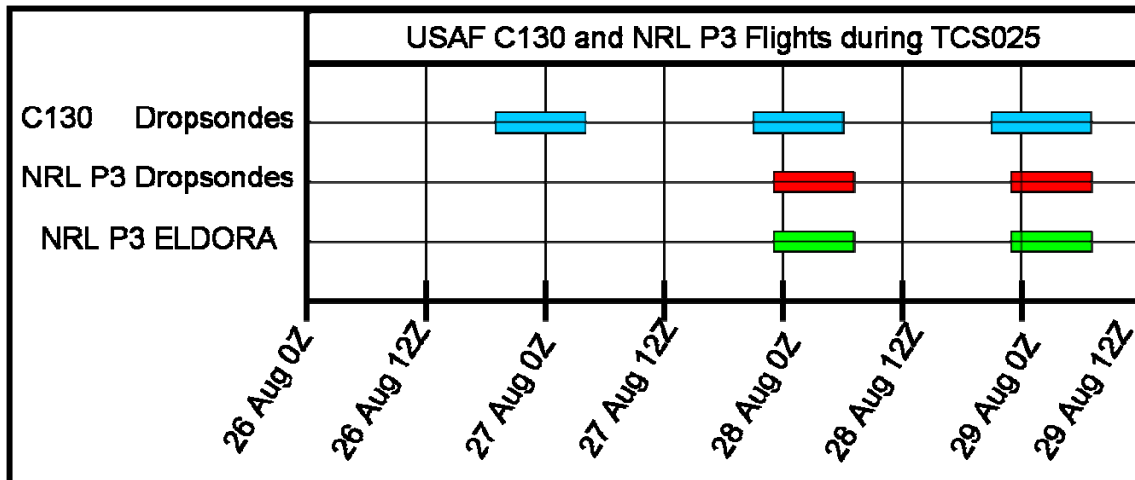


Figure 3. Timeline of USAF WC-130J and NRL P-3 missions flown on TCS025 during TCS08.

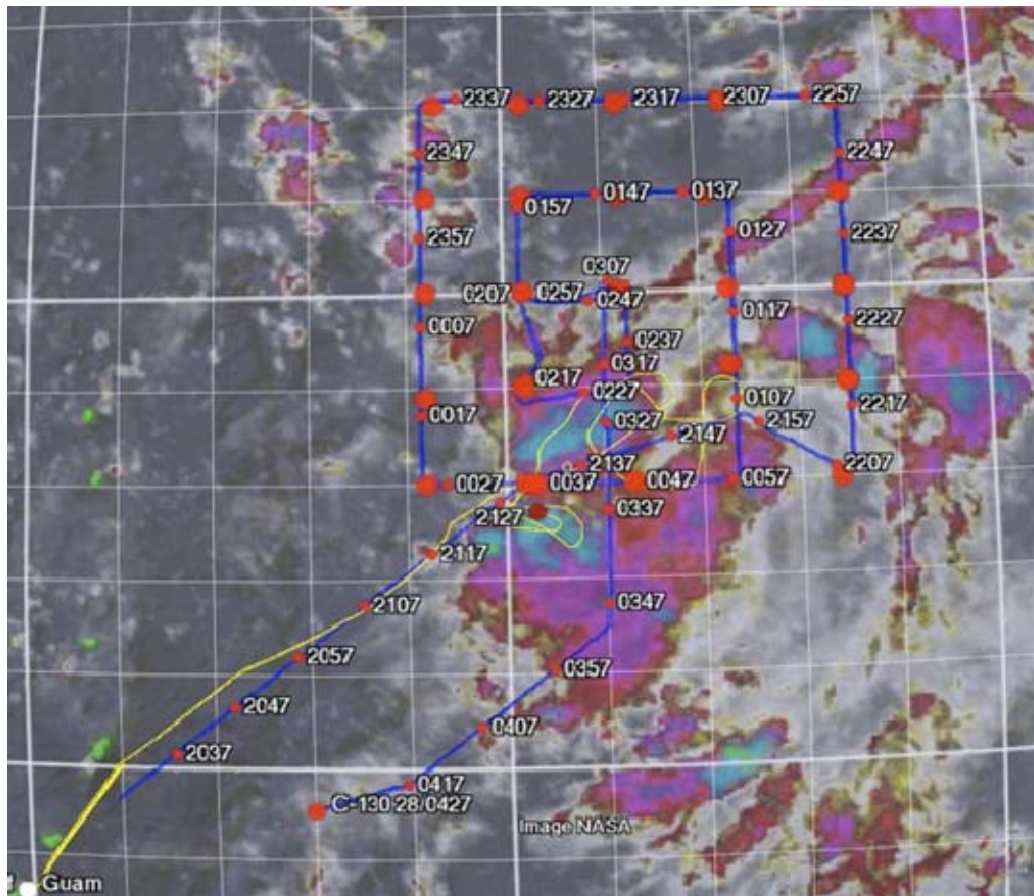


Figure 4. Flight pattern and dropwindsonde locations for the second USAF WC-130J flight of TCS025 during 1953 UTC 27 August - 0515 UTC 28 August. Yellow line is the flight path of the NRL P-3 with ELDORA.



Although the primary mission of the NRL P-3 aircraft was to collect ELDORA observations during the two flights (Figure 3) into TCS025 (RF05 and RF06), GPS dropwindsondes were also launched at pre-determined locations. To optimize ELDORA coverage, the P-3 flew at approximately 2500 m (~750 hPa) in circular patterns around small regions of deep convection (Figure 5). Because of the low altitude flight path, vertical atmospheric profiles were only available in the lower troposphere below 750 hPa. During RF05 (0030 UTC - 0630 UTC 28 August), 23 dropwindsondes were launched as the NRL P-3 circled regions of deep convection (Figure 5). During RF06 (2240 UTC 28 August - 0615 UTC 29 August), 29 dropwindsondes were launched in an elliptical pattern as the NRL P-3 circled an area of stratiform convection (Figure 6).

#### **D. ELDORA DATA**

This examination of TCS025 using ELDORA is based on two NRL P-3 flights during TCS08. The first flight (RF05) took off from Andersen Air Base in Guam at 0030 UTC (1030 local time (LT)) 28 August. At the time, TCS025 was a broad area of convection approximately 600 km northeast of Guam (Figure 5a). The flight plan was to circle some of the deep convection in multiple MCSs and search for any low-level circulation. The location of the portion of TCS025 that was flown during RF05 is identified in Figure 5a. The second flight (RF06) took off from Guam at 2240 UTC (0840 LT) 28 August 2008. The flight plan was supposed to be a square, 180 n mi on each side, around the TCS025 convection. However, the path changed to an elliptical pattern (Figure 6b) following the periphery of a large area of deep stratiform cloud bounded by deep convection (Figure 6a). The location of the portion of TCS025 that was flown during RF06 is identified in Figure 6a.

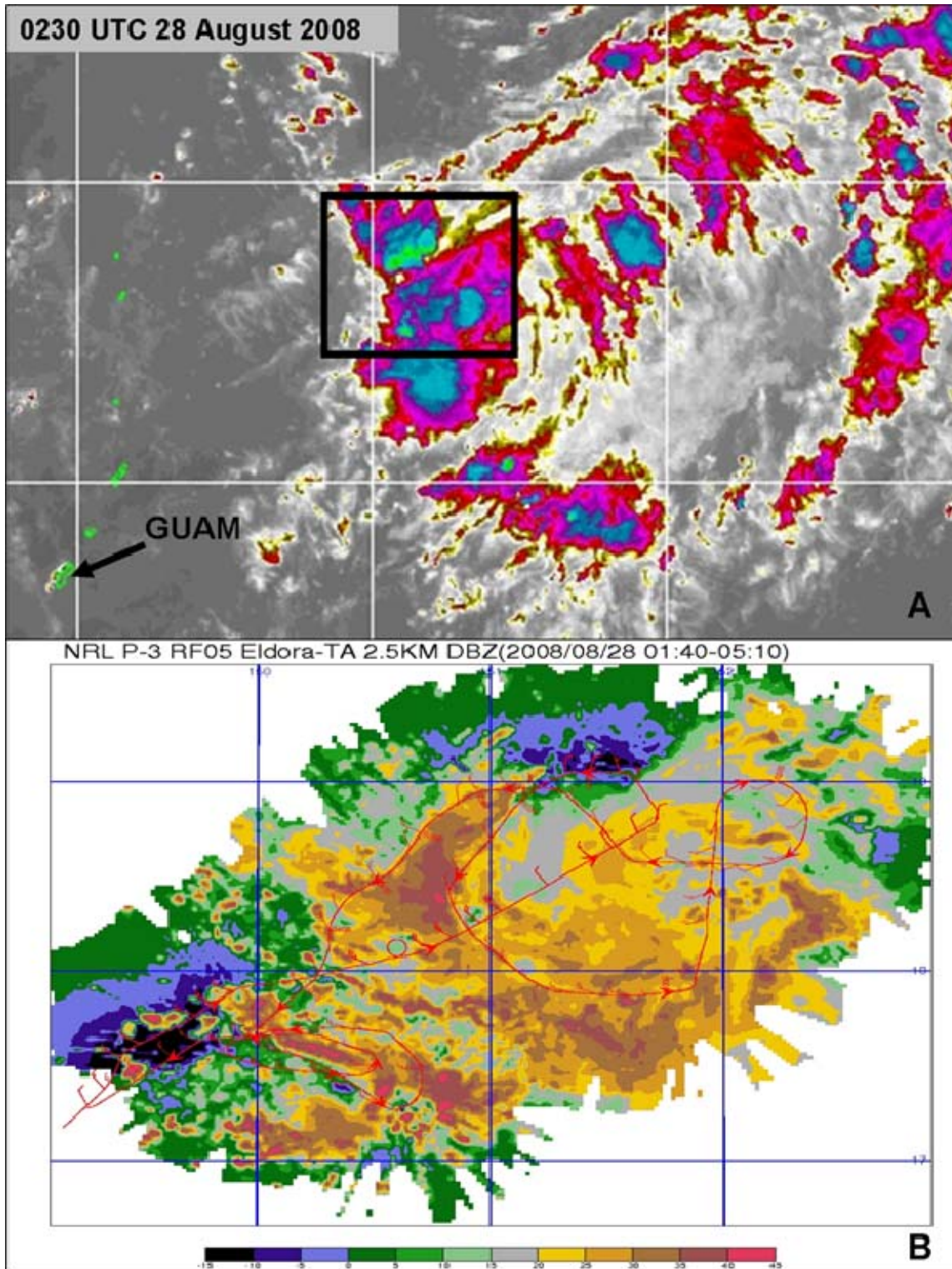


Figure 5. (a) MTSAT IR imagery of TCS025 at 0230 UTC 28 August. (b) RF05 ELDORA reflectivity and NRL P-3 flight path for portion of TCS025 indicated by the black box in (a).

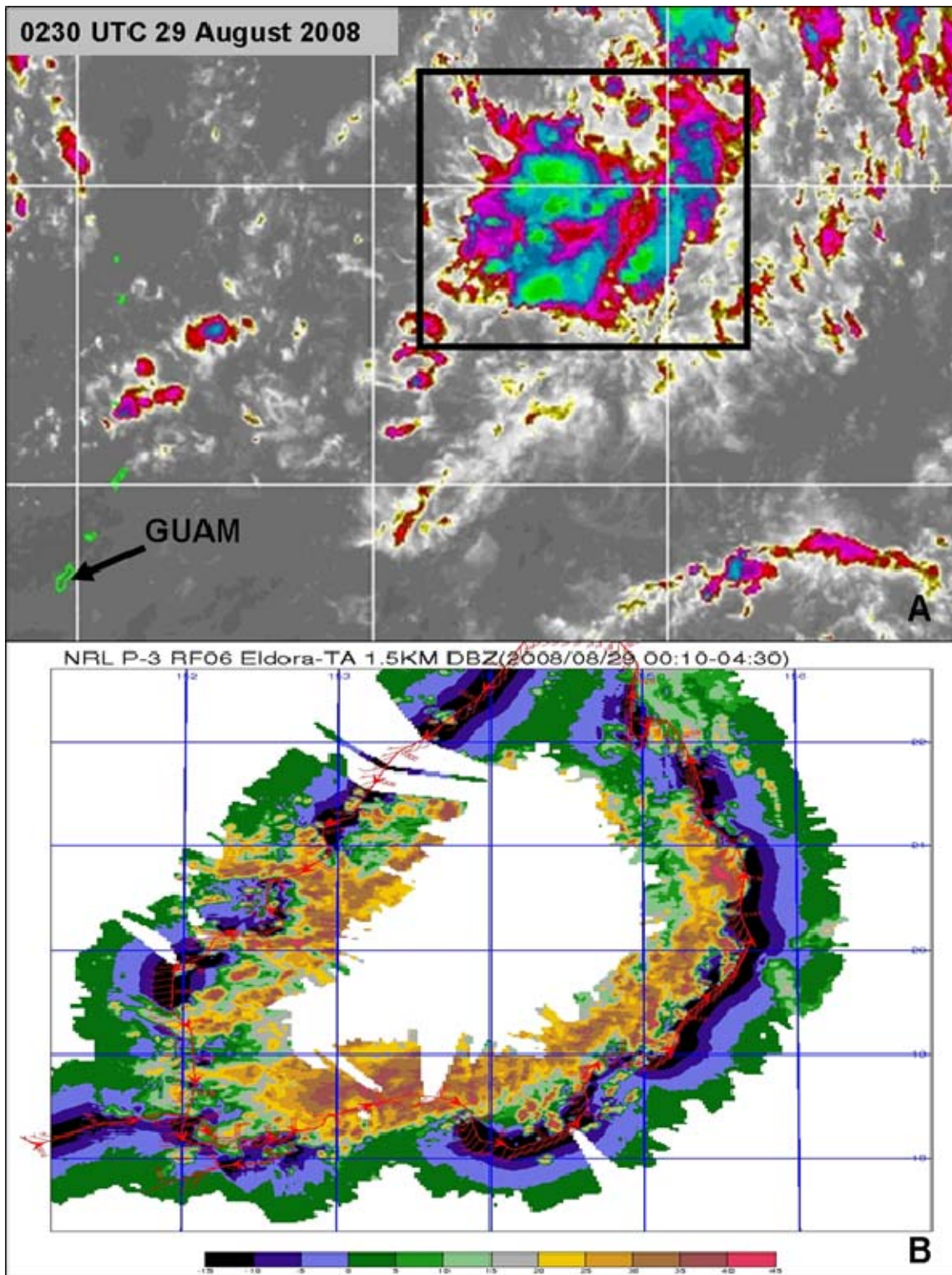


Figure 6. (a) MTSAT IR imagery of TCS025 at 0230 UTC 28 August. (b) RF05 ELDORA reflectivity and NRL P-3 flight path for portion of TCS025 indicated by the black box in (a).



The large ELDORA data sets required several processing steps for this analysis. The raw field format data, which were collected in real-time during the flight, were translated into Doppler Radar Data Exchange (DORADE) format sweep files. Correction factors (CFACs) were also included to correct for navigation issues such as aircraft tilt, drift, and ground speed. The next step was to edit the sweep files to remove ground echo, noise, clutter, and radar side-lobes. These processing steps were done through an interactive radar processing tool called Solo (NCAR/EOL 1993). Several automated algorithms were provided, which eliminated the time-consuming process of manual editing. The resulting sweep files then gave a relatively close representation of the monitored convection (Figure 7).

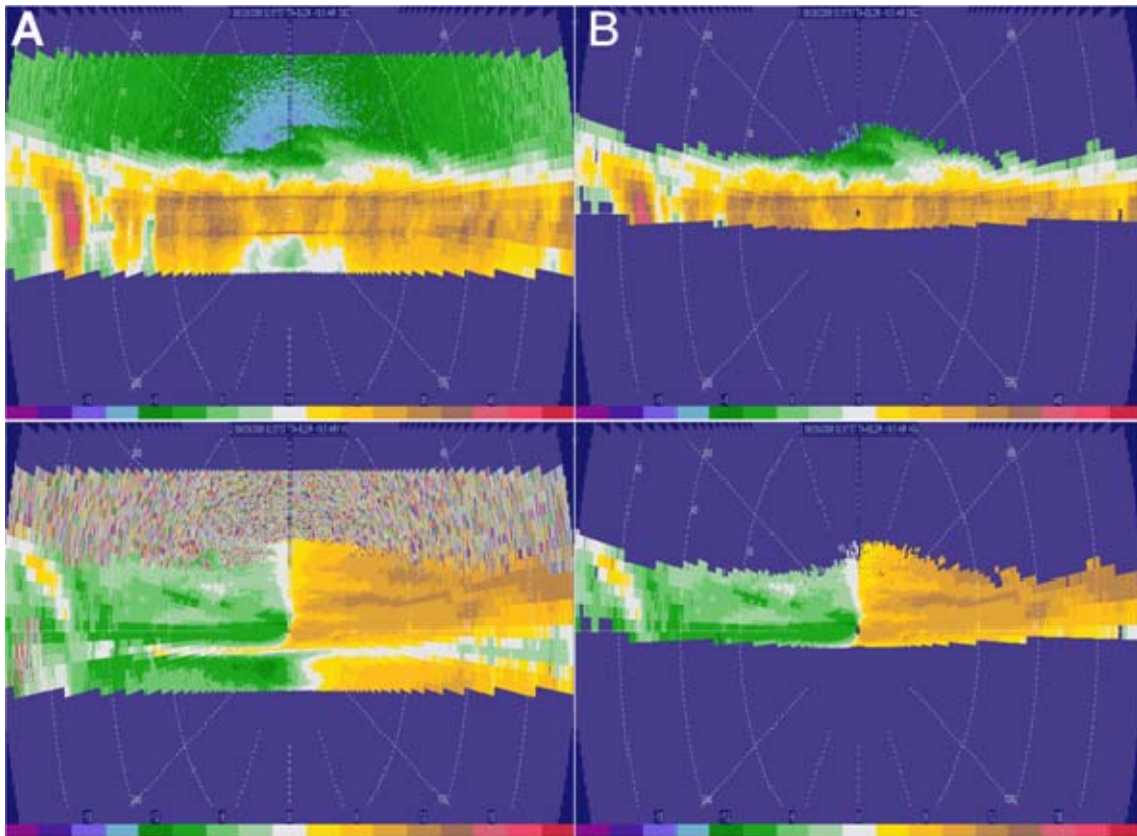


Figure 7. (a) Forward-looking raw ELDORA reflectivity (dBz) (top) and velocity over ground ( $\text{m s}^{-1}$ ) (bottom) before processing with Solo. (b) Processed reflectivity (top) and velocity over ground (bottom) using automated algorithm in Solo.

Once the sweep files had been edited, they needed to be interpolated into a gridded format. The program REORDER, developed by UCAR/NCAR, was used to transform the radar data from radar space to Cartesian space. The datasets produced were then synthesized and displayed using the Custom Editing and Display of Reduced Information in Cartesian space (CEDRIC), which was developed by UCAR/NCAR. To display the datasets in a graphical format, the CEDRIC files were converted into Grid Analysis and Display System (GrADS) format. A cursory examination of the ELDORA wind fields indicated a relatively large uncertainty in the horizontal wind components ( $u$ ,  $v$ ) during aircraft turns. Additionally, vertical velocity ( $w$ ) was not represented well due to  $w$  being calculated using the  $u$  and  $v$  components in the continuity equation. An accurate depiction of the three components of the wind vector was only evident when the flight path was straight.

Due to the tendency of large errors in the ELDORA wind fields using REORDER, another technique was employed. A program developed by John Gamache of the National Oceanographic and Aviation Administration's (NOAA) Hurricane Research Division (HRD) provided a more accurate interpolation and synthesis for ELDORA's datasets. In this technique, ELDORA reflectivity and observations are interpolated to a regularly spaced Cartesian grid (Reasor et al., 2009). The winds are then matched to ELDORA observations while satisfying several weighted constraints, including the mass continuity equation. The Gamache program allows for high resolution analysis with a minimum horizontal and vertical resolution of 500 m. This program also includes numerous calculations of useful meteorological variables such as vorticity and divergence along with radar reflectivity and a three-dimensional representation of the wind field. The output from this program was converted to GrADS format for visual analysis.

## **C. SATELLITE DATA**

Because of the limited coverage of conventional observations in the WNP, remote sensing has been the predominant tool for tracking the motion and intensity of TCs. Satellites also provide a visual tool to aid in the verification of model forecasts, detection

of low-level circulation centers (LLCCs), and the distribution of deep convection. The Multifunctional Transport Satellite (MTSAT-1R) from the Japanese Meteorological Agency was utilized as the primary remote sensing tool during TCS08/T-PARC. This geostationary satellite consists of five separate channels, including one visible and four infrared (IR), and has a resolution of one km in the visible and 4 km in the IR. For this analysis, color-enhanced images from the thermal IR channel (ch2) are utilized. This imagery is used to trace convection throughout the life of TCS025 from 24 August through 30 August. Additionally, MTSAT-1R imagery is used to identify circulations associated with the system as well as monitoring variability in convection.

THIS PAGE INTENTIONALLY LEFT BLANK

### **III. ANALYSIS**

#### **A. SYNOPTIC OVERVIEW OF TCS025**

On 24 August 2008, the broad area of convection identified in infra-red (IR) satellite imagery, approximately 600 n mi northeast of Guam between 150°E-160°E and 15°N-25°N, was designated as TCS025 (Figure 1). At the time, synoptic conditions were deemed favorable for further development as sea-surface temperatures (SST) were generally above 29° C, satellite imagery indicated a cyclonic rotation in the convection, and upper-level conditions were favorable. The TCS025 complex was monitored for signs of development for 10 days, from 24 August through 3 September. Although convection was persistent throughout the life cycle of this TCS, surface winds never exceeded minimum TD strength and a LLCC was never defined. In this analysis, MTSAT-1R IR satellite imagery and ECMWF model fields are used to describe the synoptic-scale conditions during the first week of the TCS025 life cycle.

##### **1. 24 August 2008**

When first identified on 24 August, TCS025 was an area of multiple MCSs (Figure 8a) that seemed to develop between two upper-level cyclonic circulations within the tropical upper tropospheric trough (TUTT) (Figure 8b). The area between the upper-level circulations was a region of persistent upper-level divergence (Figure 9) and enhanced upper-level equatorward outflow (Figure 8b). The deepest convection associated with TCS025 appeared near 23°N, 153°E in association with low-level convergence that was evident between 147°E-154°E (Figure 8c). Although many MCSs were present and convection appeared in satellite imagery to rotate cyclonically (Figure 8a), a LLCC could not be identified in either remotely-sensed scatterometer data or model analyses.



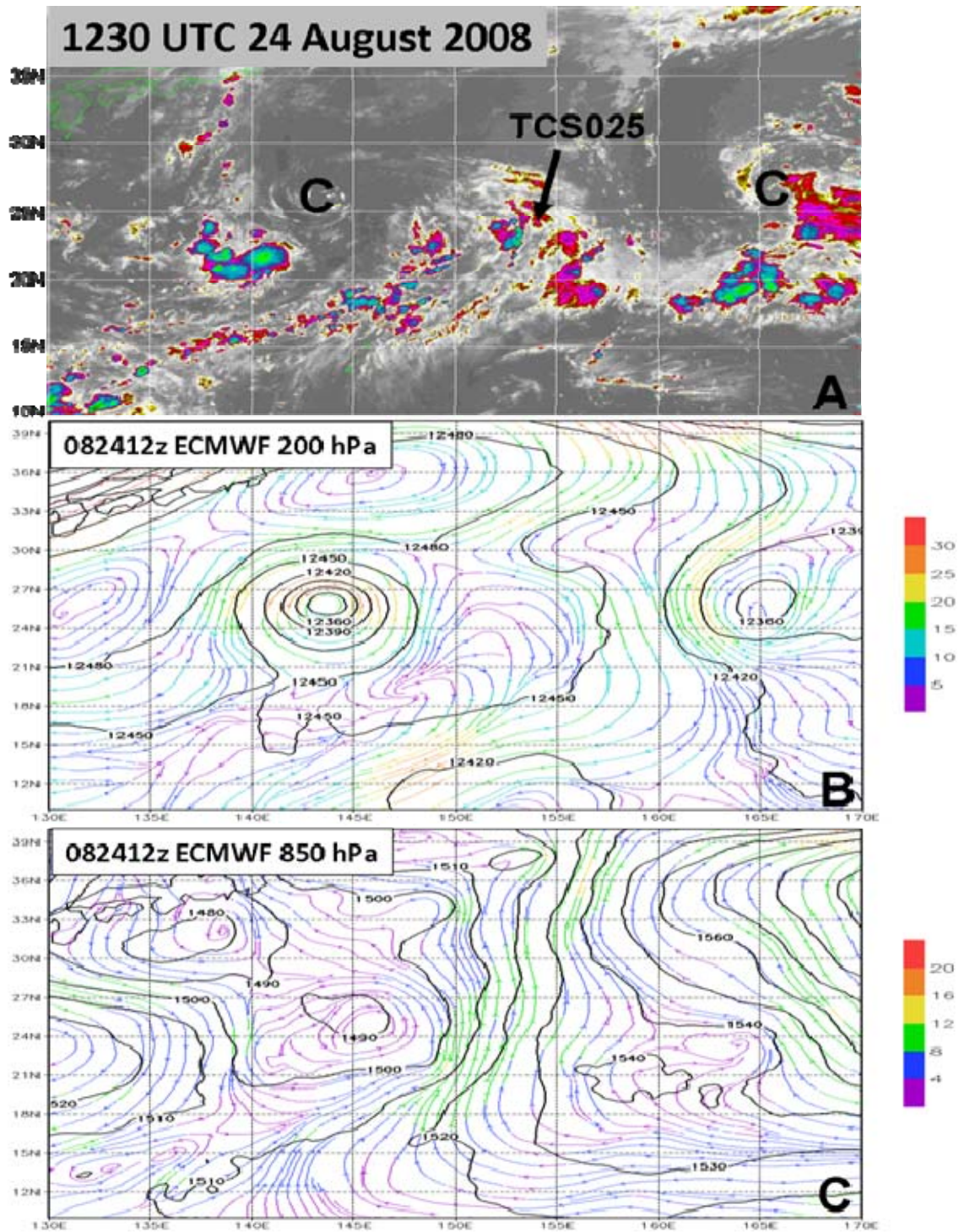


Figure 8. (a) MTSAT IR imagery at 1230 UTC 24 August 2008, and the 1200 UTC 24 August (b) ECMWF analyzed 200 hPa streamlines and geopotential (m), and (c) 850 hPa analyzed streamlines and geopotential (m). Streamline color indicates speed according to color scale on right in  $\text{m s}^{-1}$ .

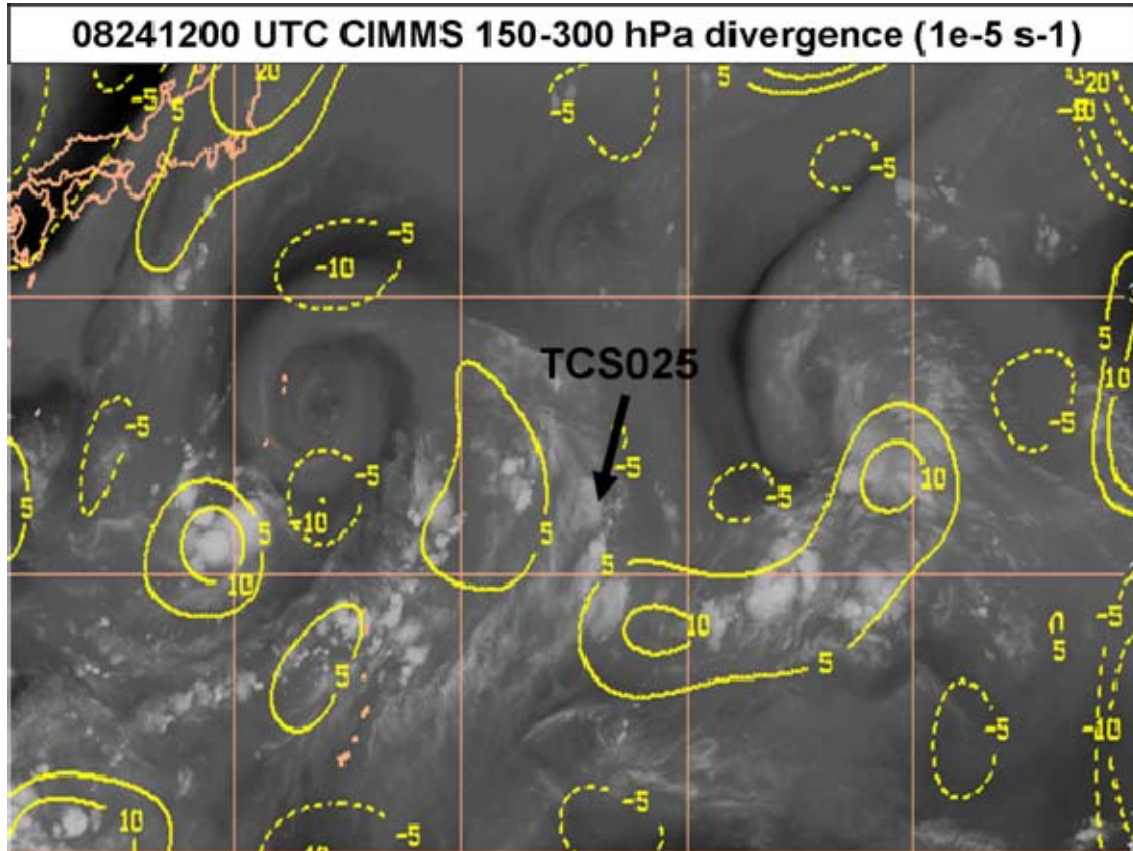


Figure 9. Upper-level divergence (contoured at  $10^{-5} \text{ s}^{-1}$ ) at 1200 UTC 24 August between 150-300 hPa superposed on MTSAT water vapor imagery.

## 2. 25 August 2008

An increase in deep convection to the south and southeast of TCS025 was identified in IR imagery at 1230 UTC 25 August (Figure 10a). By contrast, convection that had existed to the north the previous day was nearly non-existent. Convection associated with the two TUTT cells had decreased substantially but in upper-level ECMWF analysis (Figure 10b) the cells were well defined. The cell to the east of TCS025 had moved slightly to the west but did not appear to be affecting TCS025. The cell to the west of TCS025 was nearly stationary. The upper-level analysis (Figure 10b) continued to indicate relatively strong equatorward flow directly above the convection at  $21^{\circ}\text{N}$ ,  $152.5^{\circ}\text{E}$ . Low-level convergence near  $21^{\circ}\text{N}$ ,  $152.5^{\circ}\text{E}$  was weak (Figure 10c).



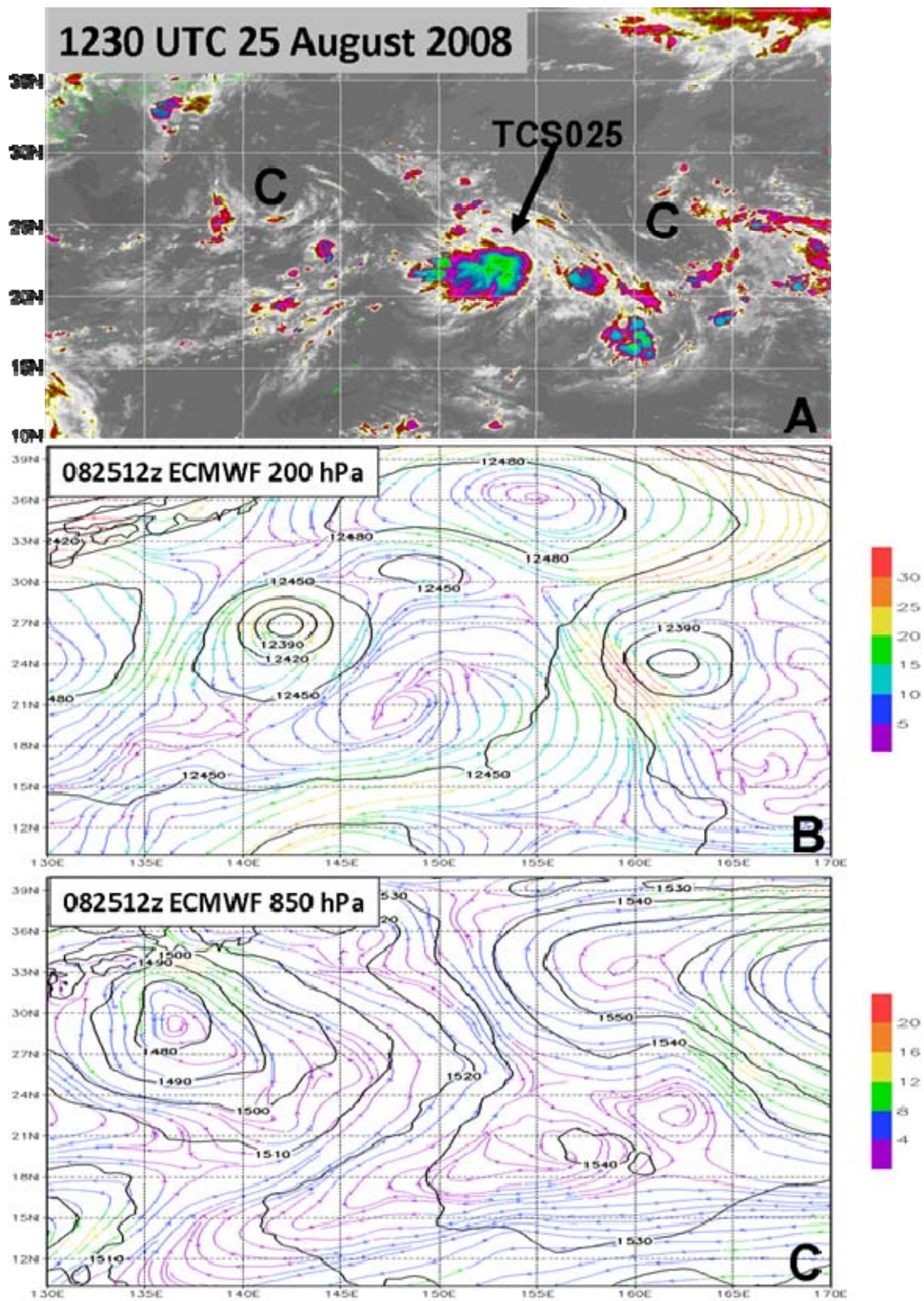


Figure 10. As in Figure 8, except MTSAT imagery at 1230 UTC 25 August and ECMWF analyses at 1200 UTC 25 August.

### 3. 26 August 2008

Strong upper-level divergence (Figure 11) and equatorward flow (Figure 12b) remained directly above TCS025 and continued to support deep convection. The upper-level cyclonic cell (Figures 12a, b) to the west of TCS025 continued to remain nearly stationary. The cell to the east of the system had moved farther to the west and the associated convection was nearly indistinguishable from convection related to TCS025. The deepest convection associated with TCS025 (Figure 12a) continued to persist to the south of the system in the form of several individual MCSs. At 850 hPa (Figure 12c), the low-level cyclonic circulations associated with the two upper-level lows were beginning to merge across the region of TCS025. A saddle point in the low-level winds existed near the region of TCS025 between 21°N-25°N and 152°E-155°E. Low-level winds were generally less than 4 m s<sup>-1</sup> and a weak convergence persisted. The first WC-130J flight for this system commenced at 2000 UTC on this day.

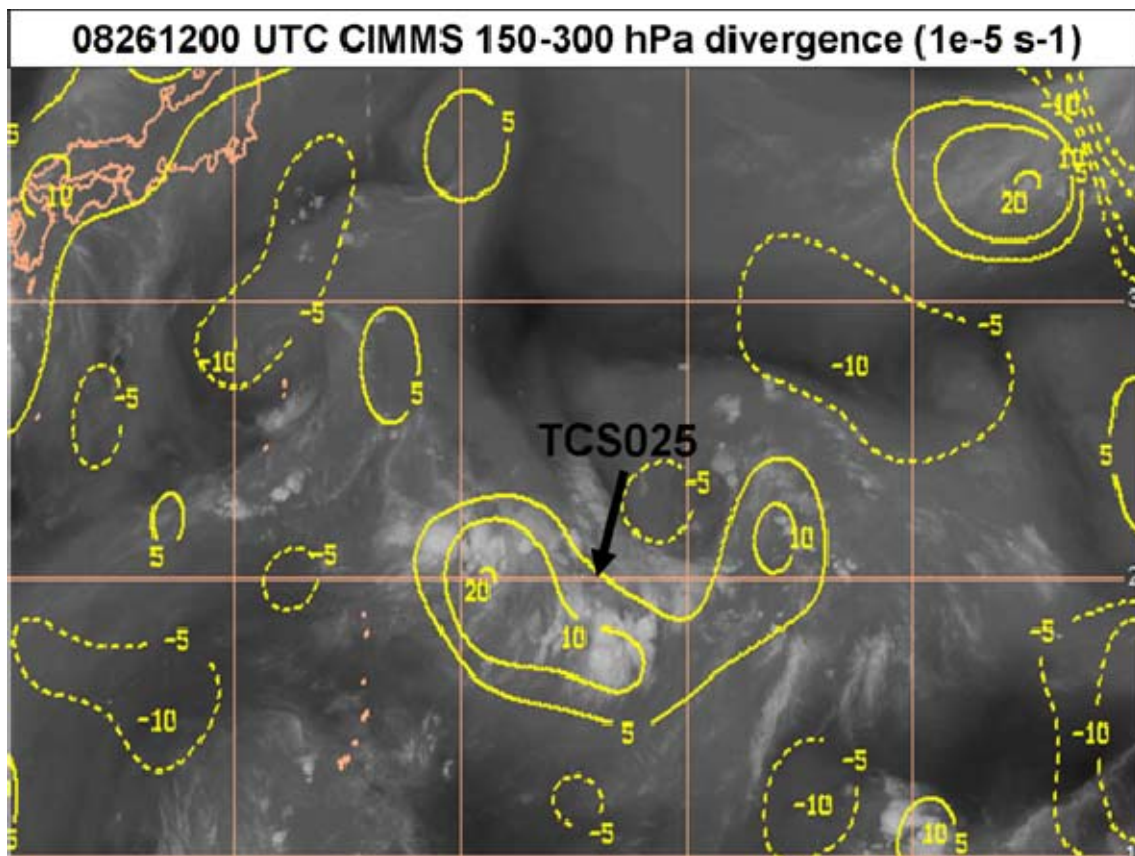


Figure 11. As in Figure 9, except at 1200 UTC 26 August 2008.



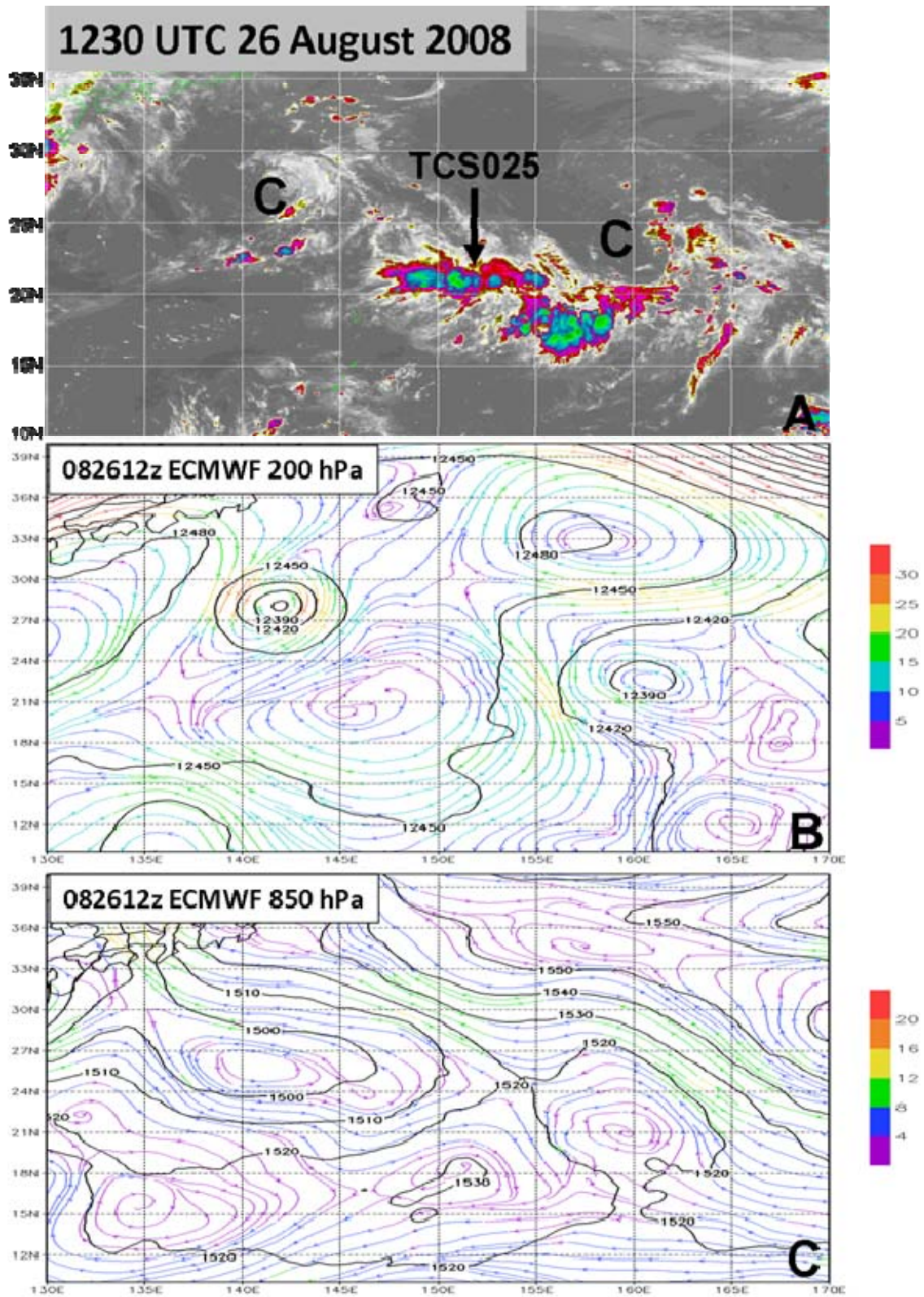


Figure 12. As in Figure 8, except MTSAT imagery at 1230 UTC 26 August and ECMWF analyses at 1200 UTC 26 August.

#### **4. 27 August 2008**

Several MCSs continued to exist along the southern portion of TCS025 (Figure 13a). The upper-level TUTT cell to the northwest of TCS025 (figure 13b) moved slowly to the north and away from the vicinity of TCS025. The primary convection of TCS025 existed along the eastern periphery of an upper-level anticyclonic circulation that was centered near 20°N, 144°E. This circulation contributed to strong equatorward outflow (Figure 13b) from the convection in TCS025. Northwesterly vertical wind shear suppressed convection from developing on the north side of the system (Figure 14). The TUTT cell to the east continued to move westward into the vicinity of TCS025 near 23°N, 157°E and contributed to the vertical wind shear (Figure 13b). Upper-level wind speeds were  $15 \text{ m s}^{-1}$  or less. Weak low-level winds were widespread (Figure 13c) and a low-level cyclonic circulation associated with the TUTT cell to the east of TCS025 had extended westward to define a cyclonic circulation associated with TCS025 near 147°E-152°E and 18°N-24°N. Throughout this four day period, TCS025 and its associated convection had remained nearly stationary.



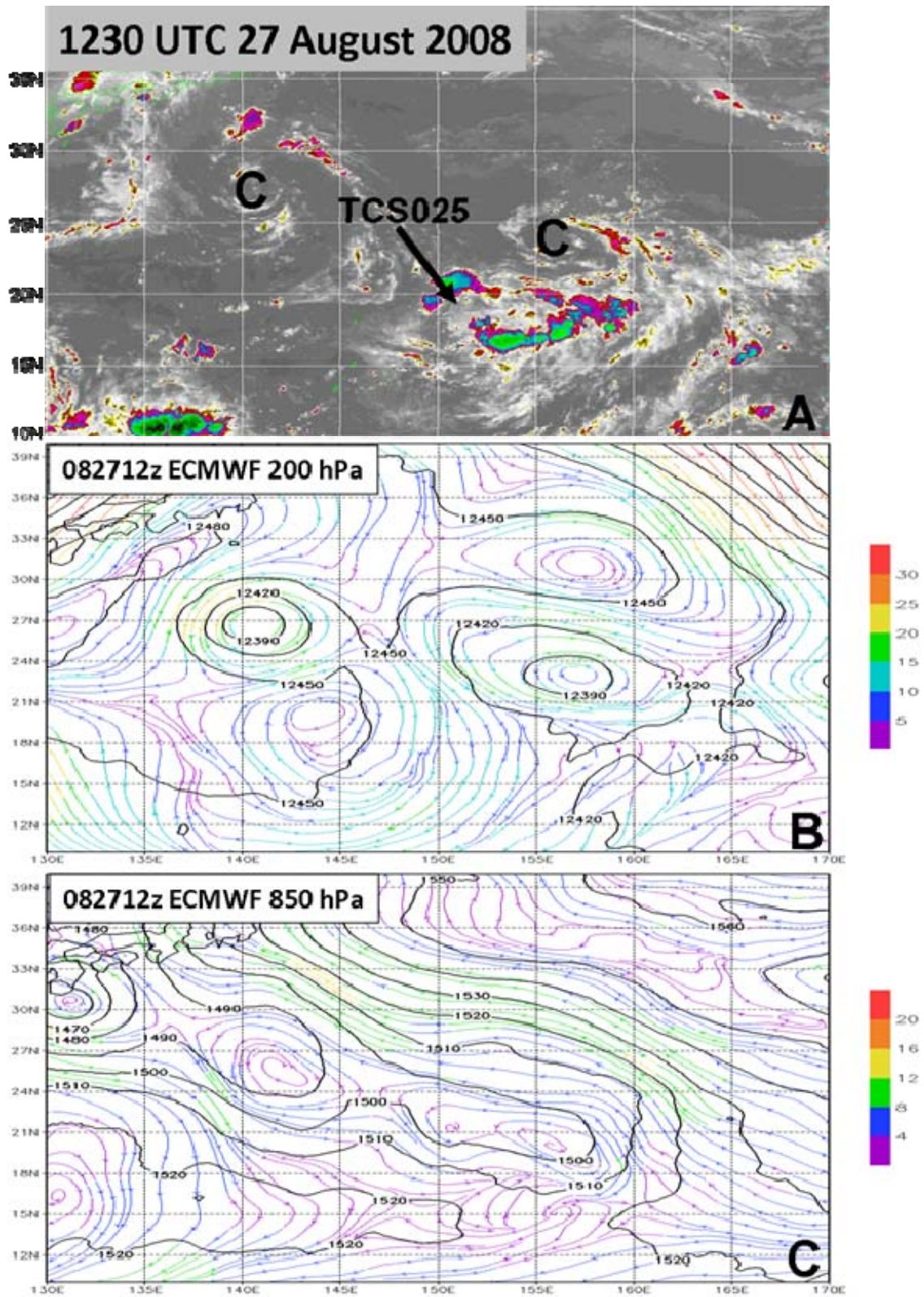


Figure 13. As in Figure 8, except MTSAT imagery at 1230 UTC 27 August and ECMWF analyses at 1200 UTC 27 August.

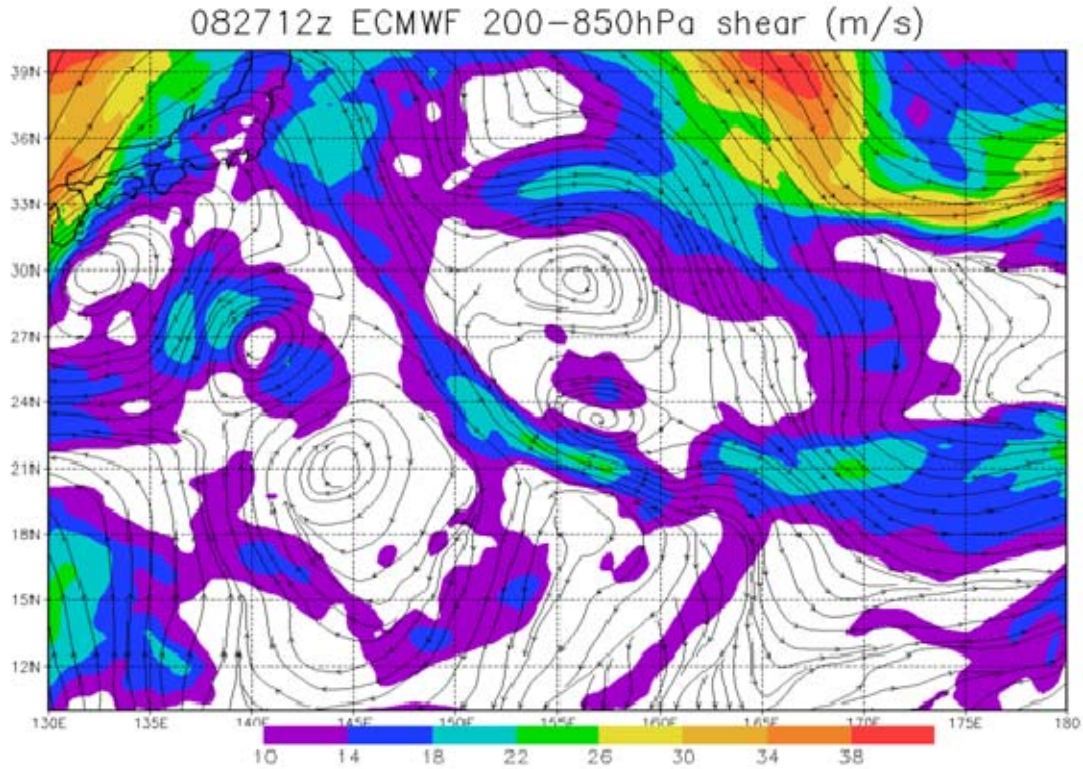


Figure 14. The analyzed 200 hPa – 850 hPa streamlines of vertical wind shear ( $\text{m s}^{-1}$ , see color bar) at 1200 UTC 27 August 2008 from the ECMWF.

## 5. 28 August 2008

By 1230 UTC 28 August 2008, convection associated with TCS025 was very weak (Figure 15a) and was being displaced southeastward under influence of the flow around the upper-level TUTT cell centered near  $25^{\circ}\text{N}$ ,  $151^{\circ}\text{E}$ . This cell had moved west and was now located directly poleward of TCS025. Strong upper-level southerly flow was present to the east of the TUTT cell and the remaining convection of TCS025 existed east of a col region near  $20^{\circ}\text{N}$ ,  $152^{\circ}\text{E}$  between two broad anticyclones. A weak low-level closed low was present near  $20^{\circ}\text{N}$ ,  $153^{\circ}\text{E}$  (Figure 15c). This low was nearly below the upper-level col defined above. However, convection was very weak near the low-level circulation except for the southeast side where low-level convergence was present near  $18^{\circ}\text{N}$ ,  $156^{\circ}\text{E}$  (Figure 15c). Low-level winds on the eastern side of TCS025 had increased from  $4\text{--}8 \text{ m s}^{-1}$  to  $8\text{--}16 \text{ m s}^{-1}$  but winds to the west and north remained weak.



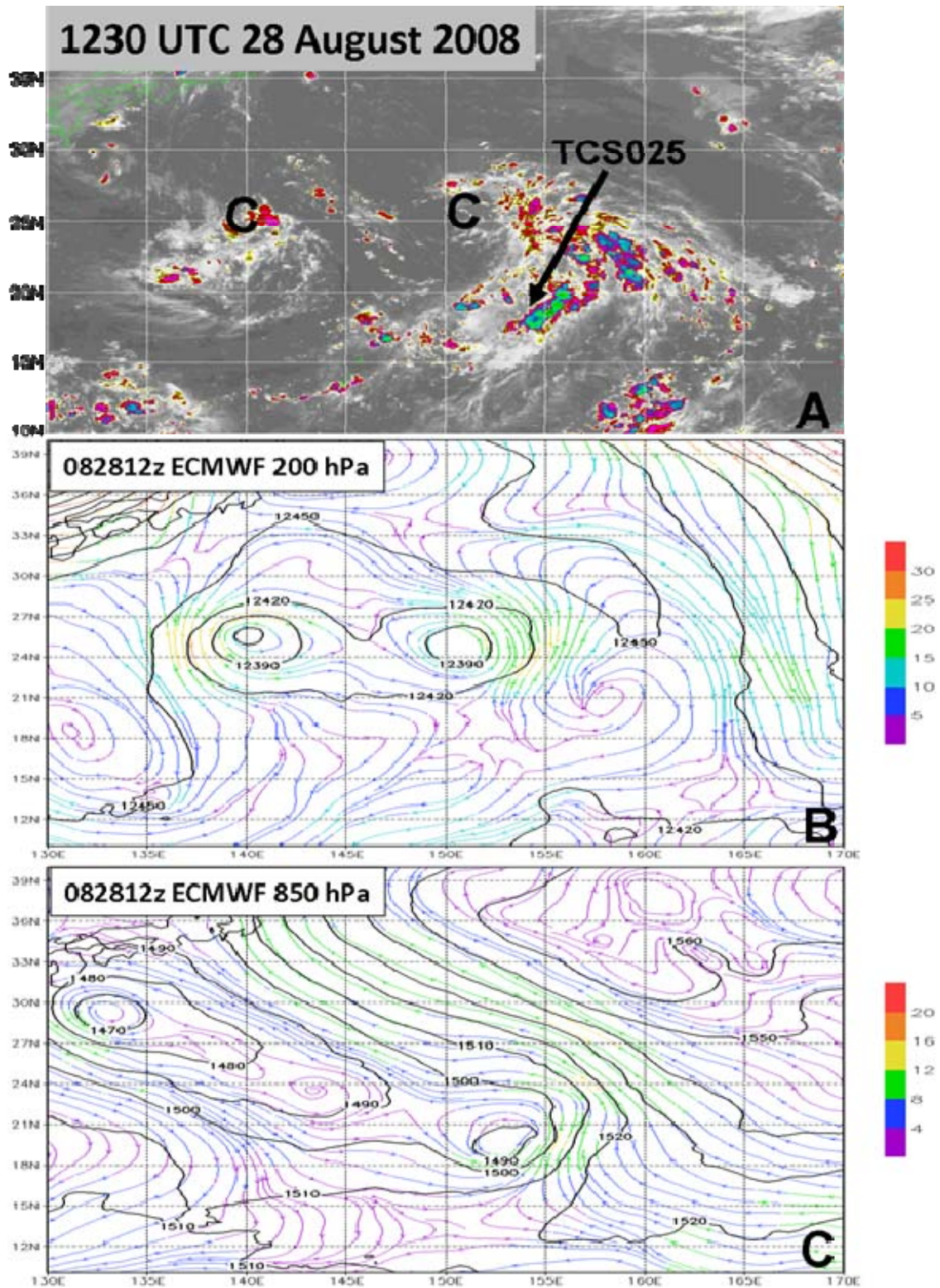


Figure 15. As in Figure 8, except MTSAT imagery at 1230 UTC 28 August and ECMWF analyses at 1200 UTC 28 August.

## **6. 29 August 2008**

By 1230 UTC 29 August 2008 (Figure 16a), deep convection was present on all sides of TCS025 except for a small portion on the western side. The upper-level TUTT cell that was directly poleward of TCS025 the previous day had progressed to the northwest and had weakened considerably (Figure 16b). The upper-level cyclonic circulation had been replaced by a broad area of anticyclonic flow that extended from 140°E to 160°E and from 10°N to 35°N. The low-level closed low was still present but had filled slightly (Figure 16c) and moved north-northwestward to be centered near 25°N, 152°E. Low-level winds to the east of TCS025 continued to be strong and southerly while winds to the southwest and west remained weak. The strongest low-level convergence (Figure 17) was found on the eastern side of TCS025 and was responsible for the increase in deep convection (Figure 16a). Satellite imagery and model predictions on this day presented the strongest case for TCS development as a low-level cyclonic circulation was associated with upper-level anticyclonic flow and convection appeared to be forming into cyclonic bands. However, low-level convergence was weak except for the eastern side of TCS025 and vertical wind shear from the north had increased dramatically on the eastern side (Figure 18).



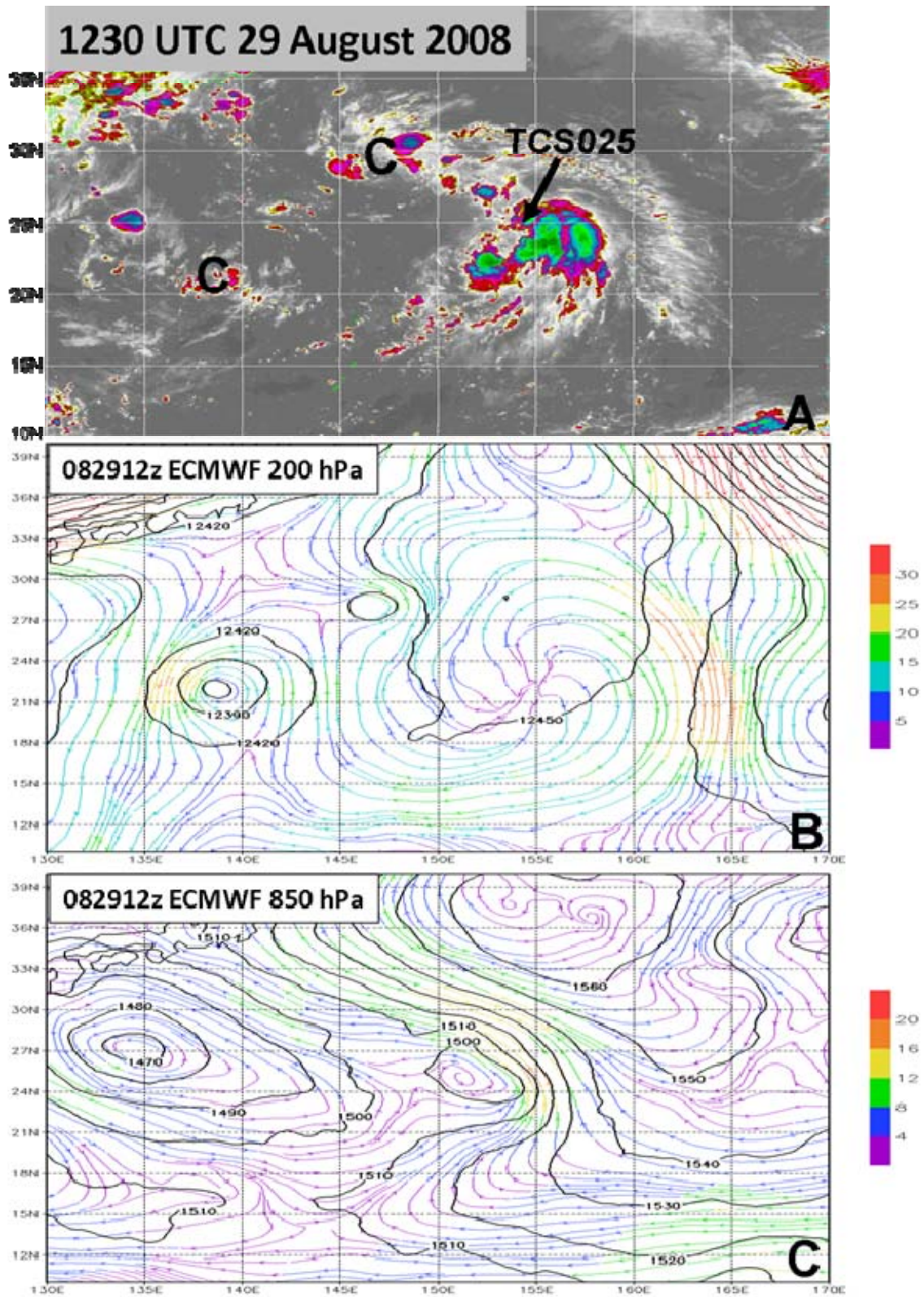


Figure 16. As in Figure 8, except MTSAT imagery at 1230 UTC 29 August and ECMWF analyses at 1200 UTC 29 August.



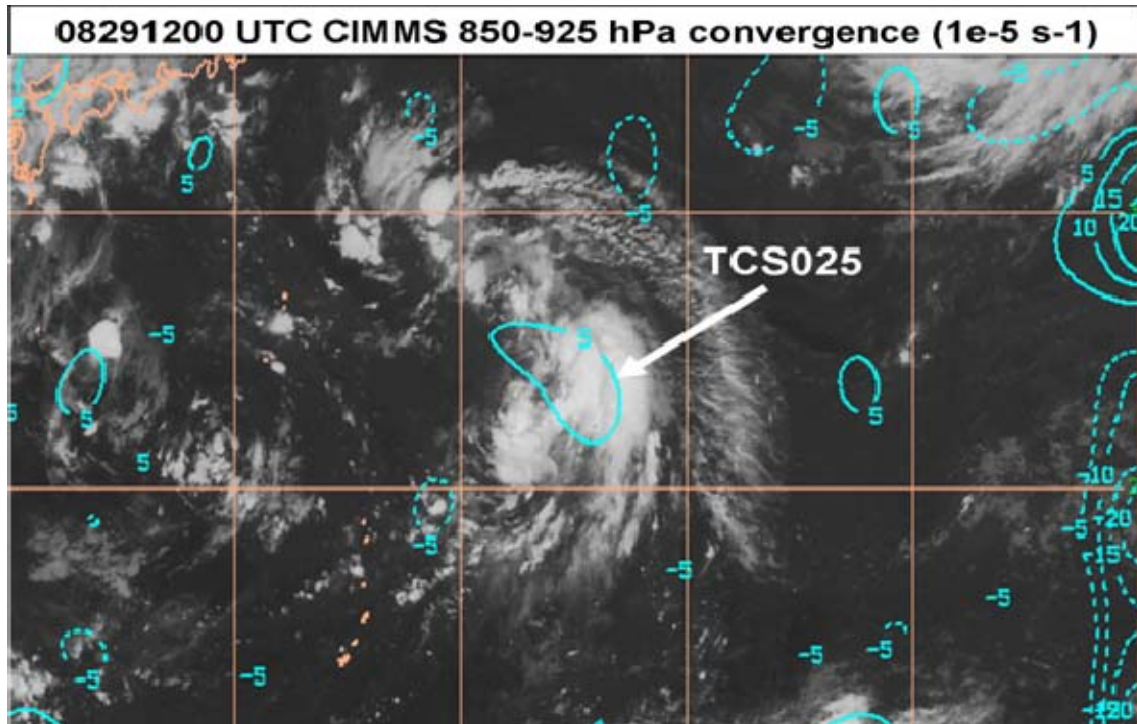


Figure 17. Convergence between 850-925 hPa (contoured units of  $10^{-5} \text{ s}^{-1}$ ) at 1200 UTC 29 August 2008 superimposed on MTSAT-IR imagery.

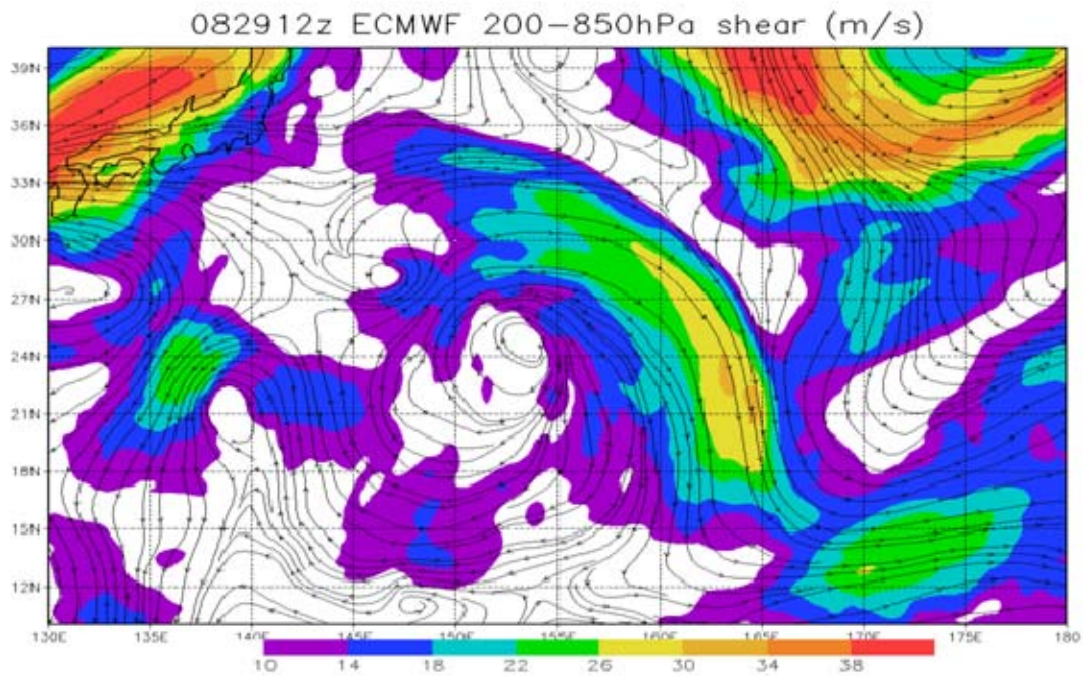


Figure 18. The analyzed 200 hPa – 850 hPa streamlines of vertical wind shear ( $\text{m s}^{-1}$ , see color bar) at 1200 UTC 29 August 2008 from the ECMWF.

## **7. Synoptic Summary**

Dominant synoptic features during the early stages of TCS025 included two upper-level cyclonic circulations associated with the TUTT. These features propagated very slowly and contributed to the formation of TCS025 in a region of upper-level divergence that existed between the two circulations. Convection associated with TCS025 was persistent but fluctuated in intensity and location relative to the broad circulation of TCS025. Upper-level winds seemed favorable for further development in the sense that anticyclonic flow dominated the region, especially during the period of strongest convection. However, upper-level winds were weak with the exception of 28 and 29 August. Fluctuations in low-level convergence were most likely the cause of the variability in convection intensity. Low-level convergence was weak except for 28 and 29 August when convection appeared to be the most intense and organized. Whereas a low-level closed low did develop, it did not persist for TCS025 to be upgraded to TD status. This LLCC was only apparent for the two days of 28 and 29 August and then quickly filled. Aircraft investigations of the system ended on 29 August. By 30 August, MCSs associated with TCS025 remained but did not show any signs of organization. For the next four days, convection continued to blow up and die down but further development never occurred. On 3 September 2008, TCS08 scientists eliminated TCS025 from further investigation.

### **B. MESOSCALE CONVECTION ANALYSIS**

From the analysis of the synoptic-scale characteristics associated with TCS025, it is clear that variability in MCS activity played an important role in the evolution of TCS025. One of the primary tools for identifying mesoscale features, including MCSs, is an examination of the MTSAT-1R infra-red satellite imagery. This color-enhanced imagery can be used to detect and trace individual MCSs from inception to dissipation. Besides MCSs and other mesoscale features such as upper-level outflow, deep convection and the overall general circulation may be inferred. In particular, the characteristics of MCS development during the times of aircraft missions are examined.

Infra-red imagery is used to describe the pre-flight environment in terms of convection. Although MTSAT 1R imagery was available every 30 minutes during TCS025, a two-hour resolution is used from the pre-flight time of 0930 UTC 25 August through 0730 UTC 29 August, which coincided with the final WC-130J and NRL P-3 flights. In the figures 20-23, the intervals of 0930 UTC to 0730 UTC on the following day are chosen to incorporate the flight times within each figure.

#### **1. MTSAT-1R Imagery 0930 UTC 25 August – 0730 UTC 26 August**

The MTSAT-1R imagery at 0930 UTC 25 August indicated a relatively large MCS at 22°N, 152°E that is identified by the circle in the first panel of Figure 19. This MCS is labeled MCS-A as it is the first in a sequence that was initiated in the same region. Although convection was deep, it appeared to be unorganized. The deepest and most uniform convection associated with the larger MCS-A occurred at 1130 UTC. By 1330 UTC, MCS-A convection began to decay and MCS-B (identified by the box in Figure 19) started to develop. Convection in MCS-B was strongest at 1530 UTC but also dissipated such that by 2330 UTC, MCS-B had disappeared. By 0330 UTC 26 August, another round of activity (MCS-C ) was developing to the north near 24°N, 153°E. This new MCS-C strengthened rapidly in roughly the same location that the MCS-A and MCS-B had developed. By 0530 UTC 26 August, convection associated with TCS025 and convection associated with an upper-level low to the northeast appeared to merge as there was no discernable separation in the cloud structure.



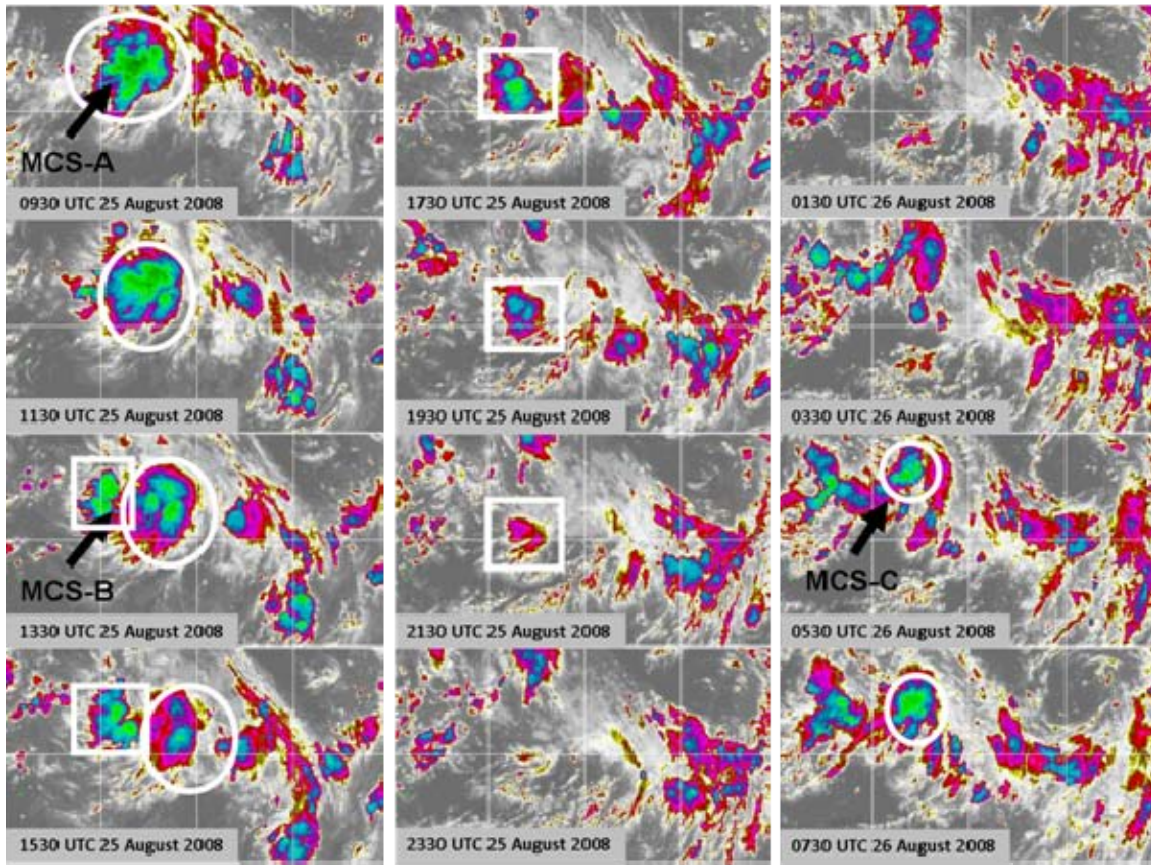


Figure 19. MTSAT infra-red imagery each 2 h between 0930 UTC 25 August and 0730 UTC 26 August. In each image, the center latitude is 20°N and the longitudinal domain is 145°E to 165°E in 5° increments.

## 2. MTSAT-1R Imagery 0930 UTC 26 August – 0730 UTC 27 August

By 0930 UTC 26 August 2008 (Figure 20), TCS025 consisted of multiple MCSs, although MCS-C and the newly formed MCS-D (identified by the box in the 0930 UTC 26 August panel of Figure 20) were the dominant features. The upper-level low to the northeast had propagated slightly to the west as a closed cyclonic circulation and its associated convection on the southern side is evident in the imagery. By 1330 UTC 26 August, deep convection developed to the southeast of MCS-C near 17°N, 160°E. This group of MCSs continued to move to the south away from TCS025. After the deep convection in this cluster had diminished, all that remained was a line of cyclonically curved stratiform clouds and weak convection, as is evident in the imagery for 0130 UTC 27 August (Figure 20). During this period, MCS-C that had developed to the north and

was near 23°N, 153°E at 0930 UTC 26 August moved slightly southward but dissipated as had MCS-A and MCS-B earlier.

As MCS-C moved southward, MCS-D developed (0930 UTC 26 August) along the northern periphery of TCS025 and drifted south-southeastward. A fifth MCS (MCS-E) was initiated near 21°N, 150°E at 1730 UTC (identified with a circle in Figure 20). Convection in MCS-E was strongest at 2130 UTC 26 August but then weakened as MCS-D had previously. By 0130 UTC August 27, MCS-F (identified by the box in Figure 20) started to develop. However, this MCS was not as strong as the previous MCSs and MCS-F also dissipated as it progressed southward.

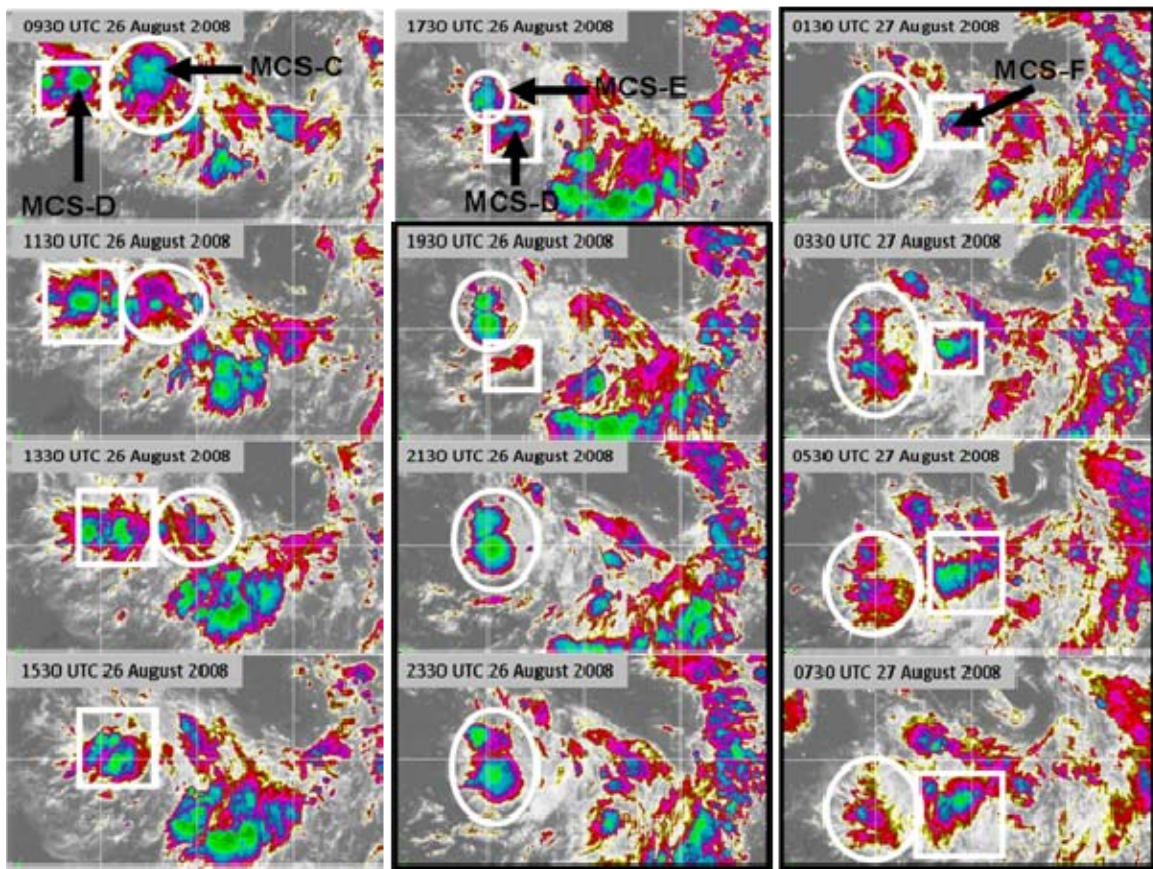


Figure 20. MTSAT infra-red imagery each 2 h between 0930 UTC 26 August and 0730 UTC 27 August. In each image, the center latitude is 20°N and the longitudinal domain is 145°E to 165°E in 5° increments. The panels outlined in black indicate the period of a NRL P-3 with ELDORA mission.



### **3. MTSAT-1R Imagery 0930 UTC 27 August – 0730 UTC 28 August**

Convection around TCS025 had weakened and became unorganized with most of the deep convective cells to the southeast (Figure 21). At 1130 UTC 27 August, MCS-G (identified by the circle in Figure 21) began to form near 22°N, 152°E, which is nearly the same location as the previous MCSs had developed. This MCS intensified rapidly over the next few hours with the strongest convection at 1530 UTC 27 August. After this time period, MCS-G slowly progressed southward and slowly dissipated. By 0130 UTC 28 August, most of the deep convection in MCS-G had subsided. This MCS was the first to be examined using ELDORA.

The NRL P-3 mission time is represented by the black outline of frames in Figure 21. The small black circle in the 0330 UTC 28 August panel is the approximate location of a mid-level circulation identified by the ELDORA data and dropwindsondes. A more in-depth examination of this circulation will be presented later.

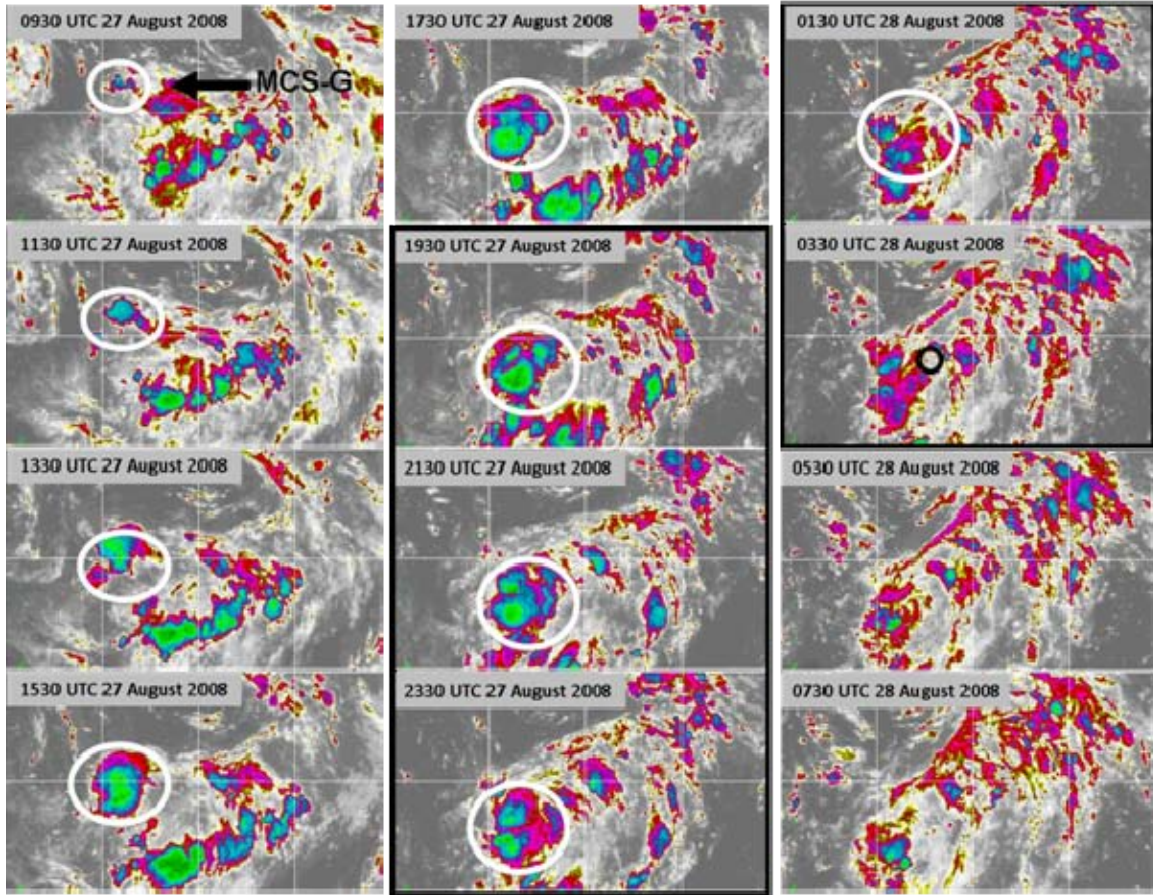


Figure 21. MTSAT infra-red imagery each 2 h between 0930 UTC 27 August and 0730 UTC 28 August. In each image, the center latitude is 20°N and the longitudinal domain is 145°E to 165°E in 5° increments. The panels outlined in black indicate the period of a WC-130J and NRL P-3 with ELDORA mission.

#### 4. MTSAT-1R Imagery 0930 UTC 28 August – 0730 UTC 29 August

By 0930 UTC 28 August 2008 (Figure 22), MCS-G continued to progress southward and, by 1130, UTC had diminished considerably (Figure 22). Several MCSs were present to the southeast and northeast of TCS025. By 1730 UTC 28 August, several smaller MCS near 20°N, 153°E merged to form a large individual MCS (MCS-H identified by the white box in Figure 22). This MCS formed just to the east of the origin location of the previous MCSs (MCSs A-G). Deep convection formed rapidly and appeared to be strongest at 1930 UTC 28 August centered near 18°N, 154°E. By 2330 UTC 28 August, MCS-H convection had diminished slightly but remained well formed.

Through the next few hours, MCS-H morphed into several small but deep convective cells within a broad area of weaker convection (Figure 22). By 0730 UTC 29 August, the remnants of MCS-H were nearly indistinguishable from the broad convection associated with TCS025.

The final WC-130J and NRL P-3 with ELDORA investigation of TCS025 was conducted on 29 August 2008. The WC-130J and NRL P-3 mission time is outlined by the black boxes in Figure 23. The small black circle indicates the approximate position of the mid-level cyclonic circulation center defined by ELDORA data and dropwindsondes. A more in-depth examination of this circulation will be presented later.

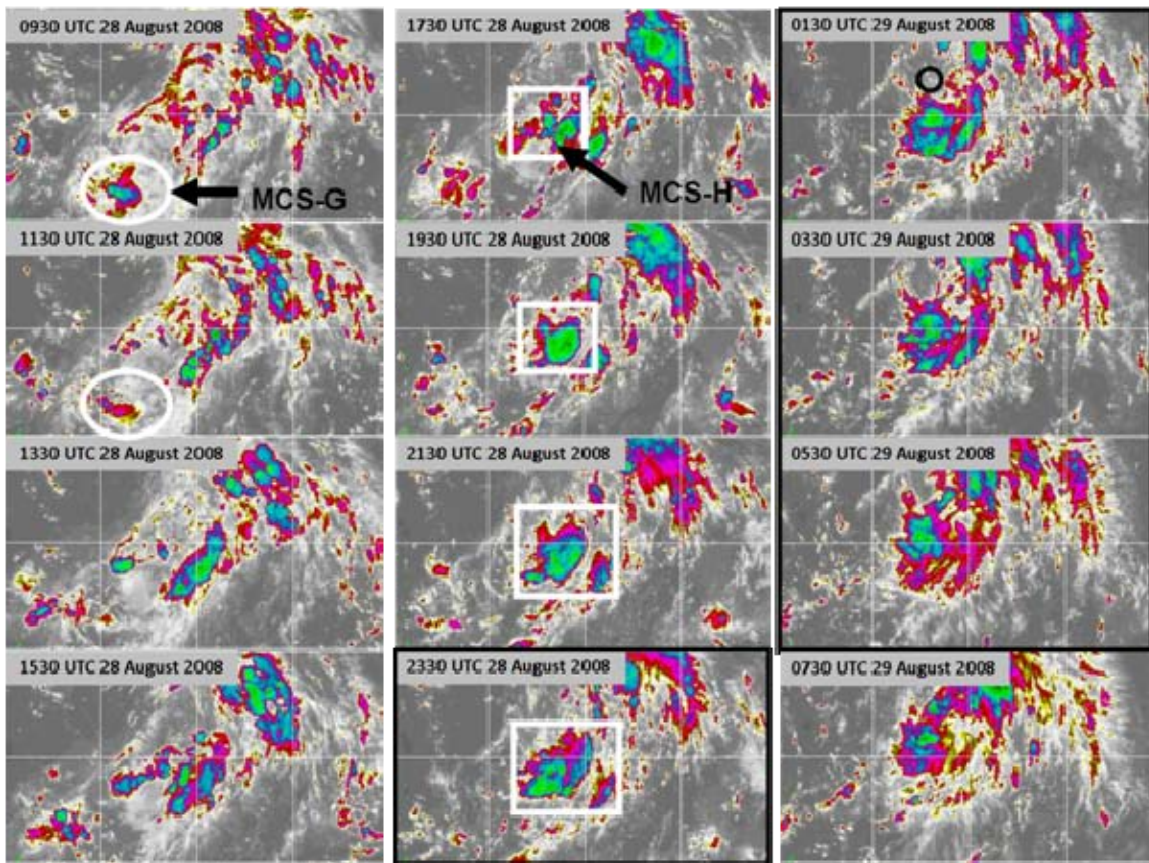


Figure 22. MTSAT infra-red imagery each 2 h between 0930 UTC 28 August and 0730 UTC 29 August. In each image, the center latitude is 20°N and the longitudinal domain is 145°E to 165°E in 5° increments. The panels outlined in black indicate the period of a WC-130J and NRL P-3 with ELDORA mission.

## **C. AIRCRAFT DROPWINDSONDE ANALYSIS**

Remote sensing of a TCS is a valuable tool for identifying mesoscale features such as deep convection and individual MCSs. Although geostationary satellite observations are available at regular time intervals, it only provides a two-dimensional view of the entire TCS region. While microwave imagery from polar-orbiting satellites may provide a more in-depth view of the structure of the convection in a TCS, it is only available when a polar-orbiting satellite passes overhead.

Aircraft can be a very useful platform for providing a detailed and comprehensive three-dimensional analysis of a TCS. During TCS08, dropwindsondes launched from the USAF WC-130J and the NRL P-3 provided vertical profiles of the environment in the vicinity of numerous TCSs. The multiple MCSs, widespread convection, and anticipated further development of TCS025 made it an ideal target for aircraft missions. Three WC-130J missions during 26-29 August and two NRL P-3 missions on 28 and 29 August were flown in TCS025. Dropwindsonde and ELDORA observations provided a detailed three-dimensional picture of the TCS025 environment as well as several MCSs.

### **1. USAF WC-130J Dropwindsondes 26–27 August**

At 0930 UTC 26 August 2008, TCS025 was made up of several MCS including MCS-C and MCS-D (Figure 20). These MCSs appeared to be well organized and TCS025 showed promise for further development so the decision was made by TCS08/T-PARC scientists to conduct the first WC-130J mission to investigate TCS025. The WC-130J took off from Guam at approximately 1800 UTC 26 August and sampled the region with dropwindsondes until 0730 UTC 27 August (Figure 23). During this flight, especially around 2130 UTC 26 August (Figure 20), the deepest convection associated with MCS-E was located in the center of the MCS. By 0130 UTC 27 August, this MCS was weakening and became less organized (Figure 20). A new, smaller MCS (MCS-F) appeared on the eastern side of TCS025, and by 0730 UTC 27 August had formed into a large MCS (Figure 20). At this time, convection was present on three sides of TCS025 but was strongest to the southeast where MCS-F had expanded southward into a line of several MCSs that were propagating to the southeast.



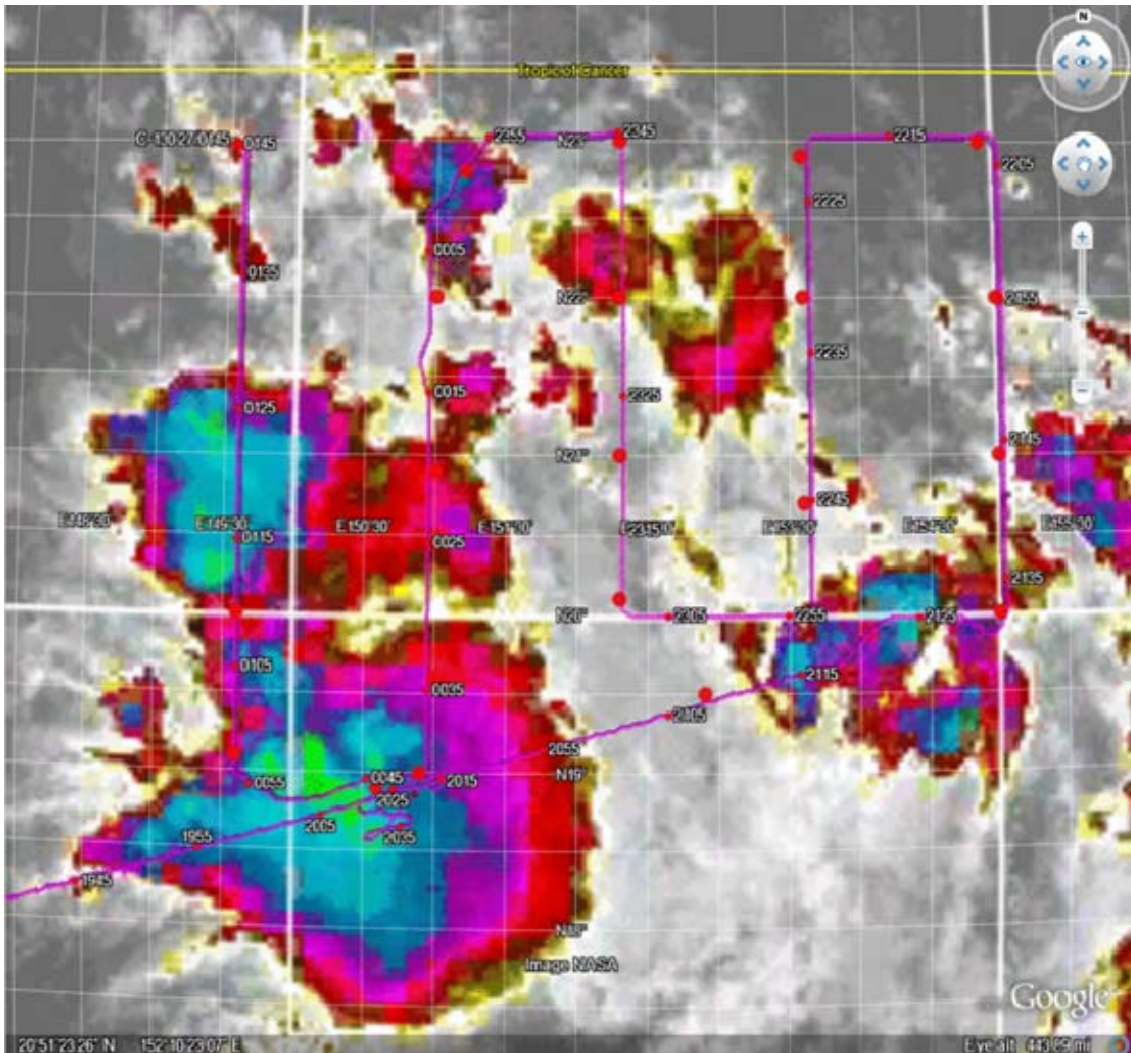


Figure 23. The WC-130J flight track between 1800 UTC 26 August – 0730 UTC 27 August 2008 displayed on the MTSAT enhanced IR imagery at 0130 UTC 27 August 2008. Circles identify approximate locations of dropwindsonde launches.

The USAF WC-130J flew a modified lawn mower pattern through TCS025 at approximately 300 hPa and launched dropwindsondes approximately every 10 minutes (Figure 23). This pattern and dropwindsonde launch locations provided a three-dimensional profile of the environment that included MCS-E and MCS-F (Figure 20). Although the horizontal winds at 950 hPa did not define an organized low-level circulation (Figure 24a), the 850 hPa winds were somewhat more organized as there appeared to be two regions of cyclonic turning of the winds. One was centered at 21°N, 150°E and was associated with MCS-E. The other region of cyclonic wind was centered

to the east of 155°E (Figure 24b). Winds at 700 hPa (Figure 24c) and 500 hPa (Figure 24d) were more uniform and generally out of the north to define the western portion of the upper-level cyclonic circulation east of TCS025 that was discussed above (Figure 24). Therefore, the horizontal distribution of winds seemed to define a broad upper-level cyclonic circulation that extended down to 700 hPa. At 850 hPa, the broad cyclonic circulation was identified along the eastern end of the flight area as a weak 850 hPa cyclonic circulation existed to the west in MCS-E. At low levels, only weak disorganized flow was observed.

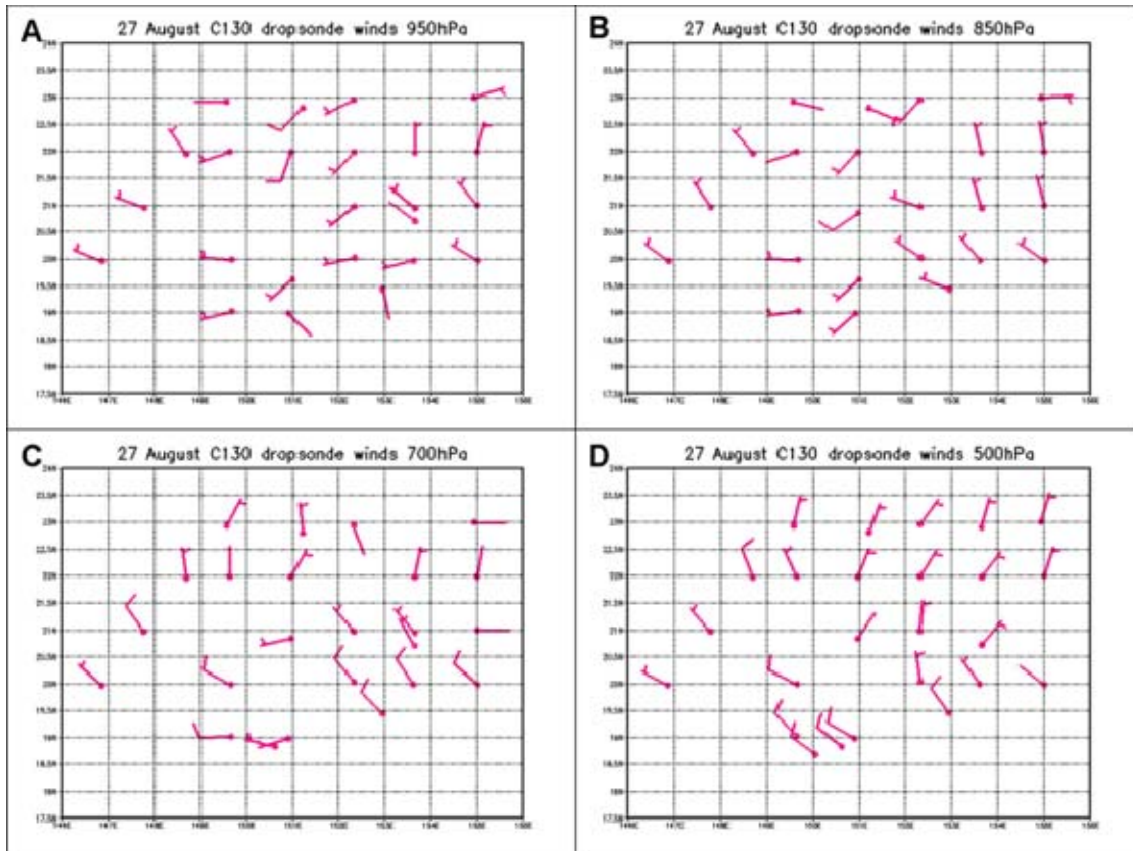


Figure 24. Dropwindsonde winds for WC-130J flight 1800 UTC 26 August - 0730 UTC 27 August at (a) 950 hPa, (b) 850 hPa, (c) 700 hPa, and (d) 500 hPa.

A vertical cross-section along approximately 20°N from 150°E to 155°E (Figure 25a) identifies very moist low-level flow (Figure 25b) to the east of the deep convection (Drop location C4) and moist mid-levels in the convection (Drop locations A3 and B4). Horizontal winds are generally out of the northwest at all levels above 850 hPa, which as discussed above defines the vertical extent of the western portions of the upper-level low off to the northeast. Low-level winds are weak southerly. The very moist mid-levels are most likely due to remnants of MCS-E that had moved through the region between 1930-2330 UTC 26 August. The largest vertical velocities in the region of highest moisture content correlate well to the location of MCS-E. Therefore, this cross-section at the time of the first TCS025 flight further identified the relative contributions of MCS-E and the upper-level cyclone in defining the overall structure of TCS025.



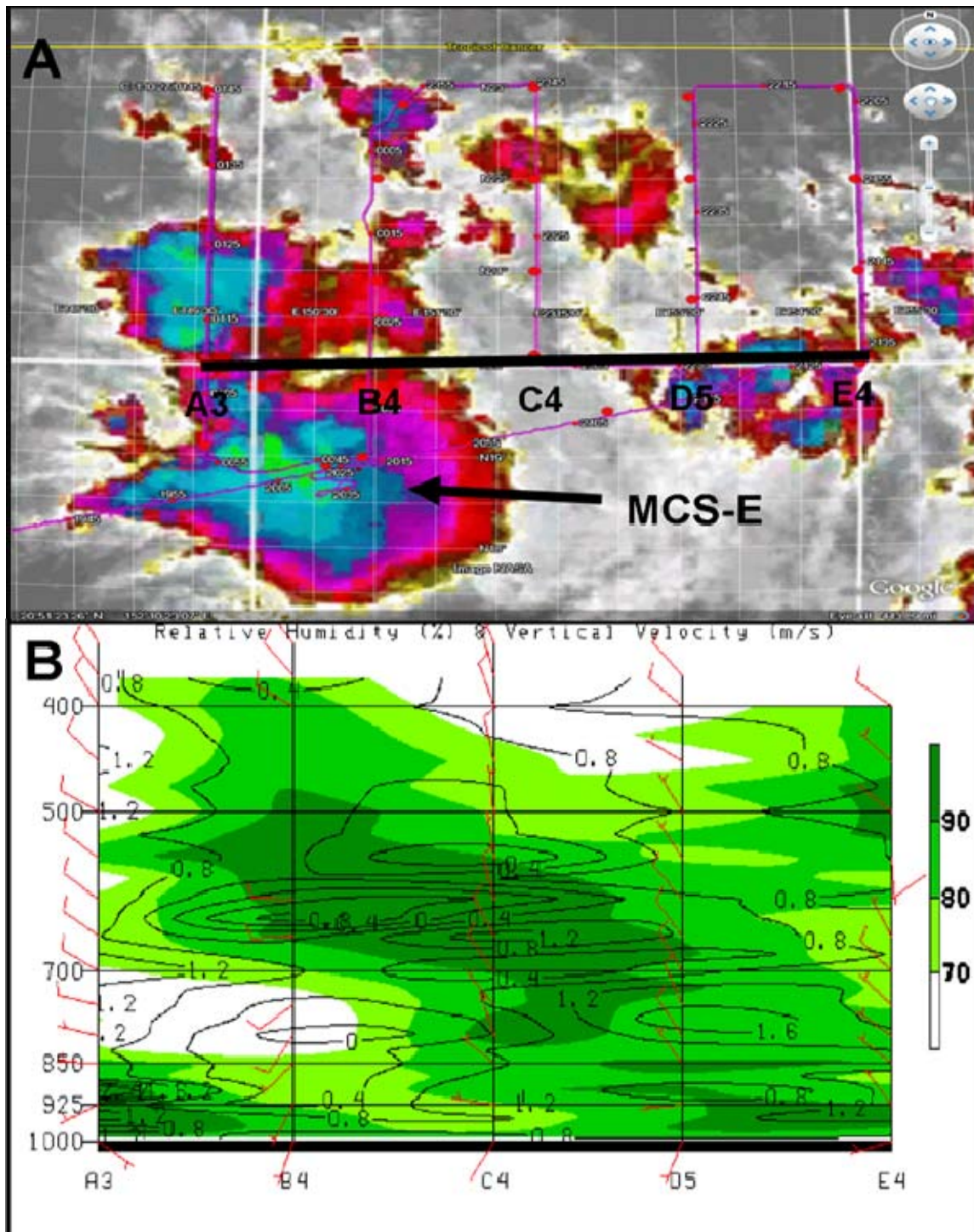


Figure 25. (a) Geostationary MTSAT IR imagery and WC-130J flight track from 1800 UTC 26 August – 0730 UTC 27 August 2008. (b) East-west vertical cross-section along 150°E-155°E at 20°N (black line in the MTSAT imagery panel (a)). Horizontal winds are defined by the barbs with one long barb equal to  $10 \text{ m s}^{-1}$ . Contours are vertical velocity in  $\text{m s}^{-1}$  and relative humidity in percent shaded.



## **2. USAF WC-130J and NRL P-3 Dropwindsondes 27–28 August**

The second WC-130J flight into TCS025 took off from Guam at 1953 UTC 27 August 2008. Based on observations during the previous flight, the objective of this flight was to locate a circulation center in TCS025. A modified square wave spiral pattern was flown to achieve maximum coverage (Figure 26). Additionally, the NRL P-3 mission equipped with ELDORA was planned to examine the developing MCSs associated with TCS025. The largest MCS (MCS-G in the 1930 UTC 28 August panel in Figure 21) was the target for this mission. The NRL P-3 departed from Guam at 0030 UTC 28 August 2008 and flew a circular pattern around the remaining deep convection of MCS-G. Besides ELDORA, the NRL P-3 was equipped with dropwindsondes that were launched approximately every 10 minutes after the flight had reached the targeted convection. Because the primary mission of the NRL P-3 was the use of ELDORA, a maximum flight level of 3 km was chosen.

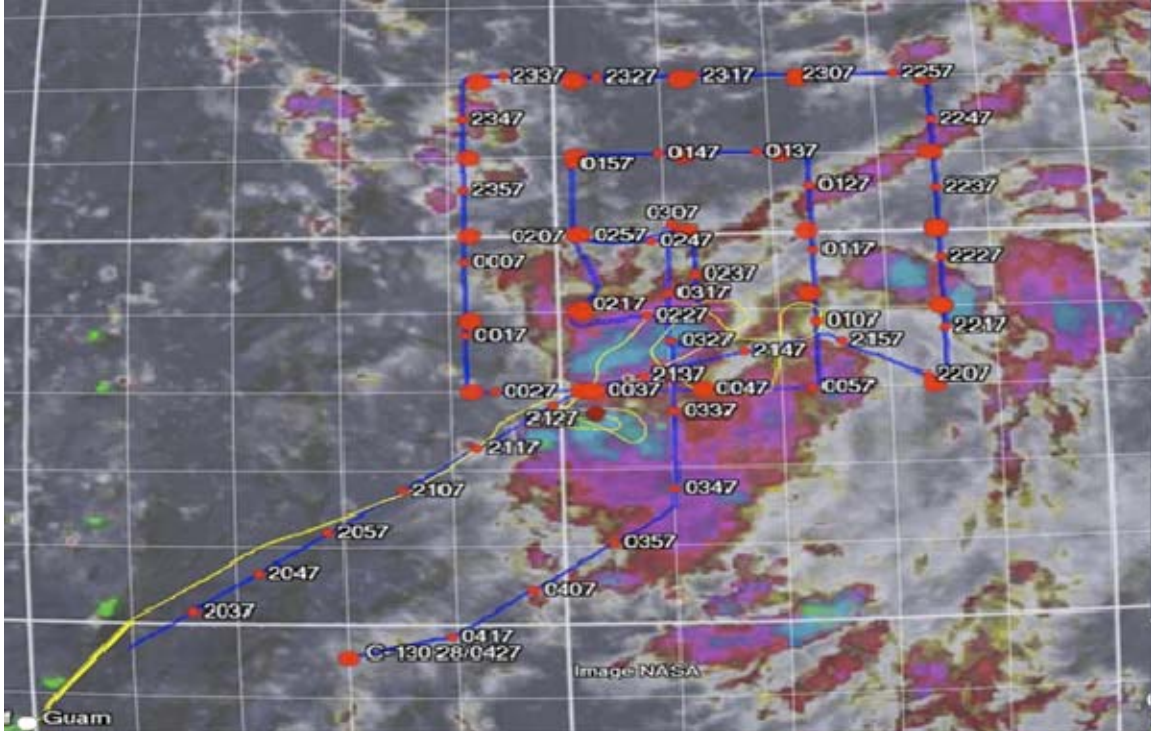


Figure 26. WC-130J flight track from 1953 UTC 27 August – 0515 UTC 28 August 2008 superposed on MTSAT IR imagery from 0330 UTC 28 August. Larger red circles identify approximate locations of dropwindsonde launches. Yellow line indicates flight path of the NRL P-3.

Low-level winds were much better organized during this second day of WC-130J operations (Figure 27). Winds at 950 hPa were generally between 5 and 10  $\text{m s}^{-1}$  and an obvious low-level cyclonic circulation existed at approximately 19.5°N, 152°E (Figure 27a). This was in the vicinity of the location where the deepest convection of MCS-G had formed. Winds at 850 hPa also define a broad cyclonic circulation that was centered at approximately 19.5°N, 152°E (Figure 27b). Dropwindsonde data at 700 hPa were only available from the WC-130J flight since this was above NRL P-3 flight level. Wind barbs at this level clearly show a cyclonic circulation approximately centered at 18.5°N, 151.8°E (Figure 27c), which is south of circulation centers at lower levels. Winds were generally between 5 and 10  $\text{m s}^{-1}$ . The center of the cyclonic circulation at 500 hPa (Figure 27d) was shifted even farther to the south and east. Winds at this level were also weak with a maximum velocity of 10  $\text{m s}^{-1}$ . Therefore, the dropwindsondes identify a circulation above 700 hPa that is located along the southern portion of the flight area

where deep convection (MCS-G) existed (Figure 26). The track of MCS-G was such that it had traveled southeastward through the region of the WC-130J square-spiral pattern where dropwindsonde data defined a circulation below 700 hPa.

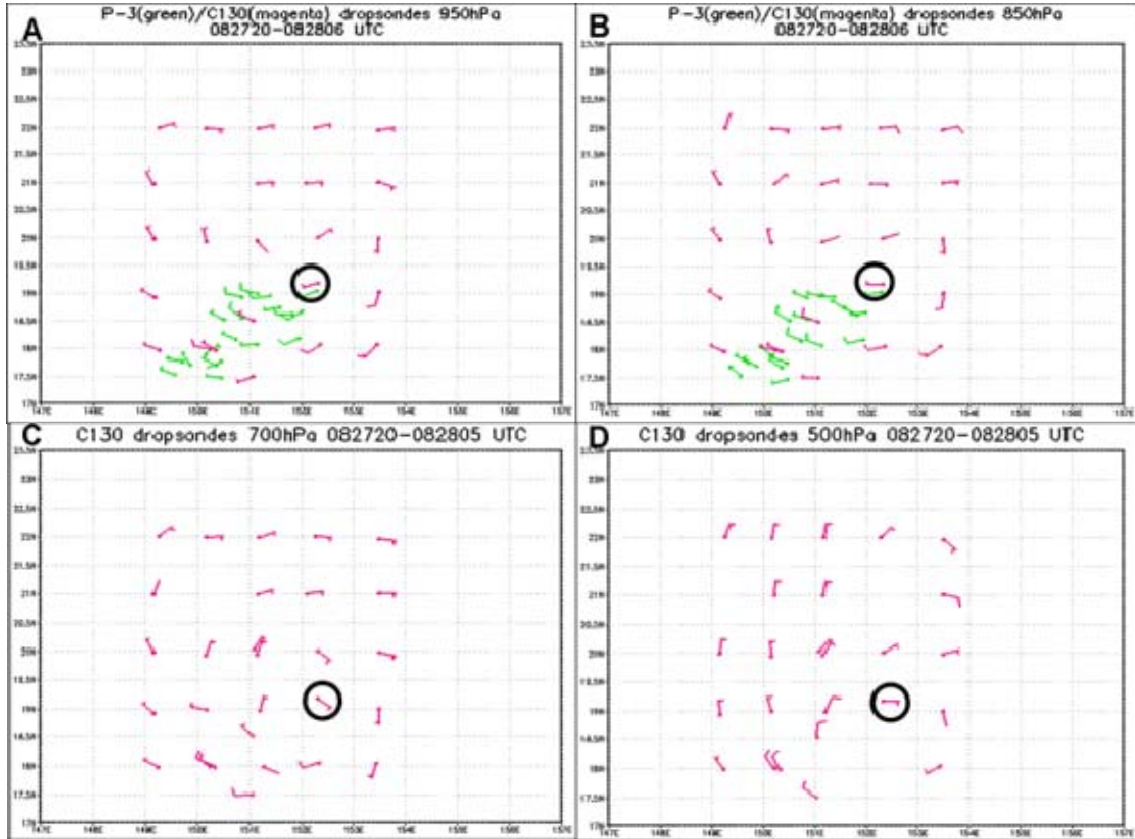


Figure 27. Dropwindsonde winds for WC-130J flight 2000 UTC 27 August - 0500 UTC 28 August at (a) 950 hPa, (b) 850 hPa, (c) 700 hPa, and (d) 500 hPa. The circled wind barb coincides to the skew-T plot in Figure 29.

A dropwindsonde sounding of TCS025 at 19.2°N, 152.3°E (Figure 28), which was near the center of cyclonic circulation, showed a very moist vertical profile from the surface up to the highest dropwindsonde level. Winds were from the west below 850 hPa but changed to the east-southeast at 750 hPa. This would indicate that the center of circulation was to the north of the dropwindsonde location below 850 hPa and to the south of the dropwindsonde location above 850 hPa. This is consistent with horizontal analysis of dropwindsonde winds in Figure 27. Comparison of the sequence of satellite images in Figure 21 it is clear that MCS-G had moved southeastward during the period of

the WC-130J flight. The dropwindsonde in Figure 28 was launched during the later portion of the flight as the aircraft flew through the southeast portion of TCS025 for the second time. It appears that the presence of the circulation to the south and above 750 hPa is related to the deep convection that had recently passed through this region. The circulation to the north and below 750 hPa is older and is apparently a remnant from the earlier traverse of MCS-G through that region.

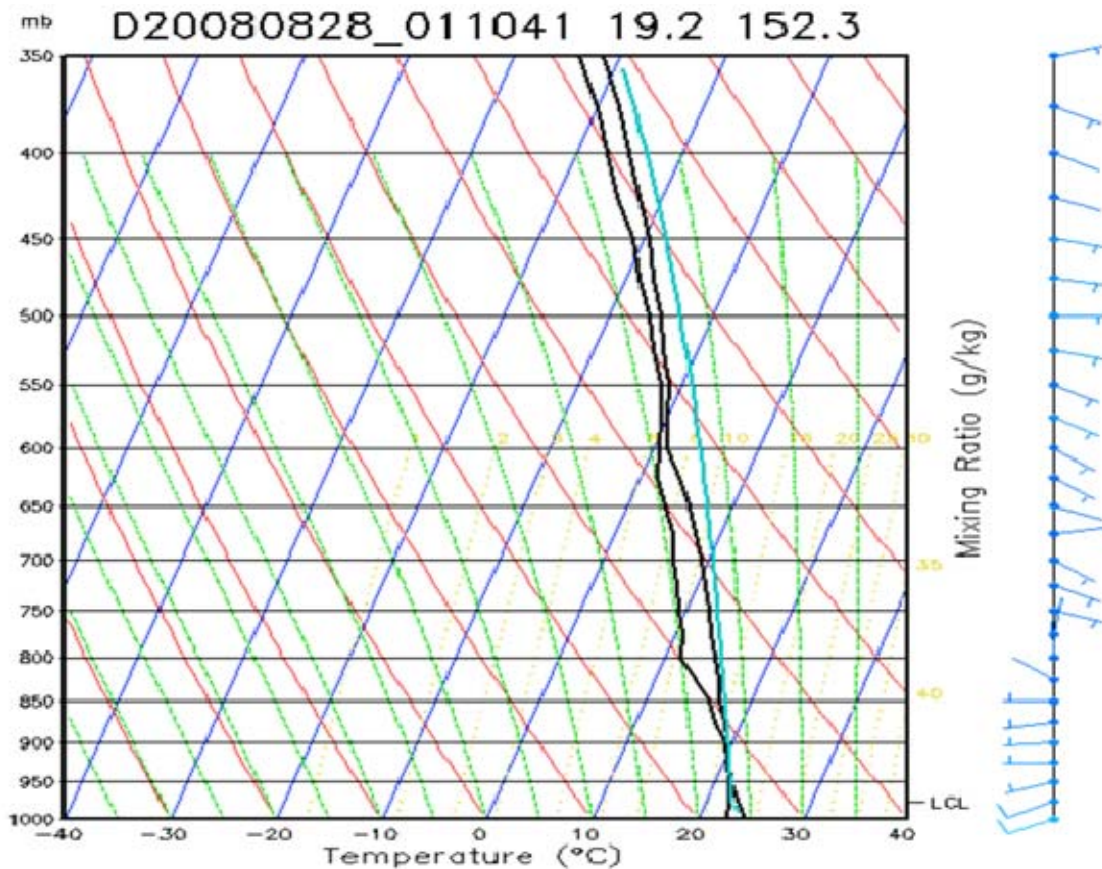


Figure 28. Skew-T profile of TCS025 at 19.2°N, 152.3°E at 0110 UTC 28 August 2008.

Following the second WC-130J and first NRL P-3 flight, satellite-derived upper-level winds (Figure 29) confirmed an upper-level cyclonic circulation center near the same location at 18.5°N, 152°E, as indicated in upper-level dropwindsonde winds. At this time, infra-red satellite imagery (Figures 21 and 29) indicated convection was strongest near the center of this upper-level cyclonic circulation. Since upper-level



dropwindsonde winds and satellite-derived winds all identified a circulation center near 18.5°N, 152°E, and convection was strongest near this location, the third WC-130J and second NRL P-3 with ELDORA flights were planned to further examine TCS025 focused on the region centered at 18.5°N, 152°E (identified by the red “I” in Figure 29).

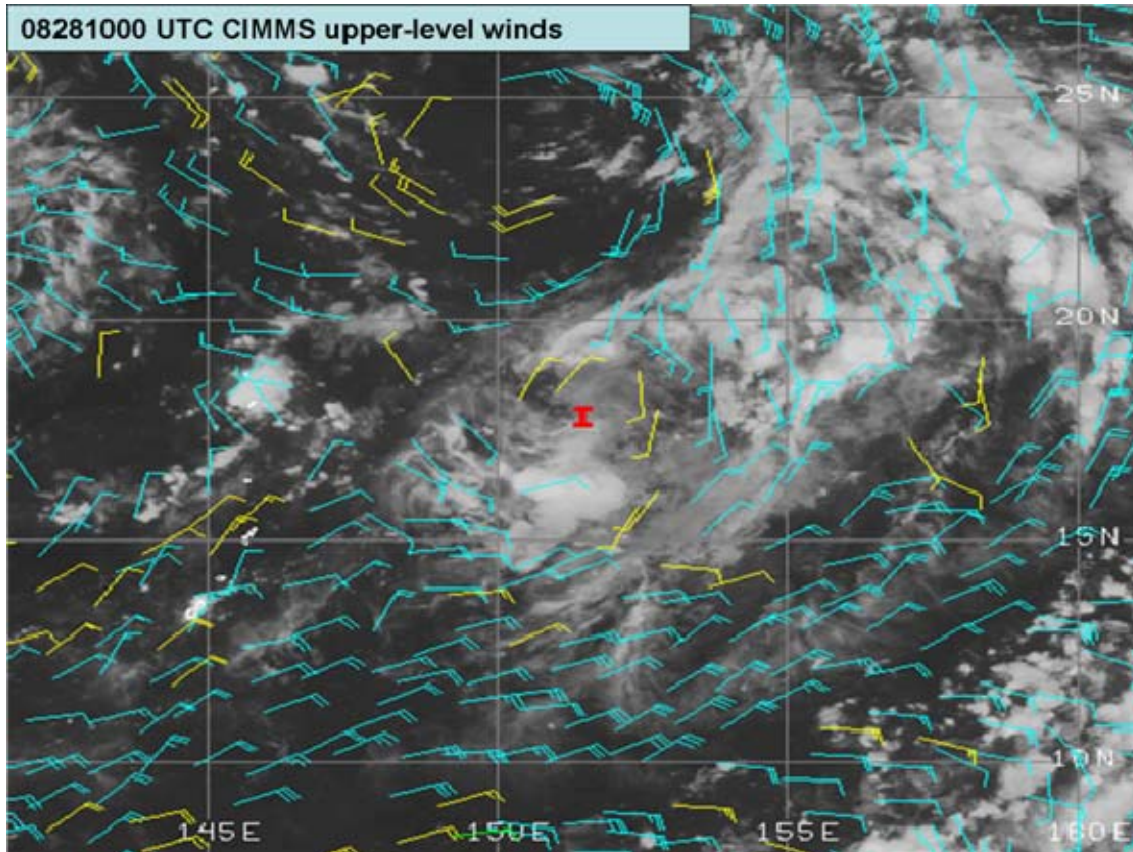


Figure 29. Satellite-derived upper-level winds from CIMMS at 1000 UTC 28 August between 150-300 hPa superposed on MTSAT water vapor imagery.

### 3. USAF WC-130J and NRL P-3 Dropwindsondes 28–29 August

The third and final WC-130J investigation into TCS025 took off from Guam at 2100 UTC 28 August 2008. A spiral box pattern was flown to map the three-dimensional winds, temperature, and moisture fields in the region of the strongest TCS025 convection (Figure 30). This four-degree box was centered on what was thought to be a low-level circulation based on satellite imagery. The NRL P-3 departed Guam at 2240 UTC 28 August 2008. The NRL P-3 flew an elliptical pattern around the periphery of a large

region of deep stratiform cloud bounded by convection (Figure 30). Dropwindsondes were launched approximately every ten minutes along the flight path.

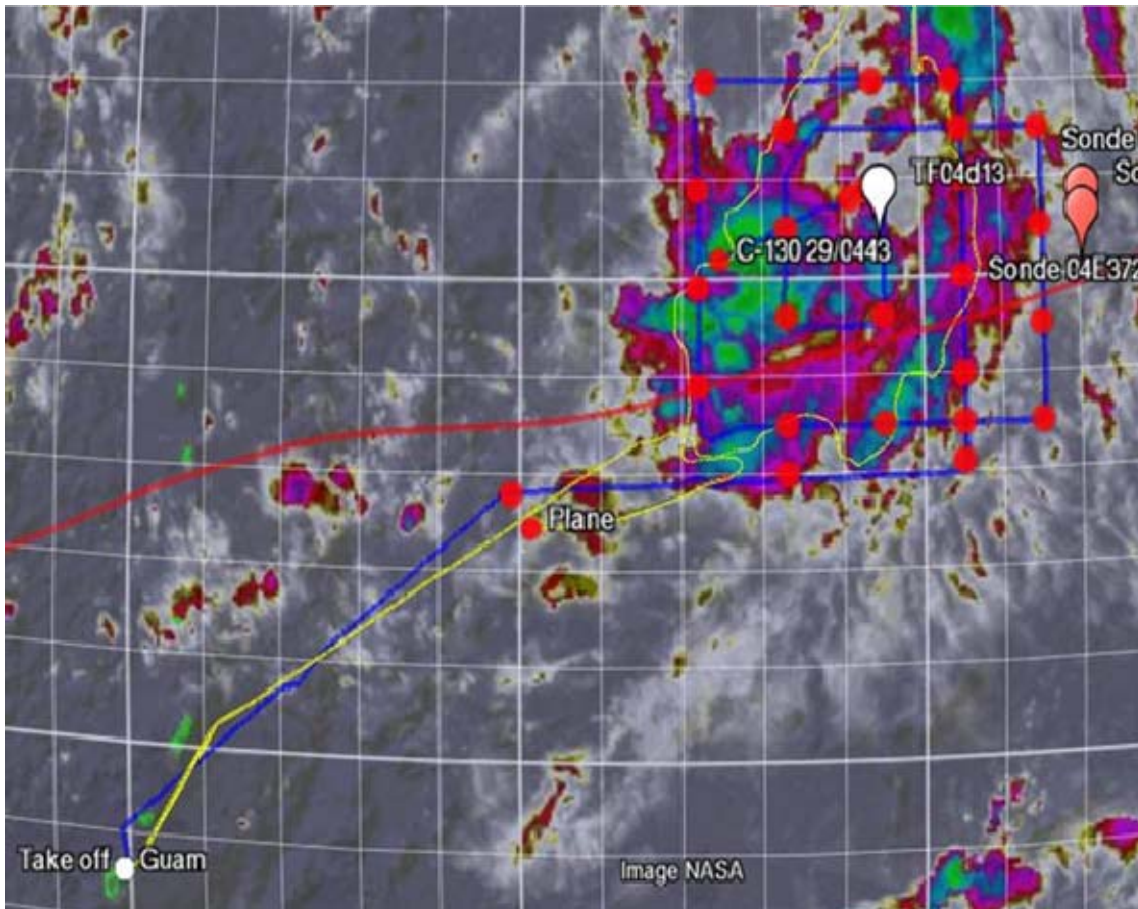


Figure 30. WC-130J flight track from 2100 UTC 28 August – 0700 UTC 29 August 2008 superposed on MTSAT IR imagery from 0330 UTC 29 August. Red circles identify approximate locations of dropwindsonde launches. Yellow line indicates flight path of the NRL P-3 from 2240 UTC 28 August – 0615 UTC 29 August 2008. Red line is the path of the T-PARC Driftsonde launched from Hawaii.

Although the WC-130J dropwindsonde launch pattern was designed to be centered on the low-level circulation thought to be coincident with the deep convection in Figure 30, it was obvious from dropwindsonde winds at 950 hPa (Figure 32a) that the low-level cyclonic circulation was displaced to the northwest of all dropwindsonde locations. Near-surface winds in QuickSCAT imagery (Figure 31) identified a low-level cyclonic circulation near 22°N, 152.5°E. Winds at 950 hPa were also much stronger for this flight than they were the previous days. Winds in excess of  $8\text{--}10\text{ m s}^{-1}$



were common between 154°E and 156°E. Winds at 850 hPa also defined a broad cyclonic circulation that was approximately centered at 22.5°N, 153°E based on WC-130J dropwindsonde wind (Figure 32b). Maximum wind speeds at this level were between 8-12 m s<sup>-1</sup> on the east side of the flight pattern. The 700 hPa and 500 hPa level also identify the cyclonic circulation to the north (Figure 32c and d). From the MTSAT IR imagery (Figure 30), the low-level and mid-level cyclonic circulation identified by dropwindsonde winds was north of the strongest convection of TCS025. However, convection in this region was very weak and disorganized (Figure 30).

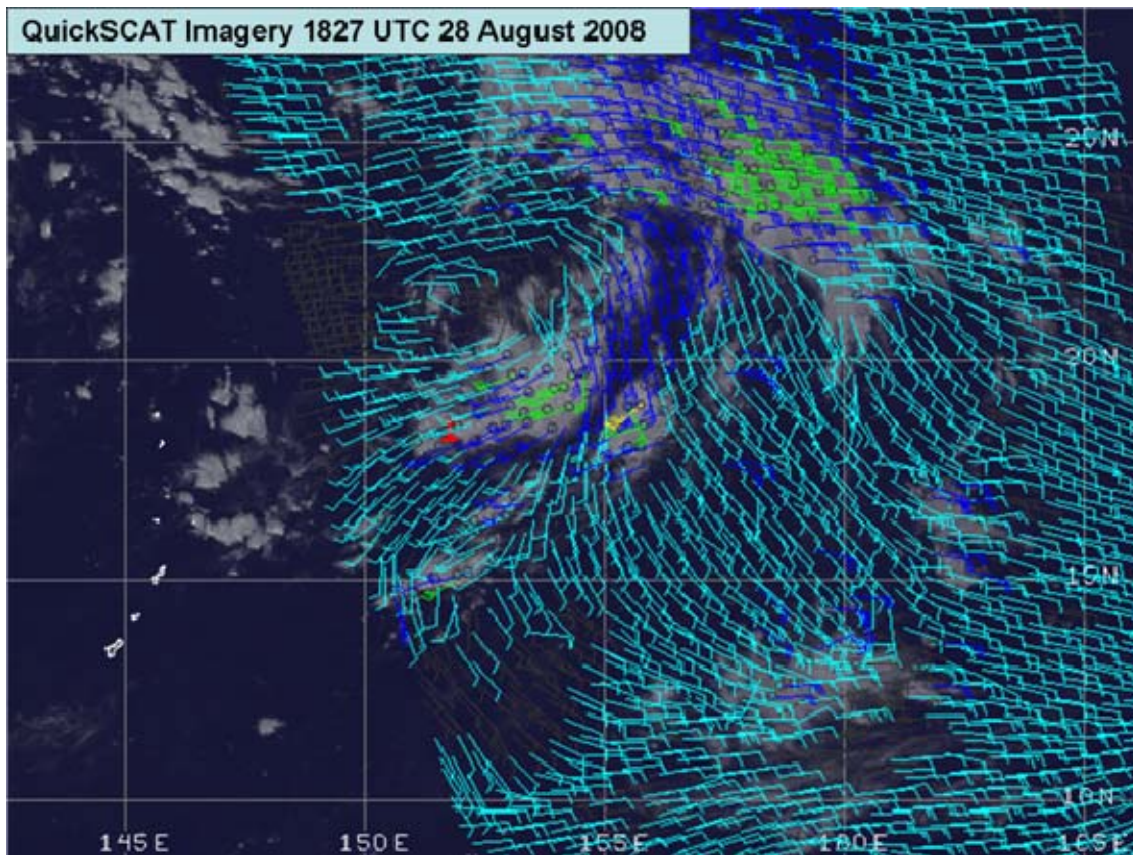


Figure 31. Low-level winds from QuickSCAT imagery at 1827 UTC 28 August.

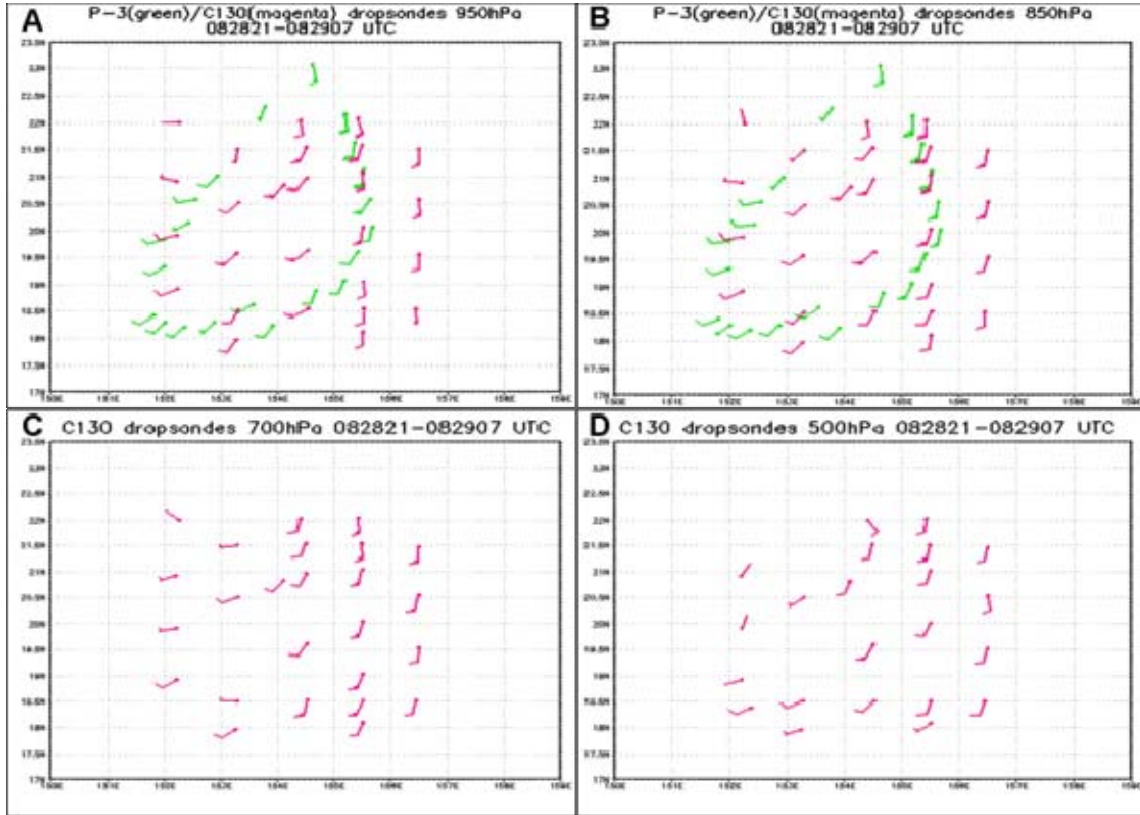


Figure 32. Dropwindsonde winds for WC-130J flight 2100-0700 UTC 28 and 29 August at (a) 950 hPa, (b) 850 hPa, (c) 700 hPa, and (d) 500 hPa.

#### D. ELDORA ANALYSIS

Whereas dropwindsondes provided a coarse three-dimensional analysis of the TCS025 environment, a more detailed approach was needed to examine the three-dimensional mesoscale processes that defined the multiple circulations of TCS025. The multiple MCSs that were associated with TCS025 offered a unique opportunity for an analysis using ELDORA. Because of the high resolution of ELDORA, small-scale changes in the horizontal and vertical wind components and the reflectivity patterns can be identified. One of the primary goals of this analysis is to describe the role these processes had in the non-development of TCS025.

As described earlier, multiple MCSs formed throughout the life cycle of TCS025. These MCSs were the target for the two NRL P-3 ELDORA missions on 28 and 29



August 2008. Post-processing of the ELDORA observations produced high-resolution data that defined atmospheric variables such as the horizontal and vertical wind components, reflectivity, vorticity, divergence, and convergence. In this analysis, ECMWF model fields, dropwindsondes, and ELDORA data are used to describe the three-dimensional environment of TCS025.

### **1. NRL P-3 ELDORA Flight 28 August 2008**

The fifth ELDORA mission during TCS08 departed Andersen Air Base in Guam at 0030 UTC 28 August 2008 to investigate the deep convection of multiple MCSs associated with TCS025 (MCS-G in Figure 21) that had developed in the pre-flight hours. By the time the NRL P-3 reached the TCS025 convection at approximately 0145 UTC 28 August, MCS-G had weakened but still contained regions of deep convection (Figure 21). Because the NRL P-3 was not designed to pierce the strongest convection, these deep convective cells were circled multiple times to obtain ELDORA data from all sides. Several deep convective cells associated with MCS-G were targeted (Figure 33).

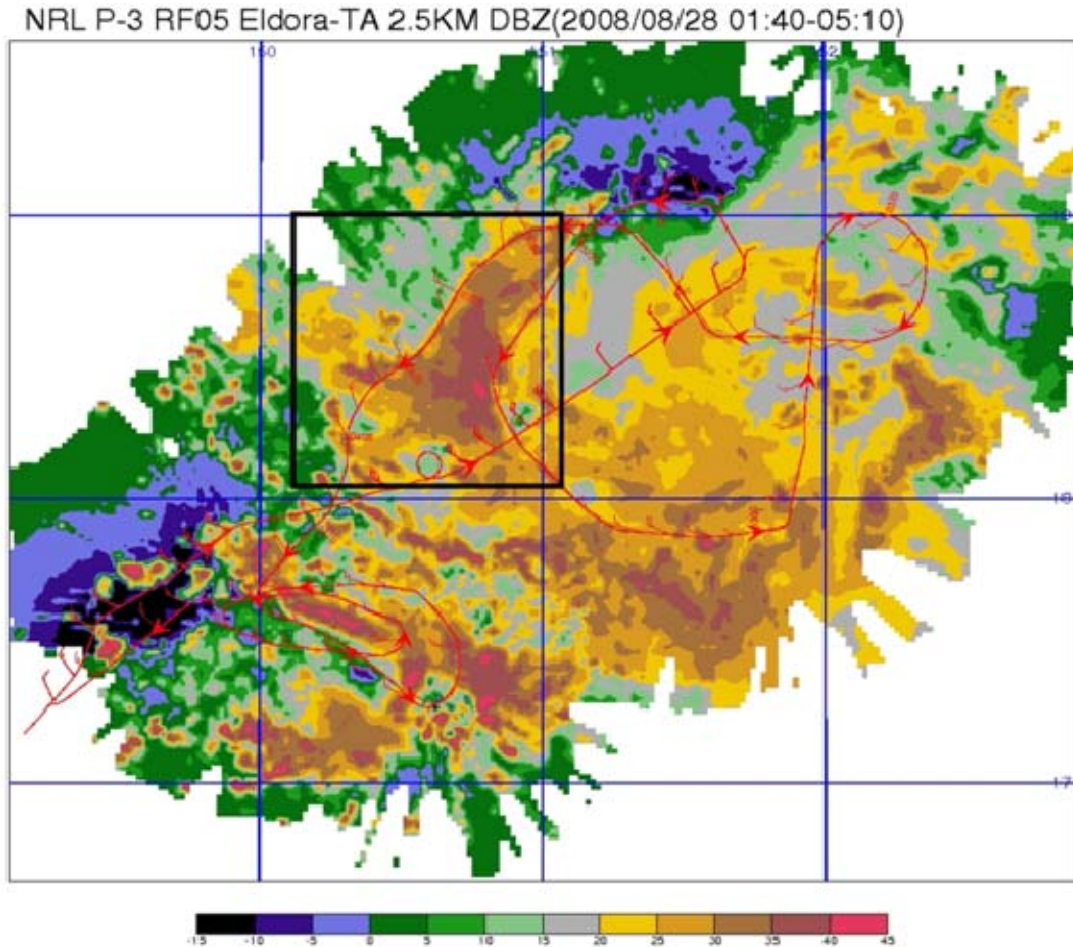


Figure 33. The P-3 flight path, flight-level winds, and ELDORA reflectivity (dBz; scale at the bottom) at 2.5 km altitude 0140-0510 UTC 28 August 2008.

To examine the variation in winds from the surface to upper levels, dropwindsonde wind barbs and ELDORA-derived winds are examined at standard levels in the vertical. A low-level 850 hPa cyclonic circulation in the ECMWF wind analysis is approximately centered at 19.5°N, 152.5°E (Figure 34). As described in the previous section, dropwindsonde winds from the WC-130J and P-3 also define this low-level circulation. The deepest convection identified by ELDORA reflectivity is just to the southwest of the analyzed closed cyclonic circulation (Figures 33 and 34). At 1.5 km altitude (Figure 34), ELDORA wind vectors also define a cyclonic circulation just to the north of the convection. Winds are weak with only a small region of winds greater than  $10 \text{ m s}^{-1}$  on the southeastern side of the circulation. One challenge in the processing of

ELDORA winds is the definition of winds in close proximity to the flight path of the NRL P-3. Due to this uncertainty, wind vectors that are co-located with the flight path are ignored.

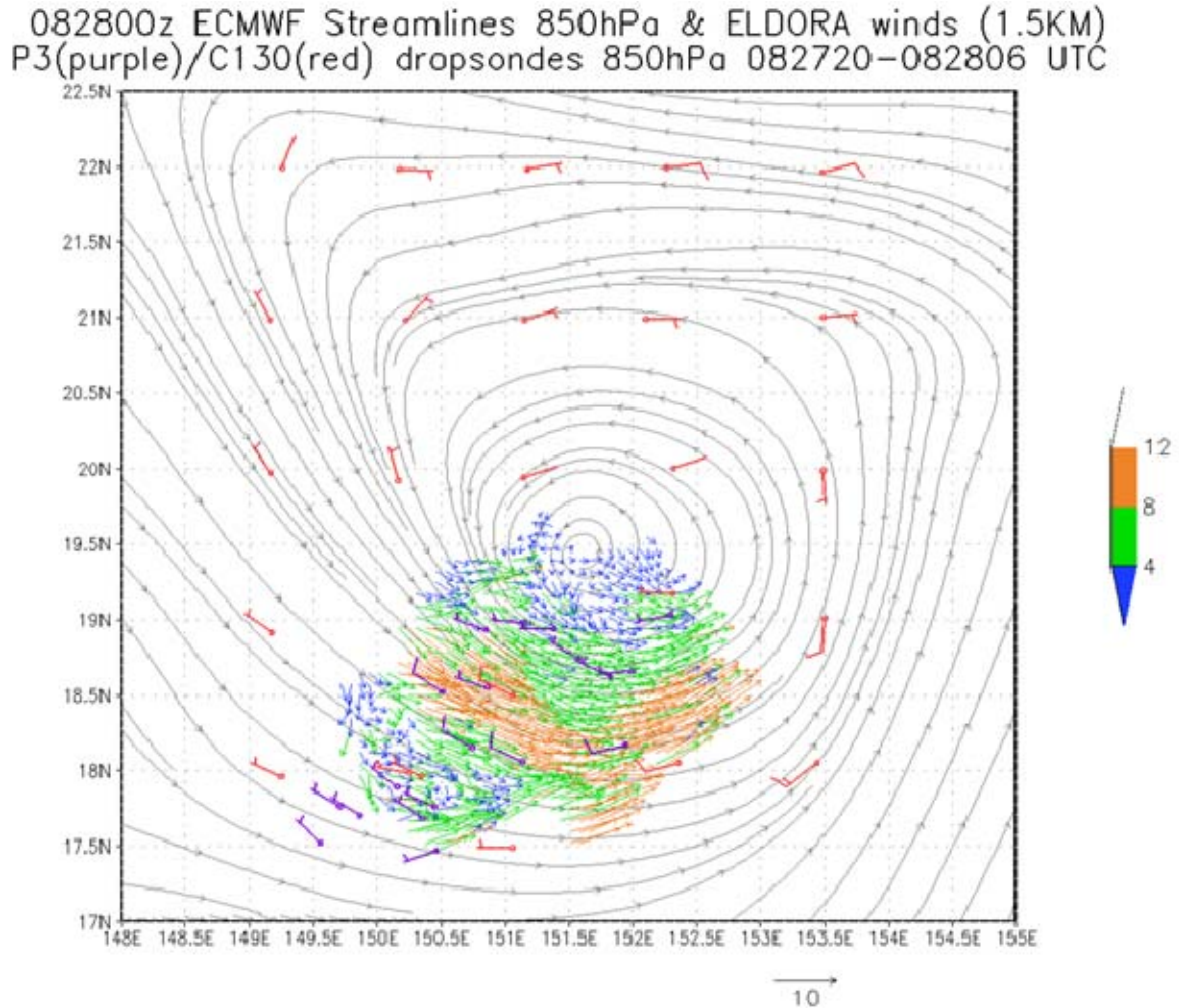


Figure 34. Analyzed ECMWF streamlines, WC-130J and P-3 dropwindsondes at 850 hPa between 2000 UTC 27 August – 0600 UTC 28 August, and ELDORA winds ( $\text{m s}^{-1}$ :  $10 \text{ m s}^{-1}$  scale at bottom) at 1.5 km between 0150-0410 UTC 28 August 2008.

At 700 hPa (Figure 35), the cyclonic circulation identified from the dropwindsondes (Figure 27) was shifted slightly to the south and centered near  $18.5^\circ\text{N}$ ,  $152^\circ\text{E}$ . Wind vectors derived from ELDORA were in agreement with the shift in the center of circulation. The strongest winds remained to the south and east of the circulation center. Convection was strongest to the southwest of the circulation center as

indicated by ELDORA reflectivity (Figure 33). Analyzed EMCWF streamlines correlate well with the winds from dropwindsondes and the ELDORA winds as well as the location of the center of circulation (Figure 36).

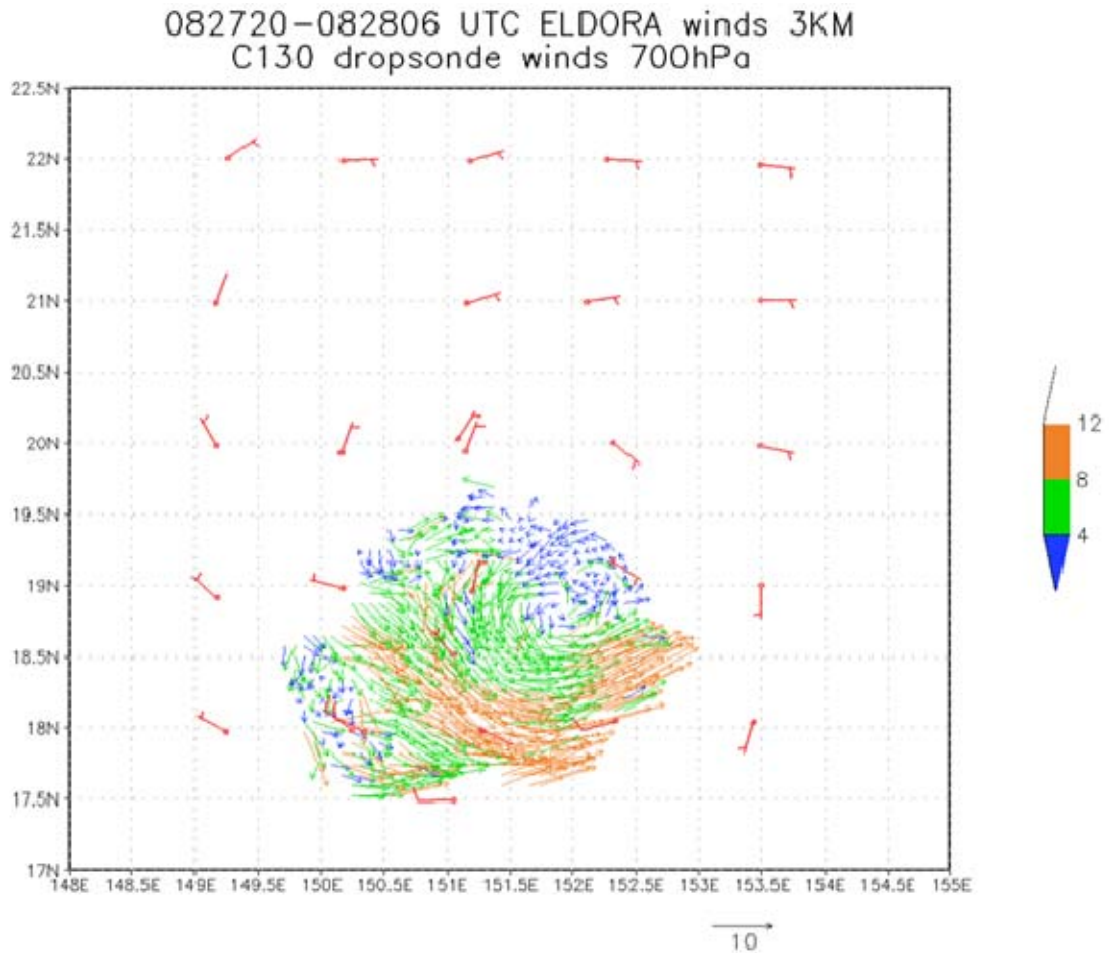


Figure 35. Analyzed ELDORA winds at 3 km ( $\text{m s}^{-1}$ :  $10 \text{ m s}^{-1}$  scale at bottom) and WC-130J dropwindsondes at 700 hPa during 0150-0410 UTC 28 August 2008.

ECMWF Streamlines 700hPa 082800 UTC & ELDORA winds(3KM)  
C130 dropsondes 700hPa 082720–082806 UTC

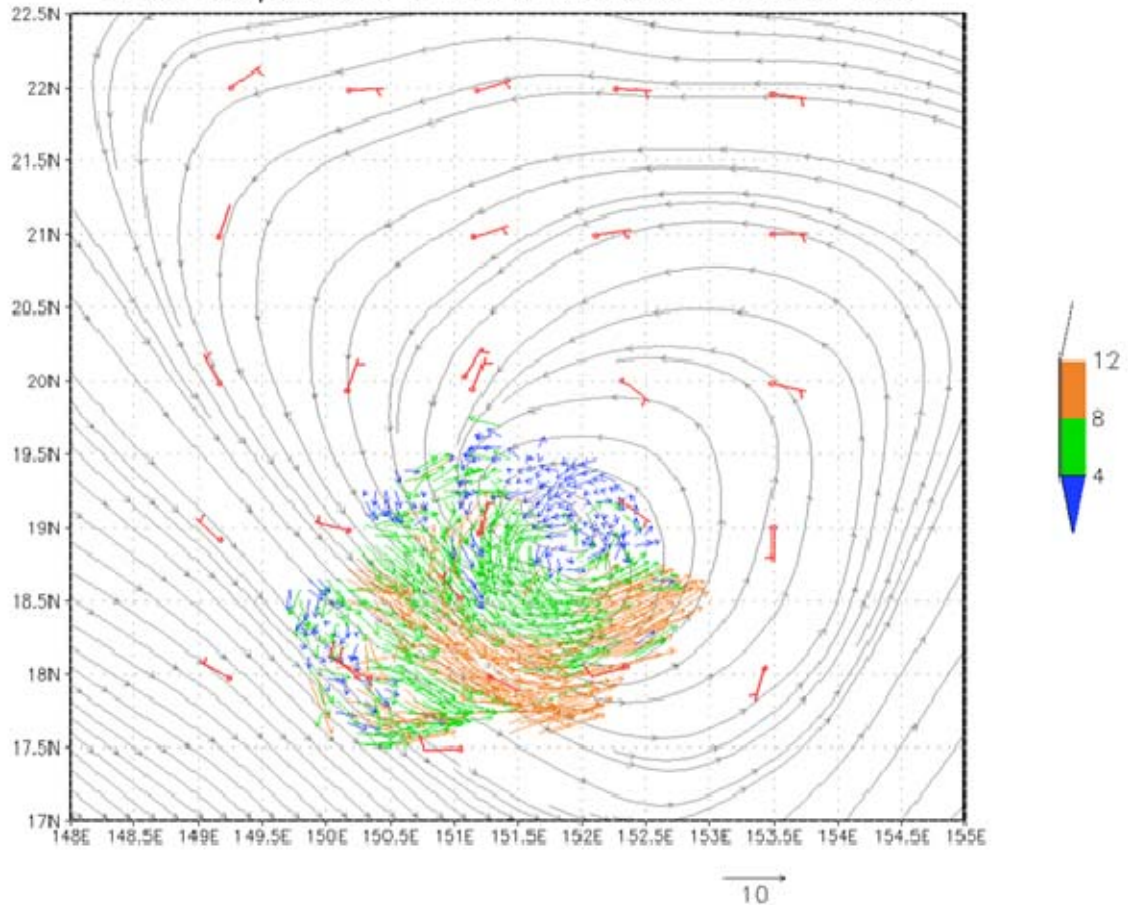


Figure 36. As in Figure 34, except for 700 hPa and 3 km.

At 500 hPa (Figure 37), the center of circulation was at 18.5°N, 152°E, which is approximately the same location as 700 hPa. Winds in excess of  $10 \text{ m s}^{-1}$  were present to the south and west of the center of circulation. Winds quickly abated to  $5 \text{ m s}^{-1}$  or less away from the center as indicated by the dropwindsonde observations (Figure 37). The analyzed ECMWF streamlines at 500 hPa were in general agreement with dropwindsonde and ELDORA winds, as well as being aligned with the center of circulation (Figure 38).



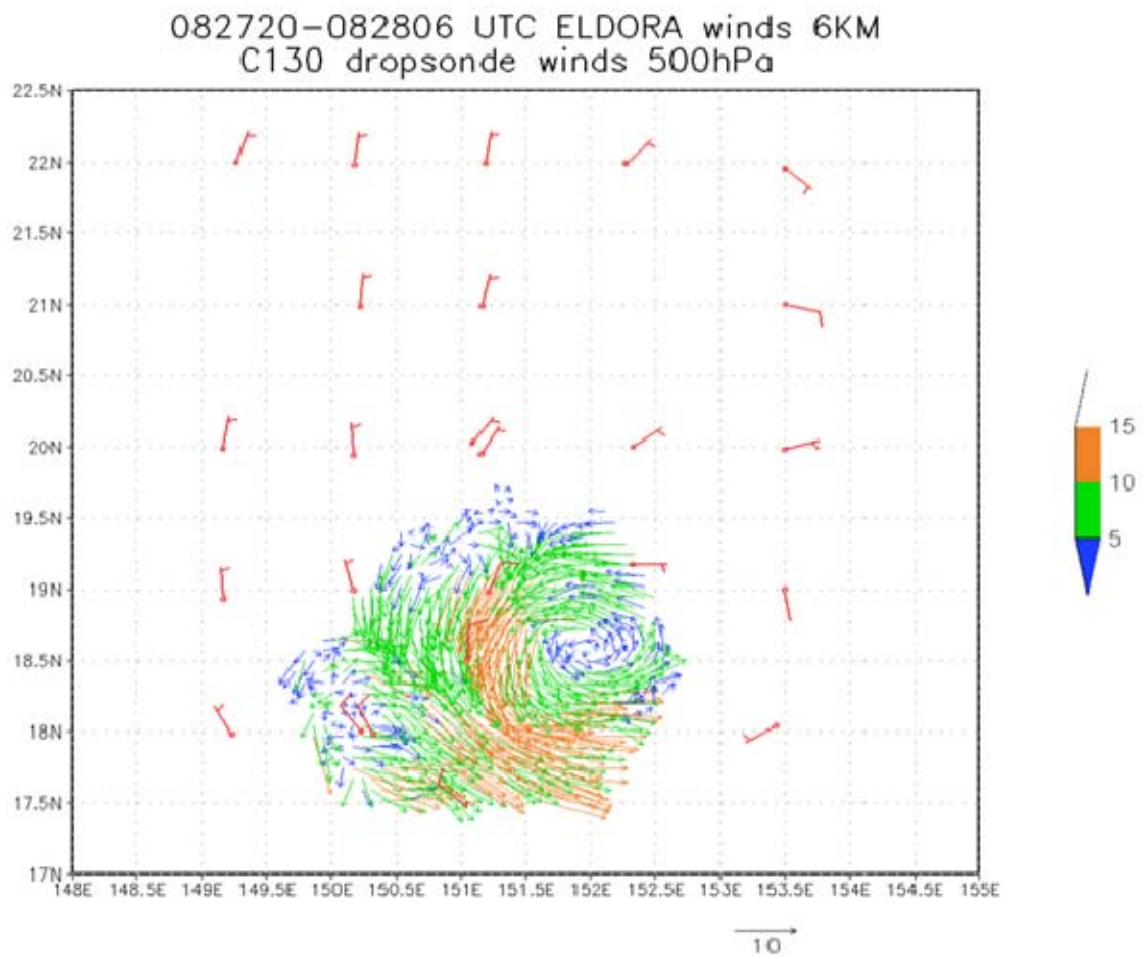


Figure 37. As in Figure 35, except for 500 hPa and 6 km.



ECMWF Streamlines 500hPa 082800 UTC & ELDORA winds(6KM)  
C130 dropsondes 500hPa 082720–082806 UTC

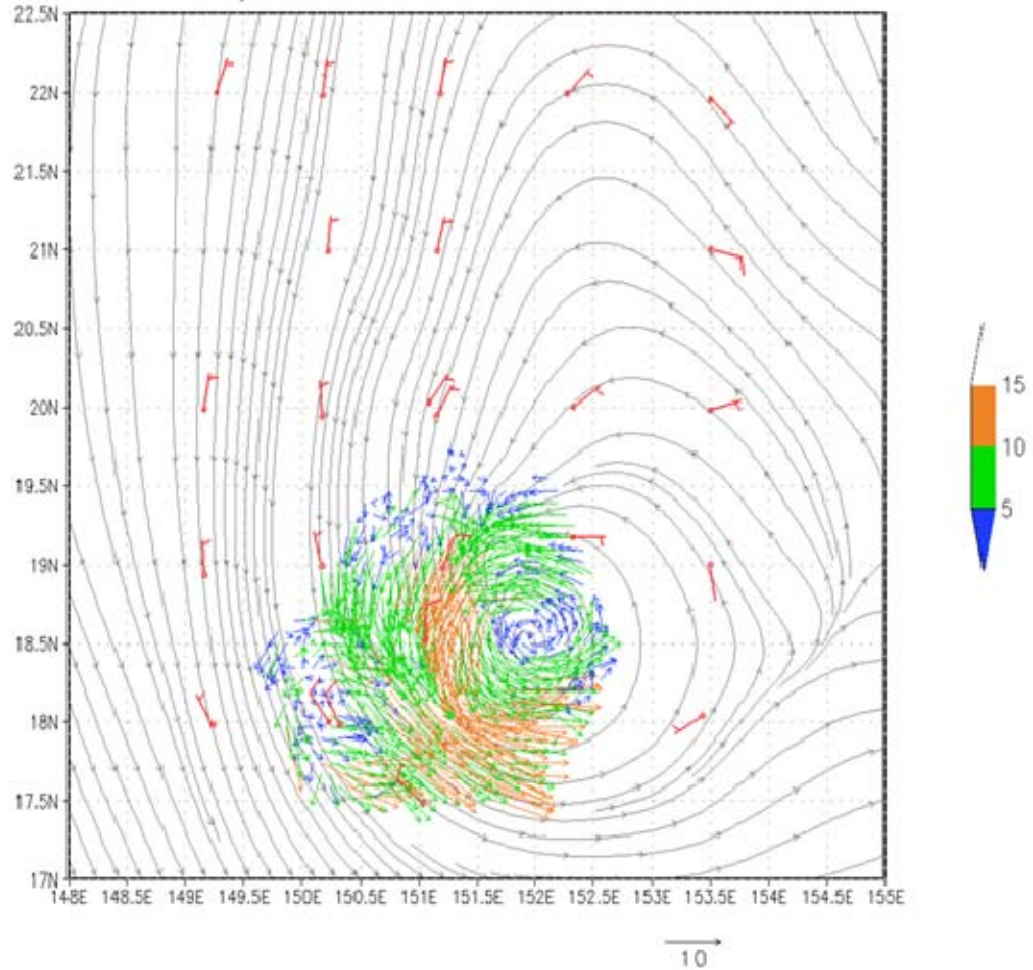


Figure 38. As in Figure 34, except for 500 hPa and 6 km.

Analyzed EMCWF streamlines at 300 hPa (Figure 39) define an anticyclonic circulation to the northeast and a trough centered over the region of ELDORA wind analysis (Figure 39). Winds from ELDORA at 9.5 km indicated this region contains a closed cyclonic circulation that is also identified at 500 hPa and 700 hPa. The center of this cyclonic circulation is approximately at 18.5°N, 152°E, which is the same location as the low and mid-levels. However, the analyzed ECMWF streamlines do not depict the closed cyclonic circulation that is evident only from the ELDORA winds.

# ECMWF Streamlines 300hPa 082800 UTC & ELDORA winds (9.5KM)

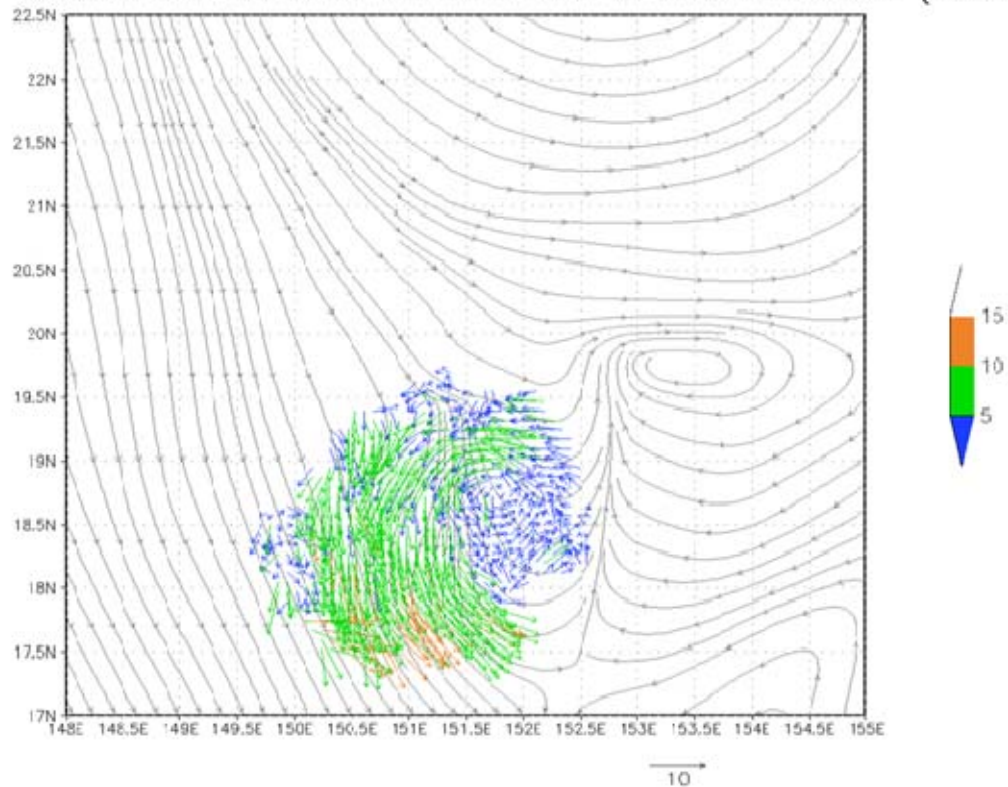


Figure 39. As in Figure 34, except for 300 hPa and 9.5 km.

The horizontal wind fields from the ELDORA indicated that a closed cyclonic circulation was present in TCS025 throughout all standard levels in the vertical. The low level (850 hPa) ELDORA winds indicated the center of circulation was at 19.5N, 152.5°E. At the middle and upper levels, the circulation was centered to the south and west at 18.5°N, 152°N. This cyclonic circulation was associated with MCS-G (Figure 21) that passed through the region during the WC-130J and NRL P-3 flights on 28-29 August. As the dropwindsonde sounding at 19.2°N, 152.3°E (Figure 28) indicated, these two cyclonic circulations seemed to be separated around the 800 hPa level.

One of the benefits of employing ELDORA is the ability to produce high-resolution wind analyses which allows for a detailed examination of reflectivity and winds for a small portion of TCS025. A 500-m resolution, 25 minute segment of ELDORA observations during 0345-0410 UTC 28 August 2008 (identified by the black box in Figure 33) is given in Figure 40. At 850 hPa (Figure 40a), winds were from the

northwest as this segment was on the southwest side of the larger cyclonic circulation identified earlier. At 3 km (700 hPa), winds were more variable with the strongest winds in the deepest convection (Figure 40b). The 4.5 km (600 hPa) level had a highly variable wind field (Figure 40c). However, a cyclonic turning of the winds around 18.5°N, 150.7°E was evident. This turning of the winds was associated with the strongest reflectivity. The void in wind vectors near 18.4°N, 150.8°E was due to the inability of the ELDORA radar beams to penetrate the deepest convection directly to the south of the flight path. The wind field at 6 km (500 hPa) was also highly variable (Figure 40d). Winds turn cyclonically near 18.5°N, 150.7°E, which was the same region of cyclonic winds at 4.5 km. This suggested the development of a small-scale mid-level cyclonic circulation associated with the deepest convection. However, this convection was not sustained and the circulation did not appear to persist.

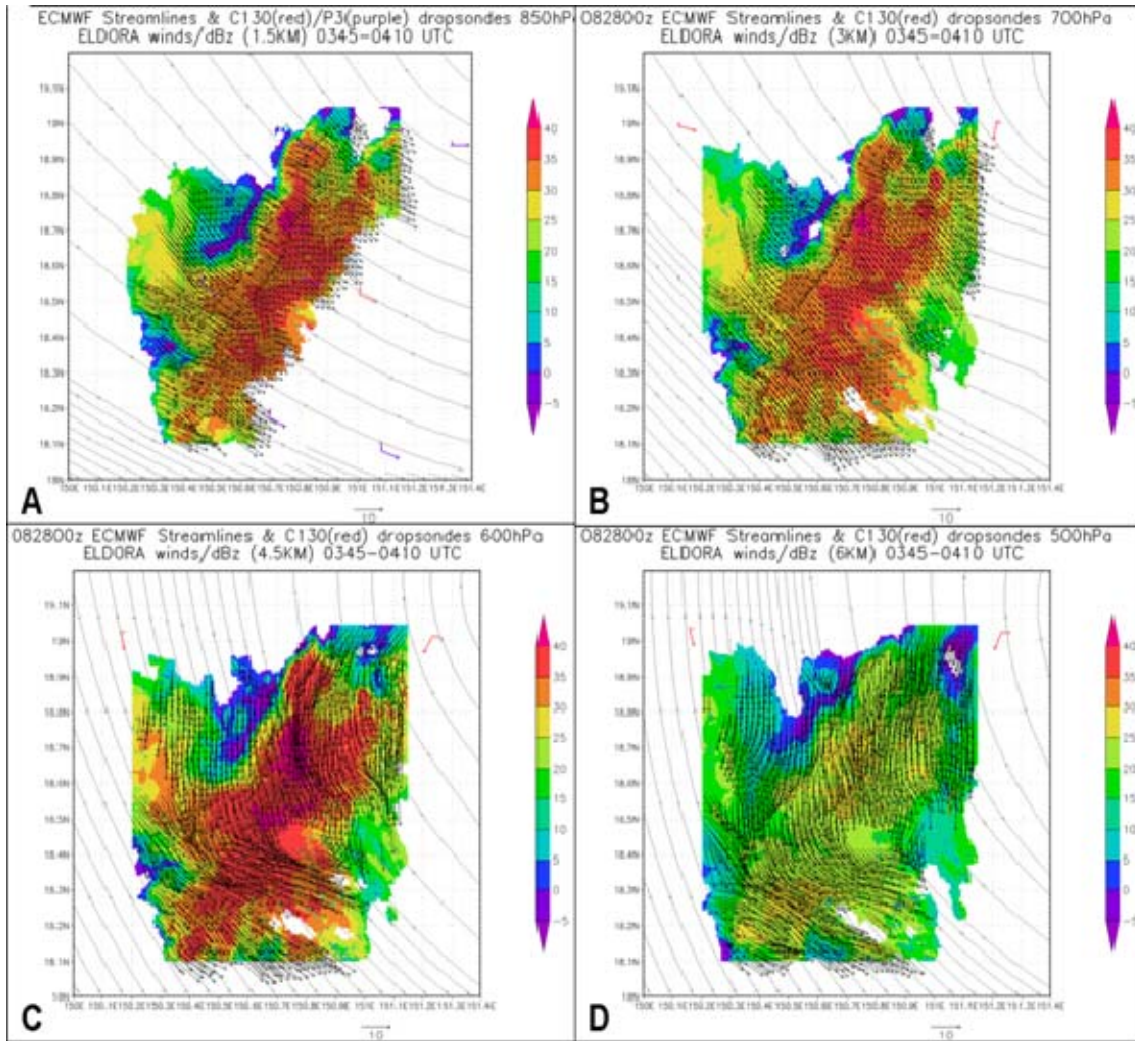


Figure 40. Analyzed ECMWF streamlines, NRL P-3 and WC-130J dropwindsondes, and ELDORA reflectivity and winds during 0345-0410 UTC 28 August 2008. (a) 1.5 km, 850 hPa, (b) 3 km, 700 hPa, (c) 4.5 km, 600 hPa, and (d) 6 km, 500 hPa.

Throughout the periods of the second WC-130J flight and the first NRL P-3 flight, TCS025 was comprised of a complex environment of deep convection in varying stages and circulations at varying levels and center locations. Over the southeast portion of the region, a circulation existed above 750 hPa in the region of deepest convection that had passed through the region. The circulation was a maximum near 500 hPa and weakened above, but was still evident at 300 hPa (Figure 38). The lowest-level circulation was near the center of TCS025, but not associated with active convection as it

had moved to the southeast. Along the periphery, new convective cells were short-lived during the flight and contained mid-level circulations (Figure 33). However, they did not seem to contribute to the organization of TCS025.

The NRL P-3 flight with ELDORA on 28 August provided a rare three-dimensional analysis of an individual MCS (MCS-G) that was embedded in TCS025. The high-resolution imagery produced by ELDORA generated a very detailed three-dimensional depiction of MCS-G reflectivity. The broad and deep convection associated with MCS-G had weakened prior to the P-3 flight (Figure 20). However, several small deep convective cells were still present. Nearly all of the convection associated with MCS-G was to the south and west of the cyclonic circulation indicated in the horizontal wind fields (Figure 34, 35, and 37). The wind field analysis indicated two cyclonic circulations separated meridionally by approximately  $1^{\circ}$  latitude ( $\sim 100$  km). The lower-level circulation was centered at approximately  $19.5^{\circ}\text{N}$ ,  $152.5^{\circ}\text{E}$  (Figure 34) and the upper-level cyclonic circulation was centered at approximately  $18.5^{\circ}\text{N}$ ,  $152^{\circ}\text{E}$ . The separation between the two circulations occurred near 1.5 km (850 hPa), which was indicated earlier in the skew-T at  $19.2^{\circ}\text{N}$ ,  $152.3^{\circ}\text{E}$  (Figure 28). This cyclonic circulation was most likely produced earlier by MCS-G when convection was strongest. As MCS-G progressed southward (Figure 21), the upper-level circulation remained with the convection while the lower-level circulation lagged behind.

## **1. NRL P-3 ELDORA Flight 29 August 2008**

The sixth ELDORA mission during TCS08 departed Andersen Air Base in Guam at 2240 UTC 28 August 2008 to continue the investigation of MCSs associated with TCS025. The mission of this flight was to search for a closed circulation and examine the deep convection on the south side of TCS025. By the time the NRL P-3 reached the TCS025 convection at approximately 0145 UTC 29 August, MCS-H (Figure 22) had weakened but still contained regions of deep convection. The NRL P-3 flew an elliptical pattern around the periphery of MCS-H (Figure 41) while deviating for deep convection. The NRL P-3 circled the convection for over four hours before returning to Guam at 0615 UTC 29 August 2008.



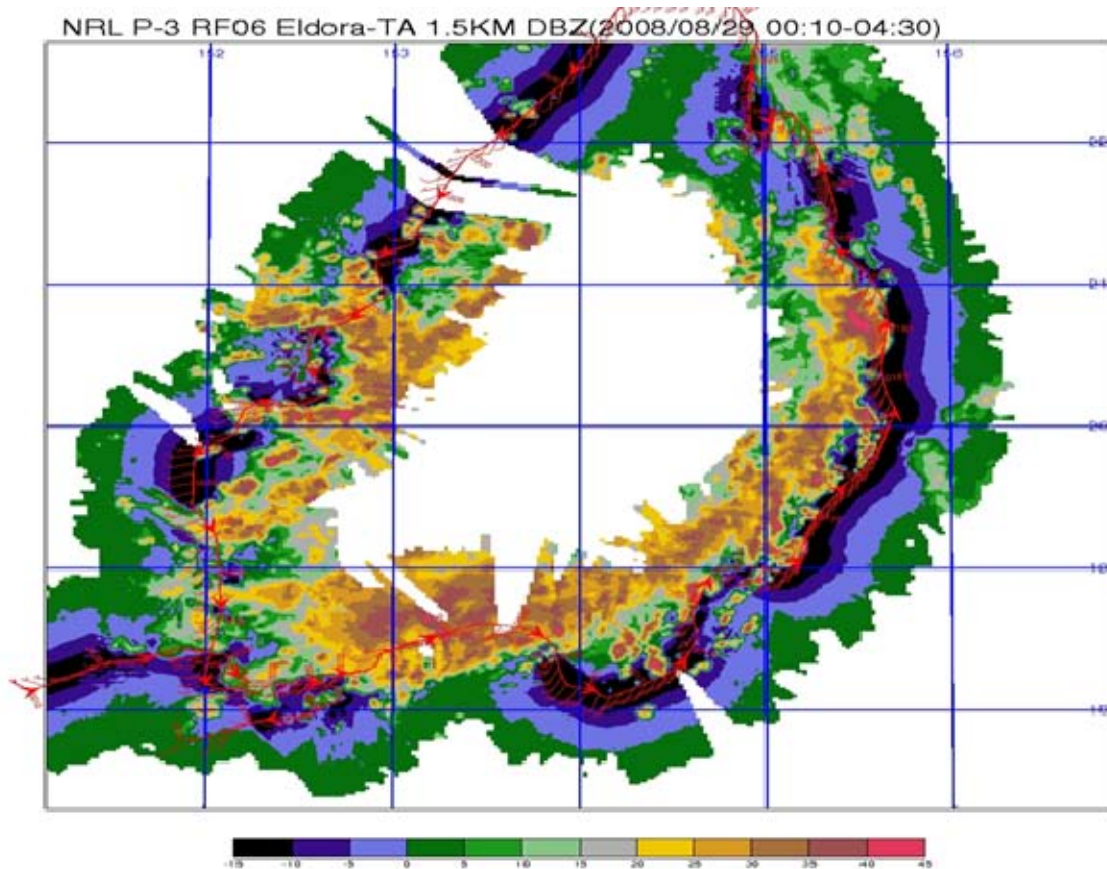


Figure 41. The P-3 flight path, flight-level winds, and ELDORA reflectivity (dBz) at 1.5 km altitude from 0010 UTC - 0615 UTC 29 August 2008.

The analysis for the previous ELDORA investigation of TCS025 on 28 August identified a low-level cyclonic circulation near 19.5°N, 152°E. A cursory examination of the ELDORA wind field, the NRL P-3 and WC-130J dropwindsondes, and the ECMWF analyzed streamlines indicated the circulation had moved to the northwest (Figure 42). However, the actual center of circulation was difficult to distinguish in aircraft data. The model analysis has a low-level circulation to the north and west of most of the aircraft data, which was likely based on the weak northerly wind from the dropwindsonde at 22°N, 152.3°E. The western side contained the least convection and winds were generally less than  $10 \text{ m s}^{-1}$ . Although convection existed in the middle of the elliptical NRL P-3 flight path, ELDORA only detected convection in proximity to the elliptical flight path.

082900z ECMWF Streamlines 850hPa & ELDORA winds/dBz (1.5KM)  
P3(purple)/C130(red) dropsondes 850hPa 082821–082905 UTC

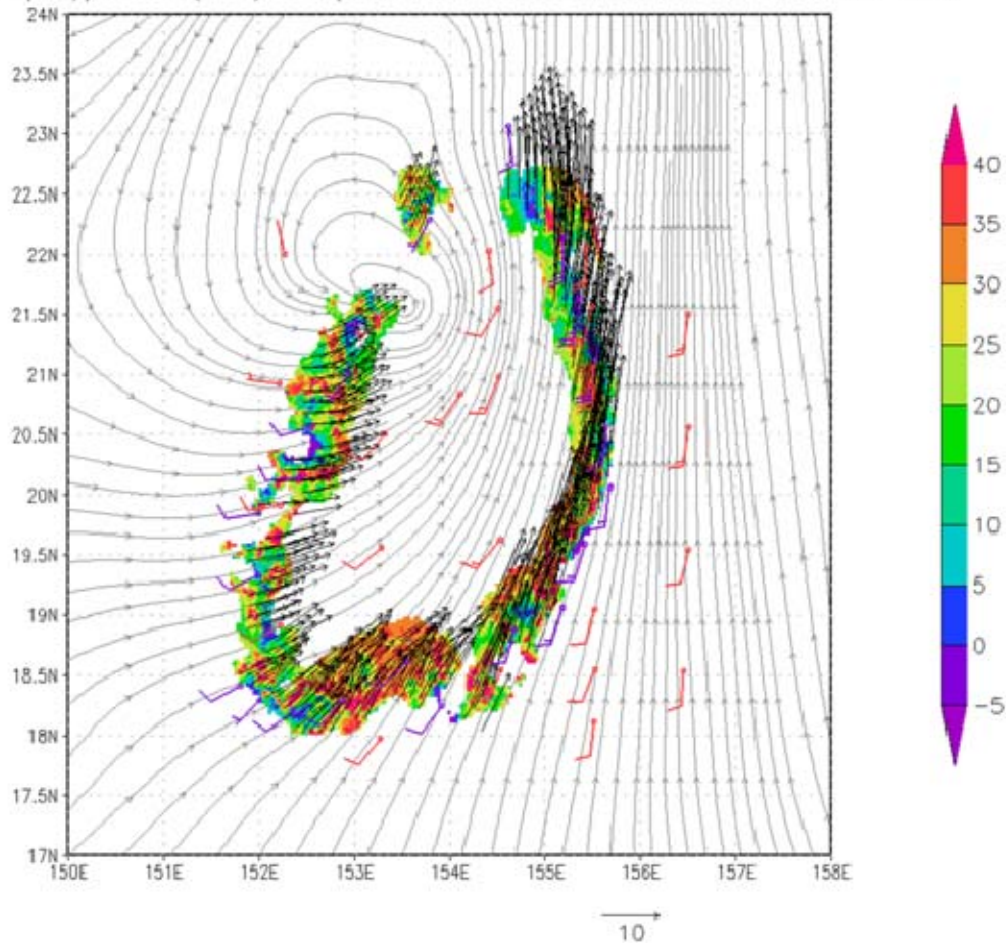


Figure 42. Analyzed ECMWF streamlines, WC-130J dropwindsondes at 850 hPa between 2100 UTC 28 August – 0500 UTC 29 August, and ELDORA reflectivity (dBz) and winds ( $\text{m s}^{-1}$ ) at 1.5 km during 0020-0415 UTC 29 August 2008.

At 1.5 km (850 hPa), ELDORA and dropwindsonde winds indicated a general cyclonic circulation associated with MCS-H, with an apparent center of circulation northwest of the region (Figure 43a). Winds in excess of  $10 \text{ m s}^{-1}$  were common on the east side of MCS-H. These high winds are consistent with a region of low-level convergence in the analyzed ECMWF streamlines (Figure 42). The 3 km (700 hPa) ELDORA and dropwindsonde winds (Figure 43b) appeared similar to the 1.5 km level with the strongest winds on the east side of MCS-H and the apparent center of cyclonic circulation to the northwest. The 4.5 km (600 hPa) level (Figure 43c) and 6 km

(500 hPa) level (Figure 43d) wind fields were also very similar to the lower levels. Winds were still strongest on the east side of MCS-H and winds on the western side were weak, as indicated by ELDORA wind vectors and WC-130J dropwindsondes. Some suggestion of a cyclonic circulation with the center to the northwest of the region was evident.

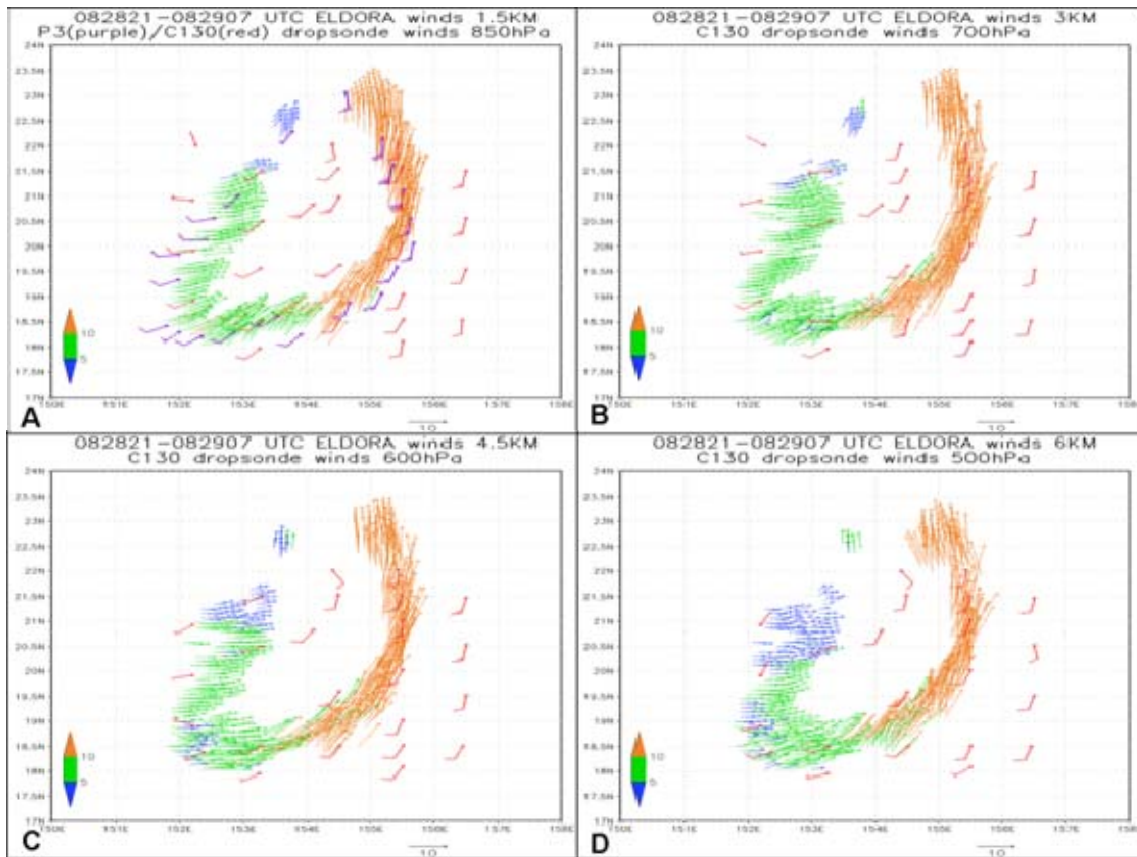


Figure 43. Analyzed ELDORA winds (3 km) and WC-130j dropwindsondes (700 hPa) during 0020-0415 UTC 29 August 2008.

The NRL P-3 with ELDORA flight for 29 August 2008 provided an opportunity to examine the periphery of the convection of MCS-H associated with TCS025. While one of the goals of this flight was to locate a low or mid-level closed cyclonic circulation, it was apparent in the ELDORA and dropwindsonde observations that the center of the circulation was missed by both the WC-130J and NRL P-3 missions. By the time that both aircraft began flying in MCS-H, the low-level circulation (identified by the black circle in Figure 22) was disassociated with the deep convection of MCS-H.

As discussed earlier, dropwindsondes (Figure 27) from the WC-130J and NRL P-3 flights on 28 August as well as satellite-derived winds (Figure 29) immediately after the flights on 28 August indicated an upper-level cyclonic circulation in the vicinity of the deepest convection associated with MCS-G (Figure 21). This circulation became the target of the WC-130J and NRL P-3 with ELDORA on 29 August. However, it appears that the cyclonic circulation associated with MCS-G during the previous flights was not sustained. The low-level circulation propagated to the north away from the convection associated with MCS-G and MCS-H.

## **E. SYNOPSIS OVERVIEW 30 AUGUST THROUGH 1 SEPTEMBER 2008**

Following the final WC-130J and NRL P-3 with ELDORA flights on 29 August, MCS-H continued to dissipate. Through the next five days, MCSs associated with TCS025 continued to develop and dissipate but a consistent low-level closed cyclonic circulation never developed. No additional flight investigations of TCS025 using WC-130J or NRL P-3 aircraft were carried out. On 3 September, TCS08/T-PARC scientists considered that TCS025 was not going to develop and the decision was made to remove TCS025 from further investigation.

### **1. 30 August 2008**

A broad area of convection was still present by 1230 UTC 30 August 2008, but the convection had weakened (Figure 44a). Multiple MCSs existed and several bands of weak convection appeared to rotate cyclonically. The two upper-level TUTT cells that had influenced TCS025 in the early stages were no longer present (Figure 44b) as the upper-level anticyclonic flow that was present the previous day had broadened considerably to cover the majority of the subtropical western North Pacific. Upper-level winds had also increased to over  $20 \text{ m s}^{-1}$  on both the east and west side of TCS025. However, the low-level closed low that was present on 29 August (Figure 14c) had completely dissipated and was replaced by a broad trough that extended eastward from a larger cyclonic circulation centered near  $27^{\circ}\text{N}$ ,  $135^{\circ}\text{E}$  (Figure 44c). As this broad trough lifted poleward, an extension of the subtropical ridge built southwestward to encompass a



broad region from 10°N-29°N and 140°E-165°E. The combination of the ridge to the south and trough along 28.5°N contributed to strong low-level southerly flow in the region of TCS025.

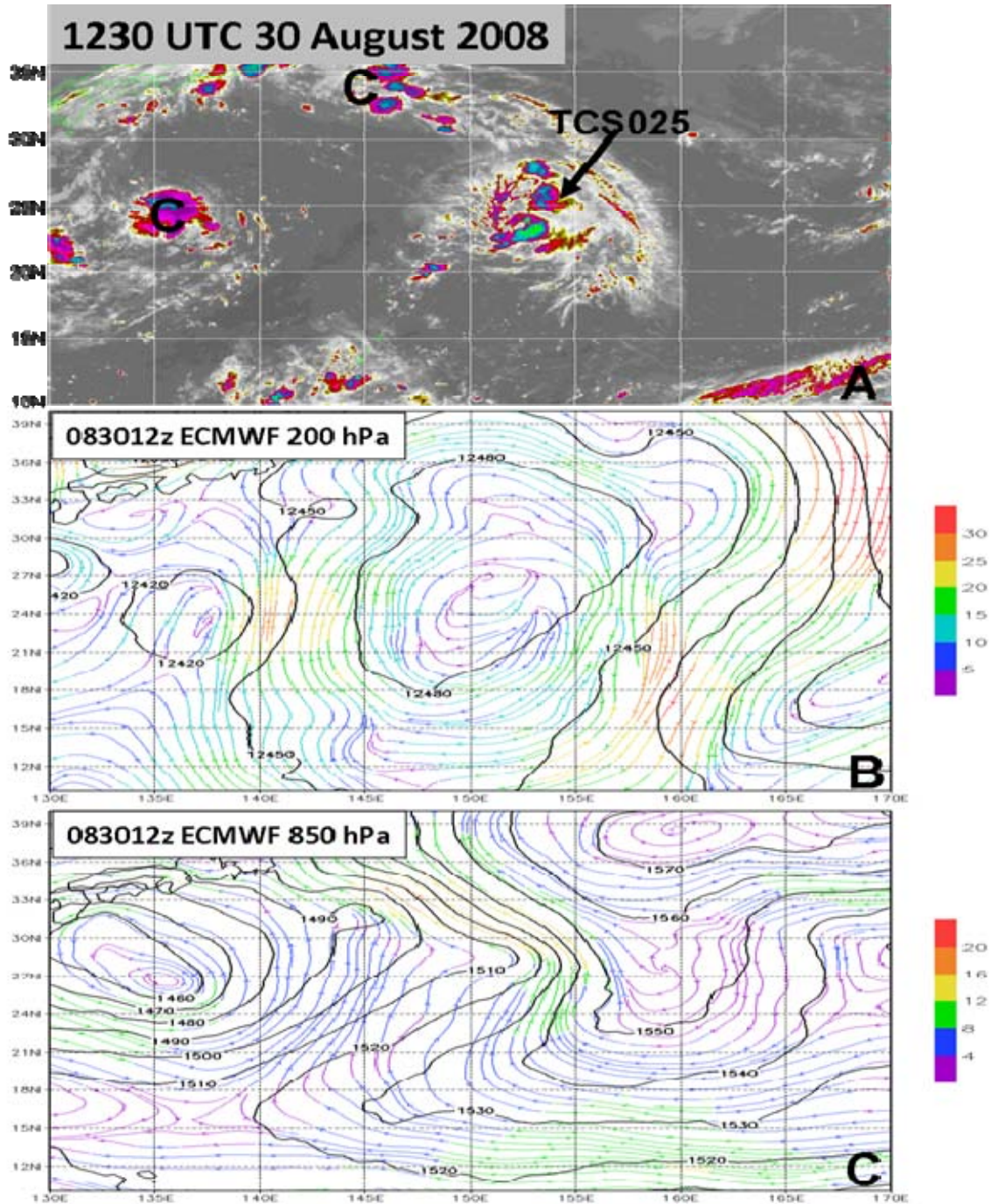


Figure 44. As in Figure 8, except MTSAT imagery at 1230 UTC 30 August and ECMWF analyses at 1200 UTC 30 August.



## **2. 31 August 2008**

Multiple MCSs continued to exist within the general cyclonic circulation of TCS025 (Figure 45a). Convection was present on all sides of the circulation but had weakened considerably (Figure 45a). Upper-level anticyclonic flow continued to dominate a large part of the WNP basin (Figure 45b). Weak equatorward upper-level flow was present directly above TCS025. The low-level analysis identified a broad closed anticyclonic circulation between 18°N-27°N and 142°E-159°E. The low-level trough that extended eastward along 28.5°N toward TCS025 at 1200 UTC 30 August (Figure 44c) had moved northward to near 33°N, 150°E at 1200 UTC 31 August (Figure 45c). The southwestward extension of the subtropical ridge became a closed anticyclone. As defined 24 h earlier, the combined ridge-trough pattern defined strong low-level southerly flow in the vicinity of the convection that defined TCS025. However, the low-level trough became separated from the convection to the south as the trough migrated northward on the cyclonic shear side of the southerly flow.

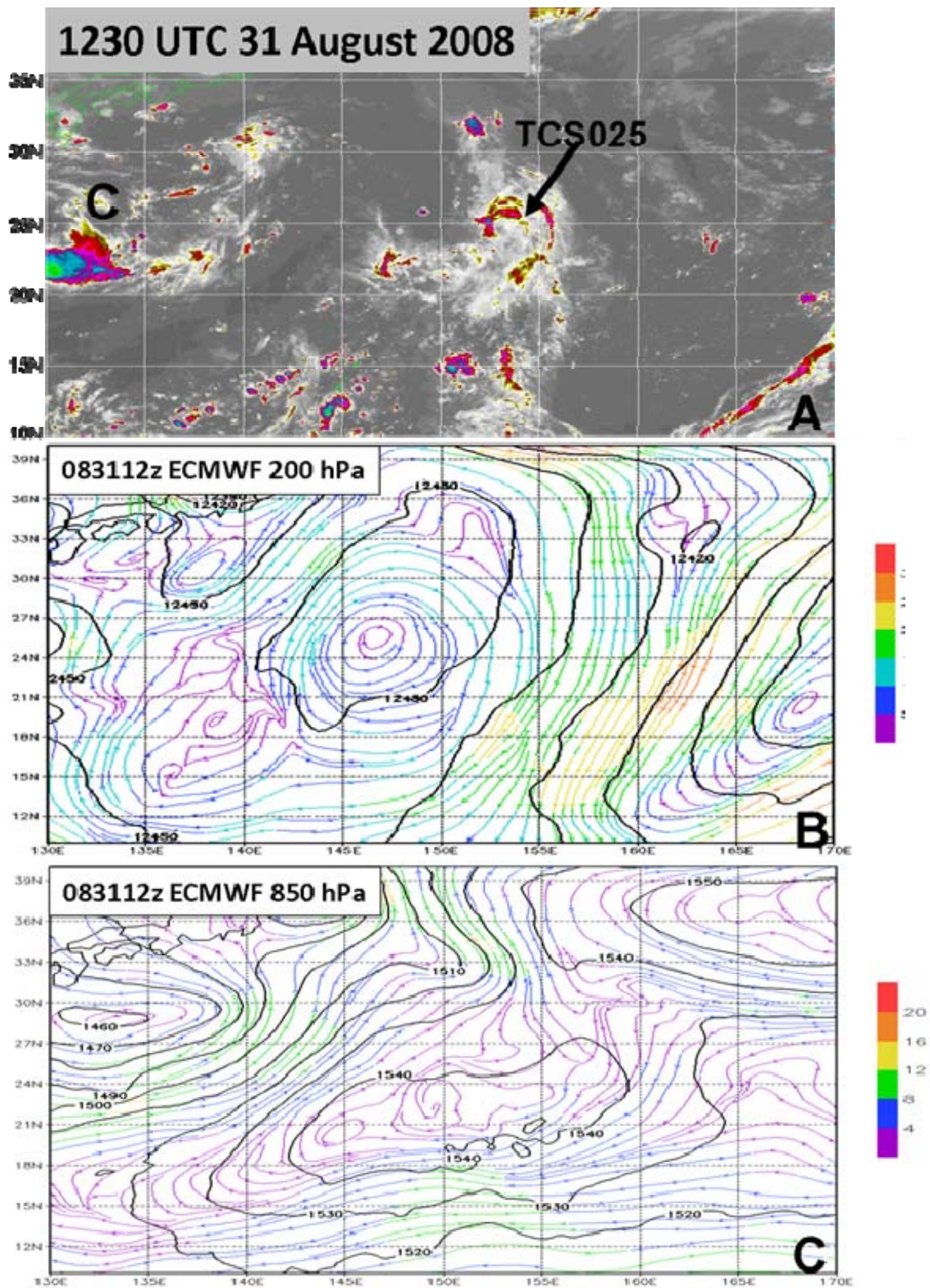


Figure 45. As in Figure 8, except MTSAT imagery at 1230 UTC 31 August and ECMWF analyses at 1200 UTC 31 August.

## **2. 1 September 2008**

By 1 September 2008, multiple MCSs associated with TCS025 persisted (Figure 46a). While some of the convection associated with these MCSs appeared to be deep, it was unorganized. The upper levels continued to be dominated by anticyclonic flow (Figure 46b). However, a deep upper-level trough was now present to the east. The interaction of the large-scale anticyclonic flow and the cyclonic flow to the east provided relatively strong upper-level equatorward flow over TCS025 (Figure 46b). At low levels (Figure 46c), the eastern portion of the west-to-east oriented trough, which had been moving northward, intensified to become a nearly closed circulation. This development may have been related to several dynamical factors associated with the poleward movement of the trough and interaction with the midlatitude environment. However, the convective signature of TCS025 remained separated to the south of the low-level circulation. Over the ensuing 24-36 h, the low-level circulation north of the TCS025 convection intensified slightly and eventually moved into the midlatitudes as a type of hybrid system. The track of the circulation was north-northwest until it was moved into the midlatitude westerlies and turned eastward to quickly move downstream.



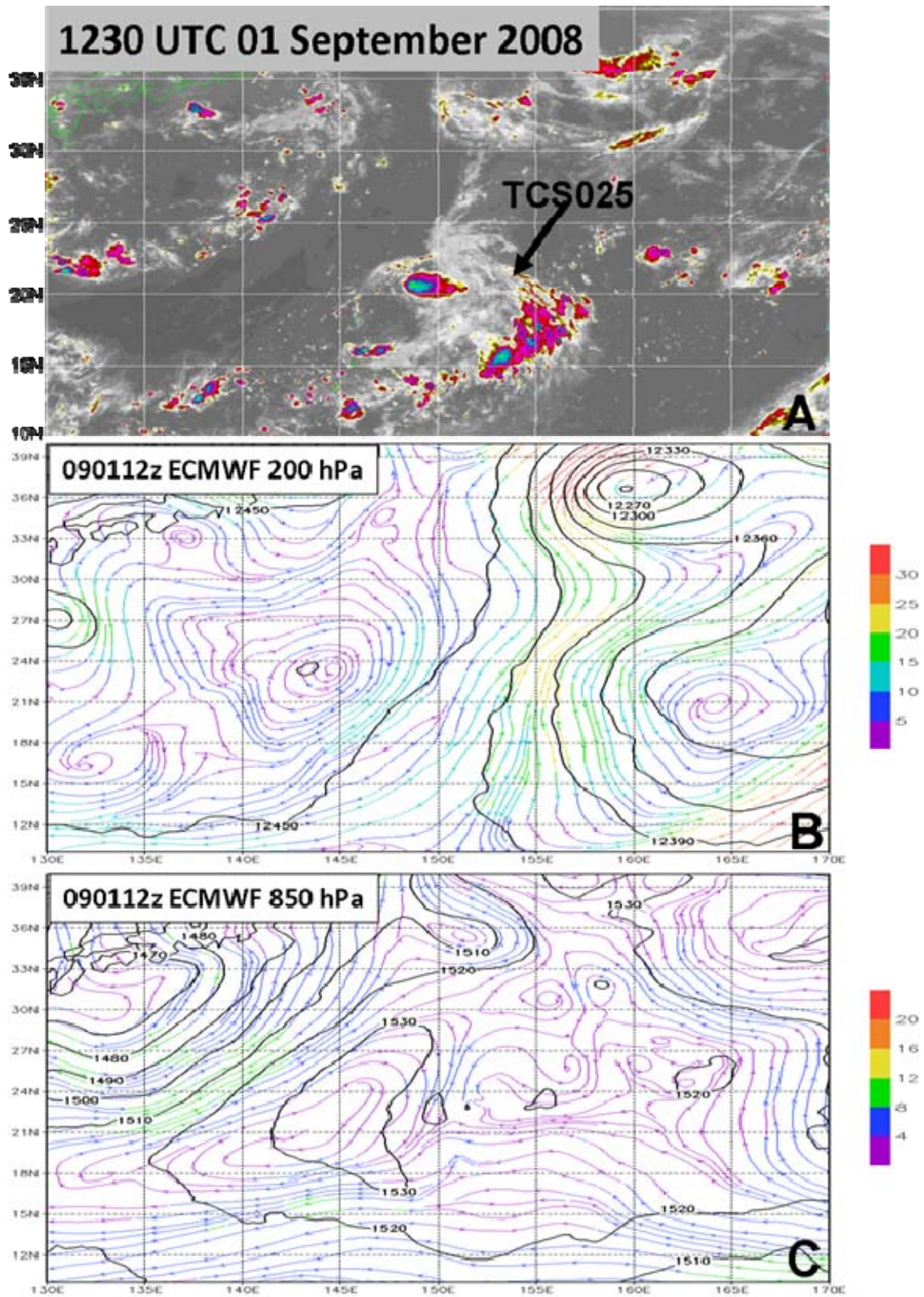


Figure 46. As in Figure 8, except MTSAT imagery at 1230 UTC 1 September and ECMWF analyses at 1200 UTC 1 September.

THIS PAGE INTENTIONALLY LEFT BLANK



## **IV. CONCLUSIONS**

### **A. SUMMARY**

The WNP is an extremely active region for TC development with an average of 31 named storms each year. Although TCs are a common occurrence in the WNP, especially in August and September, predicting the development or non-development of a TCS into a TC is a particular challenge for forecasters. Because of the immense size of the WNP basin, in situ observations are extremely rare. Therefore, forecasters have had to rely on models and remote sensing observations to forecast TC development, tracks, and intensity. During August through October 2008, the Tropical Cyclone Structure (TCS08) field experiment offered a unique opportunity to collect rare in situ data of WNP TCSs using aircraft. A total of 51 numbered TCSs in the WNP were monitored in the WNP. Of these 51, only 12 were upgraded to TD status or higher.

For this analysis, in situ measurements obtained by the USAF WC-130J aircraft and the NRL P-3 with ELDORA were used to investigate the dynamic and thermodynamic structure of a non-developing TCS (TCS025). From 24 August through 3 September 2008, TCS08/TPARC scientists monitored TCS025 for signs of development and aircraft mission possibilities. From 26-29 August 2008, a total of five missions were flown on TCS025 including three WC-130J and two NRL P-3 with ELDORA missions. In addition to in situ observations, ECMWF model fields and satellite observations were utilized.

On 24 August, TCS025 was identified as a broad area of convection between 15°N-25°N and 150°E-160°E. Conditions were favorable for development as TCS025 was in a region of low-level convergence, while two upper-level cyclonic circulations within the TUTT provided upper-level divergence and equatorward flow. Several MCSs associated with TCS025 were present but a LLCC could not be identified. By 25 August, deep convection was present on the south and southeast regions of TCS025 while convection to the north diminished. The two TUTT cells to the northwest and northeast, respectively, persisted. On 26 August, strong upper-level divergence and equatorward

flow continued to support convection. The deepest convection remained to the south and southeast in the form of several MCSs. Two of these MCSs (MCS-E and MCS-F) were the target of the first WC-130J aircraft examination.

Dropwindsondes launched from the WC-130J between 1800 UTC 26 August and 0730 UTC 27 August defined a cyclonic circulation associated with MCS-E. However, the circulation was weak and not identified in the low levels. The convection associated with MCS-E and MCS-F eventually dissipated and progressed south. By the end of the WC-130J flight at 0730 UTC 27 August, a new MCS (MCS-G) began to develop in the same region as the previous MCSs. This MCS was the target of the second WC-130J and first NRL P-3 with ELDORA mission for TCS025.

From 2000 UTC 27 August – 0600 UTC 28 August 2008, the WC-130J aircraft launched dropwindsondes on TCS025 and the NRL P-3 with ELDORA investigated the convection associated with MCS-G. A low-level cyclonic circulation was evident in the dropwindsonde and ELDORA wind field observation of MCS-G at 19.5°N, 152.5°E. From 700 hPa and above, this cyclonic circulation was shifted to the southwest and was centered at approximately 18.5°N, 152°N. A dropwindsonde sounding near the center of circulation indicated that the separation of upper and lower-level circulations occurred at approximately 800 hPa. It appears that the upper-level circulation propagated with the convection of MCS-G while the low-level cyclonic circulation, under influence of the low-level background flow, progressed northward. The convection of MCS-G eventually dissipated and the upper-level circulation associated with MCS-G did not penetrate down to the surface.

Aircraft dropwindsonde winds from 2000 UTC 27 August – 0600 UTC 28 August 2008 and satellite-derived winds at 1000 UTC 28 August indicated an upper-level circulation near 18.5°N, 152°N that became the target of the third WC-130J and second NRL P-3 with ELDORA flights. The WC-130J flew a spiral box pattern to search the convection of MCS-H for a low-level cyclonic circulation. The NRL P-3 flew the periphery of the convection associated with MCS-H while deviating for deep convection. Both the ELDORA and dropsonde wind fields did not detect a cyclonic circulation center associated with MCS-H convection. An apparent cyclonic circulation associated with

TCS025 was northwest of MCS-H convection and outside of the flight region. The cyclonic circulation that had been present when MCS-G had moved through the region had moved to the northwest.

It appears that the low-level cyclonic circulation associated with TCS025 was influenced by the background flow rather than by the convection associated with TCS025. A mesoscale circulation was produced by the convection of MCS-G. At the time of the first NRL P-3 mission, a variety of cyclonic circulations were identified at multiple levels. The circulation characteristics in terms of level and intensity appear to be related to the stage of convective development as the low-level circulation was found in a region where the clouds were low and disorganized and the mid-level circulation was found closer to the active portion of MCS-G. However, the low-level cyclonic circulation progressed to the north and did not remain with the MCS-G convection and the associated mid- and upper-level circulation.

Over the next few days, TCS025 continued to produce several MCSs but the convection never organized and a LLCC was never identified. Rather, the LLCC identified by scatterometer data and model analysis continued to move northward away from the region where convection was being forced. As the large-scale circulation over the subtropical WNP became defined by the trough to the west and a subtropical ridge to the southeast, the LLCC moved northward embedded in the cyclonic shear of the southerly flow between the trough and ridge. As the LLCC continued poleward, some intensification occurred, but eventually it was captured by the midlatitude westerlies. The northward movement of the LLCC that was related to the large-scale flow pattern kept it separate from the convection that remained to the south in low-level confluent flow between the trough to the west and ridge to the east. Since TCS025 was never upgraded to TD status, on 3 September 2008 TCS025 was eliminated from further investigation by TCS08/T-PARC scientists.

## **B. RECOMMENDATIONS**

Further studies of non-developing TCSs using aircraft data, specifically ELDORA, are recommended. Such studies could provide additional insight into the

mesoscale dynamics and thermodynamics that determine whether a TCS will develop. The unique data sets that ELDORA can produce are invaluable to TC forecasters. One of the limitations of the missions with ELDORA on the NRL P-3 was the inability to penetrate deep convection. Placing ELDORA on another aircraft that has the ability to penetrate deep convection, such as on a WC-130J, would provide scientists a valuable data set. Additionally, a modeling study to determine the relative roles of mesoscale and synoptic-scale forcing in the non-development of TCS025 would be beneficial.

## LIST OF REFERENCES

- Elsberry, R. L., and P. A. Harr, 2008: Tropical Cyclone Structure (TCS08) field experiment: Science basis, observational platforms, and strategy. *Asian Pacific Journal Atmospheric Science*, **44**, 209–231.
- European Centre for Medium-range Weather Forecasts, ECMWF Web site. Retrieved 1 August 2009. [Available online at <http://www.ecmwf.int/>]
- Gray, W. M., 1968: Global view of the origin of tropical disturbance and storms. *Monthly Weather Review*, **96**, 669–700.
- Hildebrands, P. H., W.-C. Lee, C. A. Walther, C. Frush, M. Randall, E. Loew, R. Neitzel, R. Parsons, J. Testud, F. Baudin, and A. LeCornec, 1996: The ELDORA/ASTRAIA airborne Doppler weather radar: High-resolution observations from TOGA COARE. *Bull. Amer. Meteor. Soc.*, **77**, 213–232.
- Hock, T. F., and J. L. Franklin, 1999: The NCAR GPS dropwindsonde. *Bull. Amer. Meteor. Soc.*, **80**, 407–420.
- Joint Typhoon Warning Center, cited 2009a: 2008 Annual Tropical Cyclone Report. Retrieved 13 October 2009. [Available online at [http://metocph.nmci.navy.mil/jtwc/atcr/atcr\\_archive.tml](http://metocph.nmci.navy.mil/jtwc/atcr/atcr_archive.tml)]
- Montgomery, M. T., and B. F. Farrell, 1993: Tropical cyclone formation. *Journal of the Atmospheric Sciences*, **50**, 285–310.
- Montgomery, M. T., M. E. Nicholls, T. A. Cram, and A. B. Saunders, 2006: A vertical hot tower route to tropical genesis. *Journal of the Atmospheric Sciences*, **63**, 355–386.
- NCAR Earth Observing Laboratory, Retrieved 20 October 2009: [Available online at: <http://www.eol.ucar.edu/rsf/eldora/eldora.html>]
- NRL Monterey Tropical Cyclone Homepage Retrieved 10 October 2009. [Available online at [http://www.nrlmry.navy.mil/tc-bin/tc\\_home2.cgi](http://www.nrlmry.navy.mil/tc-bin/tc_home2.cgi)]
- Reasor, P. D., M. D. Eastlin, and J. F. Gamache, 2009: Rapidly intensifying Hurricane Guillermo (1997). Part I: low-wavenumber structure and evolution. *Monthly Weather Review*, **137**, 603–631.
- Simpson, J., E. Ritchie, G. J. Holland, J. Halverson, and S. Stewart, 1997: Mesoscale interactions in tropical cyclone genesis. *Monthly Weather Review*, **125**, 2643–2661.



Franklin, J. L., M. L. Black, and K. Valde, 2003: GPS dropwindsonde wind profiles in hurricanes and their operational implications. *Wea. Forecasting*, **18**, 32–44.

Wakimoto, R. M., W.-C. Lee, H. B. Bluestein, C.-H. Liu, P. H. Hildebrand, 1996: ELDORA observations during VORTEX 95. *Bull. Amer. Meteor. Soc.*, **77**, 1465–1481.

## INITIAL DISTRIBUTION LIST

1. Defense Technical Information Center  
Ft. Belvoir, Virginia
2. Dudley Knox Library  
Naval Postgraduate School  
Monterey, California
3. Jeff Hawkins  
Naval Research Laboratory  
Monterey, California
4. Michael Bell  
Naval Postgraduate School  
Monterey, California
5. Pete Black  
Naval Research Laboratory  
Monterey, California
6. Professor Patrick Harr  
Naval Postgraduate School  
Monterey, California
7. Professor Russell Elsberry  
Naval Postgraduate School  
Monterey, California
8. Professor Michael Montgomery  
Naval Postgraduate School  
Monterey, California
9. Director, Joint Typhoon Warning Center  
Pearl Harbor, Hawaii